DISSERTATION

EXPANDING MOSQUITO CONTROL TOOLS: NOVEL APPROACHES FOR SURVEILLANCE AND CONTROL

Submitted by

Gregory (Greg) Scott Pugh

Department of Microbiology, Immunology, and Pathology

In partial fulfillment of the requirements

For the Degree of Doctor of Philosophy

Colorado State University

Fort Collins, Colorado

Summer 2025

Doctoral Committee:

Advisor: Brian D. Foy

Rebekah Kading
Elizabeth Hemming-Schroeder
Punya Nachappa

ABSTRACT

EXPANDING MOSQUITO CONTROL TOOLS: NOVEL APPROACHES FOR SURVEILLANCE AND CONTROL.

Approximately 80% of the world's population is at risk of at least one vector-borne disease. Most of these diseases are preventable through protective measures such as insecticide treated bed nets or indoor residual spraying of insecticides along the walls of a domicile. However, these measures can be cost prohibitive and due to these costs, disproportionate infection rates are found within the communities which have lower incomes. Additionally, invasive species are overtaking ecological niches where endemic vectors once thrived. Because of this, novel diseases are being introduced into naïve human populations, which could have deleterious outcomes. While vector-borne disease prevention methods, such as vaccinations, are becoming more common, for several reasons these methods can leave out the populations which need them the most, such as how vaccinations typically require cold-chain infrastructure. Furthermore, some prevention methods do not exist for some of these diseases, therefore controlling the mosquito populations with insecticides is a standard practice for preventing vector-borne disease outbreaks. However, mosquito vectors are exhibiting resistance, both biological and behavioral, to commonly used insecticide classes, resulting in cross-resistance to both old and new products. Novel approaches to mosquito control are necessary to better control vector-borne diseases while circumventing rising insecticide

resistance issues, including the development of new control methods and better characterizing mosquito population dynamics.

Mass administration of endectocides, such as ivermectin and isoxazolines, could be a novel mosquito-borne disease control method in regions where insecticide-resistant mosquitoes are feeding on human and livestock hosts and spreading disease. Ivermectin is a glutamate-gate chloride channel agonist, causing death by flaccid paralysis in arthropods which feed on treated individuals, and is highly efficacious against anopheline mosquitoes. Additionally, ivermectin is known to cause a reduction in fecundity and refeeding frequency of mosquitoes which imbibe a sublethal dose. This class of drug has been used for the last 37 years as a mass-administered antihelminth drug in rural Africa and is accepted as a beneficial drug for community health. While ivermectin has a short half-life in human plasma, newer models suggested that a change in dosing regimen may retain the mosquitocidal effects up to 28 days post-intervention. Prior studies conducted clinical trials using this dosing regimen, observing the effects on the mosquito populations. However, these studies paired ivermectin with other antimalarial treatment drugs, which could alter the pharmacokinetics and mosquitocidal effects of ivermectin. The Repeat Ivermectin Mass Drug Administration for the control of MALaria II (RIMDAMAL II) clinical trial was designed to evaluate the effect of ivermectin alone, given once a month to select villages in mass drug administration campaigns in Burkina Faso. In addition to observing the mosquitocidal effects of ivermectin on wild mosquitoes, plasma was obtained from participants to elucidate the pharmacokinetics and pharmacodynamics of human-processed ivermectin. The goal of this clinical trial was to reduce the malaria burden within

children, primarily by reducing sporozoite transmission from the older, possibly infectious mosquitoes.

The extrinsic incubation period (EIP), or the time it takes a mosquito to become infectious after consuming an infected blood meal, is dependent on both the mosquito species, the pathogen, and external factors such as temperature. Understanding the EIP is essential to determine if a mosquito population has a higher risk of transmitting a pathogen to the human population, the older a mosquito population is, the greater the risk. For instance, the EIP for *Plasmodium* development in female *Anopheles gambiae* complex mosquitoes is between 9 and 16 days before the sporozoite form of the parasite can disseminate, eventually arriving to the salivary glands, making the mosquitoes infectious when they imbibe their next bloodmeal. While the EIP of West Nile virus in *Culex tarsalis* is between 8 and 18 days, there are some instances where the virus can escape the midgut and reach the salivary glands within a few days, causing mosquitoes to become infectious before the established EIP.

This makes time crucial when assessing the age of the mosquito population. However, the current methods to age mosquito populations are slow and expensive relative to the large sample sizes and frequent sampling needed to accurately assess population age and require a high degree of technical knowledge. Additionally, the current ‘gold standard’ of mosquito age-grading is qualitative, observing the population’s parity rate, which requires an exorbitant amount of time, especially when mosquito control experts are conducting control operations. Furthermore, these parity methods are inaccurate with autogenous species, which can lay eggs without the need for a prior blood meal causing an inappropriate classification of population age. Thus, new rapid,

low-cost and simple age-grading methods are needed for mosquito control experts and researchers to identify mosquito populations which contain the greatest risk for pathogen transmission. Fortunately, we have been developing a novel technique based on older research that has all these qualities. As a mosquito ages, it loses wing scales, eventually becoming threadbare. Qualitative methods in the past placed mosquitoes into subjective categories based on the look of their wings, but we updated this method by using a novel, high-throughput, and quantitative method to age mosquito populations using machine vison algorithms to calculate the pixel intensity of wing photos.

This dissertation has investigated the pharmacodynamics of human processed ivermectin on *Anopheles gambiae* mosquitoes and observing a possible feeding aversion to imbibing ivermectin-containing blood when there is a high venous concentration of ivermectin. Furthermore, we have further refined our wing pixel intensity age grading method and developed a known age model using our colonized *An. gambiae* G3 strain. We then applied the known age model to the pixel intensities of wing photos collected from wild *An. gambiae* sensu lato mosquitoes captured during the RIMDAMAL II clinical trial to interpolate their ages. Using this novel method, we observed a significant decrease in mosquito pixel intensities once new dual-chemistry bed nets were deployed halfway through our clinical trial in both arms, suggesting the wing pixel intensity method was able to quantify the effect of this mosquito control intervention. We also applied the wing pixel intensity method to wild *Cx. tarsalis* around the Greater Salt Lake and Northern Colorado during mosquito control interventions to determine the generalizability of the method towards another mosquito vector. This age-grading technique lays the foundation for an inexpensive and high throughput

measurement for public health, mosquito control experts, and researchers to identify if a mosquito vector population has the capacity to transmit pathogens to the community.

ACKNOWLEDGEMENTS

"You know, I'm something of a scientist myself." – Norman Osborn[1]

As with all extensive projects, none of this could be possible without the unwavering and unconditional support found within mentors, friends, and family. First, I would like to thank the people of Burkina Faso for agreeing to take part in the RIMDAMAL II clinical trial. So much of my early career has been dedicated to the clinical trial and without you, I would not have been as joyous as I was during my Ph.D. training. To my advisor, Brian Foy, I truly do not believe I would have been as successful as I have been in another lab. You have allowed me to follow and forge my own path while providing a welcoming and supportive environment. Additionally, to my committee, while I have not reached out as much as I should have, each of you has provided me with the ability to learn and exercise my knowledge in your classrooms and during meetings, thank you for agreeing to be a part of my process to join you all in our field. To Jeff Wilusz, I honestly do not think I would be finishing my Ph.D. at Colorado State if you had not accepted the invitation to speak at Baylor University, thank you. To the graduate support team and the administrators of Microbiology, Immunology, and Pathology, I do not believe you all get the credit you deserve, thank you for being the unsung heroes of our department. Furthermore, to our collaborators: Chris Barker's group, Sunil Parikh's group, Salt Lake City Mosquito Control District, each of you have allowed me to graciously tag along with and have assisted me with my own research. None of this would have been possible without your acceptance, thank you all. My prior

mentors, Stephanie Randell and Jonathan Miles, thank you for your support and taking me under your wings as a young researcher.

To my Colorado family: James, Kathrine, Kenzie, and Ethan, you all accepted me and Angelica into your lives and your group you have become uncles and aunts to our daughter. You all have allowed and taught me to grow from the enlisted shackles I once wore without judgement. We have shared some of our families' most joyous occasions with one another and I am thoroughly excited to share more. You all will forever be in my mind and my heart, and I will roll polyhedra with you all at any time.

Casey, Steve, Andrew, Cody, Jordan, and Mat. You all have seen me at my lowest and stuck with me. I know I was not always pleasant to be around or talk to, but words cannot express the absolute love I have for each one of you. We all met each other in October of 2014 and since then, we have watched each other's families grow and prosper. We have seen and been there for each other during some despairing times and some extremely joyous occasions. I could not have asked for better brothers in life than the ones I have received, through a chance post on the Destiny subreddit. Thank you all, for everything and I am excited for our kids to grow and prosper with one another.

Finally, to my wonderful and supportive family: Angelica, Sylvie, and Trinh. Angie, this has been such a long and tedious journey but your support during these tumultuous years has strengthened our resolve. We have moved across the country and now perhaps overseas. We watched each other grow in unimaginable ways, ensuring that every day we become better people. We were there for each other when the floor fell and the walls caved in. We have found success in everything we have done together,

including becoming parents. Additionally, with you and with your support, I have been able to achieve goals I did not know existed. I am relieved that I can finally extend this support that you have given me over the last ten years while you explore your personal and professional goals. I have never been more excited to discover the seas and the stars with you. Let's see what our next chapter in life holds for us. Sylvie, you are entirely too young to understand this, but everything I have accomplished in my life has been for you. I do apologize I have not been able to always be there for you during this first year of your life, but I am here now, constructing a future for you, which your mom and I could not have. Everything that I own, and everything that I am is yours, forever and always. You are my north star and my heartbeat. I am so excited to see you grow and prosper in ways your mom and I could only dream of as children. To Trinh, I could not have taken on such a task without your support and help. I am forever grateful that you moved from Texas to help us when we needed you the most. Thank you Me.

TABLE OF CONTENTS

CHAPTER 1: OVERVIEW OF THE LITERATURE

1.1 The global vector-borne disease burden

The World Health Organization (WHO) estimates that vector-borne diseases (VBD) account for roughly 17% of all infectious diseases, causing more than 700,000 deaths annually[2]. Malaria alone accounts for more than 608,000 deaths per year and dengue Virus (DENV), an *Aedes*-borne pathogen, causes an estimated 40,000 deaths per year. Furthermore, 80% of the world's population is at risk of at least one VBD with disproportionate infection rates observed in lower-income areas[2]. This is primarily because most VBD are preventable though protective measures or community-led efforts, both of which have costs[3]. Significant vectors include ticks, sandflies, triatomines, and mosquitoes[2]. However, mosquitoes, such as those in the *Aedes*, *Culex,* and *Anopheles* genera, account for the highest rates of VBD transmission across the globe[2].

Globalization and climate change have compounded mosquito-borne pathogen transmission. Invasive species are being introduced, such as *An. stephensi* in east Africa, in addition to *Ae. aegypti* and *Ae. albopictus* in the United States[4–7]. Due to the introduction of *An. stephensi* in east Africa, malaria rates in urban areas are increasing as control mechanisms for other anophelines are not as effective[8,9]. *Ae. aegypti* and *Ae. albopictus*, competent vectors of dengue virus (DENV), Zika virus, yellow fever virus (YFV), and chikungunya virus, are spreading throughout the southern and western parts of the US, making *Aedes*-borne virus transmission more likely[4,10]. These invasive species are causing disruptions in vector control operations and disease risk

surveillance, making it more difficult to control VBD spread through communities. Due to the increasing range of *Aedes* mosquitoes, the propensity of the viruses they transmit to become endemic in new regions is starting to be realized. In 2024, over 6,500 reports of locally transmitted DENV were reported in Puerto Rico (6,238), Texas (2), Florida (83), US Virgin Islands (205), and California (18), compared to over 1,400 being made in 2023[11].

Most mosquito-borne pathogens share a common route in the mosquito before it can become infectious: being imbibed in an infected bloodmeal, midgut infection, dissemination out of the midgut, infection of salivary glands and dissemination into the saliva. Commonly, this process involves pathogen multiplication in the vector, although this is not the case for mosquito-transmitted filarial nematodes. For human *Plasmodium,* this process is called sporogony, and it follows a specific cycle[12]. Micro- and macrogametocytes must be ingested by a female anopheline mosquito where sexual reproduction occurs in the midgut, the zygote then transforms into an ookinete which traverses the midgut cells, and then the parasite begins to develop into an oocyst in between the basolateral membrane of midgut cell and midgut's basal lamina[12]. As an oocyst, the organism undergoes asexual multiplication, forming thousands of sporozoite forms, and the oocyst eventually bursts, flooding the hemocoel with sporozoites that disseminate to and invade the salivary glands where the sporozoites eventually can be dispersed via saliva[12]. Viruses, such as DENV and West Nile virus (WNV) follow this same course; however, they do not reproduce sexually. Instead, these arboviruses typically infect midgut cells and replicate, and eventually some escape the midgut, disseminate to, and infect numerous cells and tissues of the hemocoel, including the

salivary glands. Although in some rare cases, arboviruses can escape the midgut after being ingested without prior replication in the midgut cells. In hemocoelic tissues, including the salivary glands, further viral replication occurs before virus disseminates into the saliva being produced by the glands' acinar cells, and then virus is ultimately transmitted horizontally when a female imbibes blood from a new host[13–15].

While DENV was likely introduced into the Western hemisphere in the 18th century through the slave trade, WNV was introduced into North America via New York City in 1999[16–19]. WNV can be transmitted by a plethora of mosquito genera, however in the US, the *Culex* genus is the main vector[20,21]. Throughout the US, mosquito control districts control for *Cx. tarsalis, Cx. pipiens, and Cx. quinquefasciatus*, the three main species responsible for WNV transmission in the US[21]. Since WNV was introduced, the virus has moved across the US, becoming endemic. WNV is spread in an endemic cycle between birds and *Culex* mosquitoes[22]. Mammals who contract the virus rarely reach high enough viremia to pass the pathogen back to mosquitoes, thus making humans and most other mammals incidental or dead-end hosts[23]. Furthermore, *Culex* mosquitoes can transmit a wide range of neuroinvasive viruses including Japanese encephalitis virus (JEV), St. Louis Encephalitis virus (SLEV), western and eastern equine encephalitis viruses (WEEV & EEEV), and Rift Valley fever virus[24–28]. While *Anopheles* mosquitoes are more attributed to transmitting the parasite which causes malaria, they are known to transmit O'nyong'nyong virus, a virus with pathology resembling CHIKV[29], as well as numerous orthobunyviruses and other arboviruses more rarely[30].

The largest human burden from VBD in terms of morbidity and mortality is from malaria, which is caused by infection with *Plasmodium* parasites[2,31]. *Plasmodium species* can infect a wide range of animals, however, the five species which typically infect and cause disease in humans are *P. falciparum, P. malaria, P. vivax, P. ovale,* and *P. knowlesi*[31]. The WHO reported and estimated 263 million malaria cases and 597,000 deaths globally in 2023, an increase of 11 million from 2022[31]. While the mortality rate has decreased, the incidence rate has increased, indicating that society is finding and treating cases but more infections are occurring[31]. There are disproportionate incidence and mortality rates in the WHO African Region, with 246 million cases and 569,000 deaths occurring in 2023[31]. For example, Nigeria accounted for 25.9% of the global infections and 30.9% of the global deaths while only having approximately 3% of the world's population[31]. While malaria diagnosis and treatment is common and can be relatively straight forward, vaccines are starting to be distributed which may begin to further reduce childhood mortality[32–35]. In addition to human malaria, mosquitoes in the *Culex* genus can transmit malaria to birds; Hawai'i is trying to combat population die-offs of Hawaiian honeycreepers (*Carduelinae* species) caused by infections with the invasive *Plasmodium relictum*, transmitted by *Cx. quinquefasciatus*, another invasive species[36]. Furthermore, competent mosquitoes can transmit other parasites, including filarial worms such as *Wuchereria bancrofti*, *Brugia malayi*, and *B. timori*, the causative agents of lymphatic filariasis[37]. Mosquito-borne diseases are cause for concern, especially in developing countries with high infant mortality or morbidity. In response to these threats, researchers have developed methods to assess the epidemiological impact of VBD, constructed tools and traps to surveil mosquito populations, established

mosquito control and disease transmission prevention methods, explored the use of novel systemic insecticides, and explored new ways to discern mosquito population dynamics to control the spread of VBDs.

1.2 Epidemiological human risk assessment tools

To further our comprehension of mosquito-borne disease transmission, Ross and Macdonald created a model describing the basic reproductive rate (R_0) of these pathogens: $R_0 = \frac{ma^2bcp^n}{(-\ln(p))r}$ where *m* is the ratio of mosquitoes to human, *a* is the human bite rate (HRB), *b* and *c* are the pathogen transmission efficiencies, *p* is the daily survival rate of mosquitoes, *r* is the human recovery rate, and *n* is the extrinsic incubation period (EIP) or the time it takes for the pathogen to develop within the mosquito before transmission can occur[38,39]. This model was then modified to describe vectorial capacity (VC), or a vectors ability to transmit pathogens: $VC = \frac{ma^2bp^n}{-\ln(p)}$[40]. In this model, all variables remain the same as the Ross-Macdonald model, with *b*, *r*, and *c* removed and *-ln(p)* representing the average lifespan of a vector. In these models, the EIP (*n*) plays a significant role in pathogen transmission, requiring that an infected mosquito survive long enough to transmit to a host. While all these measures together can estimate human risk, to obtain these variables, active surveillance must occur.

To estimate *m*, the ratio of mosquitoes to humans, researchers have a multitude of tools at their disposal such as human landing capture (HLC) and collection of mosquitoes which are host seeking via traps[41–43]. HLC is considered the ‘gold-standard’ for determining the HBR as mosquitoes are actively landing and seeking a blood meal from a human host. However, the technique is prone to natural collector biases in

variation of mosquito attractiveness[42,43]. There are ethical concerns too, particularly when there are known mosquito-borne pathogens being transmitted by the mosquito population. This issue can be address by giving collectors antimalarial prophylactics, but this does not prevent arboviral or other infections. By using traps, the natural variation of attractants of host's can also be mitigated, however, trap location and the use of artificial baits, such a CO_2 can introduce biases[41,42].

To estimate HBR from captured mosquitoes not landing on a human, researchers can conduct blood meal analysis (BMA), identifying the blood meal contents of the host engorged mosquitoes fed upon[44–48]. However, these methods are passive and do not account for mosquitoes which are actively seeking a blood meal, but those who have already imbibed one. Additionally, these methods work best on newly engorged females as the biochemical markers are still intact and not degraded by the process of digestion. Furthermore, these methods allow investigators to unravel misconceptions about the feeding habits of certain mosquitoes, such as *Cx. pipiens* feeding on a wide variety of hosts[47]. To calculate p and $-ln(p)$, researchers have tried to conduct mark, release, and recapture experiments[49–53]. However, these methods are difficult to analyze due to the lack of mosquitoes recaptured. Other age-grading methods are being examined to discern these variables[54]. The pathogen transmission efficiency is dependent on the mosquito and the pathogen; however, the variable can be determined via transmission and vector competence assays. Overall, VC and R_0 are useful theoretical measures for modeling studies and understanding vector-borne disease transmission efficiencies especially when comparing different vector and pathogen pairings, but they are not easily measured and so not very useful for evaluating pathogen transmission intensity in

endemic or epidemic areas or seasons, nor for evaluating the efficacy of control measures. For these actionable measures the vector index (VI) or the entomological inoculation rates (EIR) are typically calculating from vector sampling and pathogen testing.

VI is obtained by multiplying the density of host seeking mosquitoes by the estimated proportion of infected mosquitoes, found by various molecular biological techniques such as PCR or qPCR, and typically calculated by pool-testing the entire bodies of captured arbovirus vectors (such as *Culex* tarsalis in the US) where the proportion infected is very low. While the EIR is a similar measure, but more often used with malaria vectors, and obtained by multiplying the HBR (traditionally obtained with HLC, but also by other trap catch methods with a correction factor accounting for lower catch rates or the specific proportion of human vs. other host blood meals found in the mosquito species) by the number of infectious mosquitoes that that are often tested as individuals. Anophelines that are infectious for *Plasmodium* are typically scored by detecting the presence of sporozoite forms in only the head-thorax tissues. The accuracy of VI is dependent on the choice of sampling method used to estimate biting rate, and the number of mosquitoes assessed, relative to the population size. As investigators typically perform pool-testing due to low mosquito infection rates, pool size similarly influences VI accuracy, as does the composition of the pools and the vector tissues used. Testing saliva would be considered the most accurate method, but it is practically difficult with wild mosquitoes. Nonetheless, recent efforts with sugar baits and honey-infused cards are being examined for capturing infected saliva from wild mosquitoes[55–59]. However, these methods only detect pathogens which are tested for,

and as unfamiliar or novel mosquito-borne pathogens continue to spread to into new regions by human and animal movement and the spread of invasive vectors, these pathogens may go unnoticed and misdiagnosed in certain regions and thus mosquito surveillance tools are necessary.

1.3 Mosquito population surveillance tools

Currently, mosquito population surveillance techniques use active collection of mosquitoes, both larval and adult populations, to discern the population dynamics of a given species. These surveillance techniques are used to identify breeding sites, speciate mosquitoes, and obtain the VI and EIR to calculate the relative risk to the community co-endemic with the mosquito populations[60–64]. Additionally, these surveillance techniques allow researchers and mosquito control experts to observe if any invasive species, and their pathogens, are introduced into a new region[4–10,62]. Surveillance typically involves the monitoring of the mosquito populations during different life stages, such as larvae and pupae, host seeking females, resting, and oviposition, using traps specifically designed to target the different life stages or behaviors as appropriate to the surveillance metric being used to measure actionable thresholds[65]. In addition to the traps designed for life stages, some traps are developed specifically for *Aedes* mosquitoes, attracting them via ocular or sound cues, which target male mosquitoes, seeking a female to mate with[66–69]. Furthermore, new surveillance methods are joining both traps and machine learning together, identifying mosquitoes and their sex[70,71]. As new technologies are arising, geographical information systems (GIS) are assisting mosquito control districts in their ability to provide their services[72–77]. GIS allows researchers, public health, and mosquito control experts to

visualize areas where mosquito surveillance has suggested that VI and EIP are high as well as heightened mosquito density to humans, *m* in the Ross-MacDonald and VC models. GIS technology also allows the mapping of known breeding sites, allowing control districts to easily verify and target with larvicides, should the mosquito density cross unacceptable thresholds[72,74,76]. In addition to GIS being useful for experts, it has become a source of scientific outreach, allowing citizen scientists to report actionable data for control experts to monitor[77]. Furthermore, the state of California and the CDC have tasked researchers to develop a nationwide GIS web interface, allowing districts to not only upload their mosquito capture data, but also pathogen prevalence data, which allows data sharing and cross-district collaborations for VBD control efforts [78]. While these technologies have allowed experts to identify mosquito populations, record their dispersion, and analyze their pathogen transmission potential, some communities have opted to use livestock as sentinels for pathogens.

Castillo-Neyra et al. described using dogs as sentinels for *Trypanosoma cruzi* transmission in Peru, finding that canine seroprevalence was 12.3% in the 17.4% of households infested with *T. cruzi*-infected triatomine insects, suggesting that canine xenosurveillence could be a useful tool in determining the transmission of *T. cruzi*[79]. Chickens are often utilized by US mosquito control districts for assessing the presence of circulating arboviruses, including WNV, WEEV, and SLEV[80–82]. Furthermore, pigs have been utilized as sentinels for detecting JEV circulation in south Asia[83,84]. These animals provide researchers with the opportunity to identify endemic transmission before the pathogens spill over into humans, potentially allowing public health

authorities and mosquito control experts time to alert the public and control the infectious mosquito population.

1.4 Mosquito control techniques

Mosquito control is thought to have pre-historical roots, where people living in mosquito infested areas would construct smoke fires and cover their bodies with plant-derived repellents to keep mosquitoes from biting[85]. Now, mosquito control has evolved from prehistorical roots using larvicide and adulticide chemicals to control mosquito populations.

Historical larvicides were petroleum based, spreading oils in breeding sites, keeping mosquito larvae from oxygen exchange. These methods, however, result in an oxygen exchange barrier for all animals also living in the water as well as causing ecological contamination with petroleum products. Current larvae control tools still use such methods, but the petroleum products have been replaced with plant-derived monomolecular films, and direct larval killing agents including Bacillus *thuringiensis israelensis* (Bti), *Bacillus sphericus* (Bs), spinosad, and pyriproxyfen. Bti and Bs can be placed directly into breeding sites. These spore-forming bacteria come in dissolvable granules or brickettes which are available to consumers at home improvement stores. First used against mosquitoes in 1976, Bti produces four toxic proteins which the mosquito larvae consume, killing them via cell membrane disruption in the midgut[86,87]. It has been noted that mosquitoes can gain resistance to these Bti toxins, however, this resistance is based on the individual toxins Bti produces, when a mosquito consumes all four of toxins, Bti is still efficacious and it even can overcome resistance to chemical larvicides, such as temephos, an organophosphate (OP) used as a larvicide for

mosquitoes[88,89]. In addition to Bti and Bs, *Saccharopolyspora spinosa* was discovered in soil in 1982 and creates macrocyclic lactones (ML) called spinosyns which exhibit mosquitocidal properties[90]. Since the discovery, spinosyn based products are now used for mosquito control but due to the non-specificity of spinosyn, application to mosquito larvae habitats is a preferred method of application[90]. Another class of larvicides are insect growth regulators (IGR), such as pyriproxyfen. Pyriproxyfen is effective at very low doses, mimicking the effect of juvenile hormone and preventing larval mosquitoes from developing into pupae and then adults[91,92]. It can be used in autodissemination methods, whereby adult female mosquitoes are attracted to an artificial egg laying station and land on the active ingredient in the station, contaminating their tarsi with it, and carrying it to a breeding site where they lay more eggs, and it will disseminate into the water, thus keeping her offspring and any others in the water from maturing into adults. These methods work extremely well for mosquitoes which are highly urbanized container-breeders such as *Ae. aegypti* and *Ae. albopictus*. However, if the mosquitoes are more rural, or breed in larger bodies of water, the treatment tends to be ineffective as the active ingredient is too diluted to halt the larvae population from maturing.

Adulticides have a long and storied history, which resulted in the construction of the Environmental Protection Agency[93]. Active ingredients (AI) range from organochlorines like dichlorodiphenyltrichloroethane or DDT, OPs such as naled, carbamates like that of carbaryl, and natural and synthetic botanicals like pyrethrin and pyrethroids, respectively. Organochlorines are agonists to voltage-gated sodium channels, causing mosquitoes to spasm and eventually die[94]. However, these products are long lived and accumulate in fatty tissues causing health issues in both birds and

mammals, which have resulted in a shift from organochlorines to other insecticide classes[94]. OP and carbamates target acetylcholinesterase, resulting in cholinergic receptors being overstimulated causing disrupted nerve impulses which results in death[95–97]. Pyrethroids are synthetic versions of pyrethrins, a compound found in *Chrysanthemum* flowers[98]. These classes of insecticides also target the voltage-gated sodium channels[98]. These AI are used in a plethora of different applications to reduce the mosquito population, *m* in the Ross-Macdonald model, in relation to the human population.

Indoor residual spraying (IRS) and insecticide treated bed nets (ITN) have been the main mosquito control measures used to stop the spread of malaria[99]. The AI of these methods can range from pyrethroids, carbamates, organophosphates, or organochlorines. IRS targets mosquitoes which are resting on the walls of treated homes, causing the AI to be absorbed through the tarsi, and is typically paired with ITN use to reduce nocturnal exposure to anophelines[100]. In addition to IRS and ITNs, treated eaves tubes are a relatively new control method where tubes are placed in the open eaves of traditional homes, in between the top of wall and the roof, and an insecticide treated netting insert is then placed into the eaves tube[101–103]. These tubes prevent mosquitoes from entering a household while exposing them to insecticides which can be rotated, reducing mosquito populations exposure to one type of insecticide as a way to limit the development of insecticide resistance[101–103]. Attractive toxic sugar baits (ATSB) are another newer control method which target mosquitoes which are seeking sugar meals for their daily caloric intake needs[104,105]. These devices can be treated with a variety of insecticides, including endectocides. They are also nonspecific to mosquito

sex, targeting both male and female mosquitoes thus potentially lowering their overall population density. However, these devices are subject to environmental variables, and can be rendered ineffective when precipitation dilutes the treated bait[104,105]. Furthermore, spatial repellents, like those containing transfluthrin, were developed to repel mosquitoes in a wide area and could be paired with an attractant such as an ATSB to potentially make them more effective[102,105–107]. A study conducted in Benin observed a decrease in pyrethroid-resistant *An. gambiae* s.l. activity in houses which contained a transfluthrin passive emanator when compared to houses which were treated with a placebo passive emanator. Additionally, they observed a reduction in other mosquito vector species as well[106]. A study conducted with transfluthrin on lab mosquitoes found that while described as a spatial repellant, transfluthrin can also act as an adulticide, suggesting this spatial repellant is killing some species instead of repelling them[107]. While the control of mosquitoes has been a long endeavor, control has always resulted in resistance development to commonly or overly used AIs.

Insecticide resistance (IR) is a growing issue for current mosquito control efforts that has presented itself in varied ways to current formulations of adulticides and larvicides, requiring insecticide developers to constantly investigate new chemicals and formulations to control mosquito populations[89,108–116]. Target-site mutations have resulted in the alteration of binding sites resulting in resistance to a wide-range of insecticide classes[108,109,112,114,116]. These changes are most studied in pyrethroid resistant populations and known as *knock down resistance (kdr)*, which refers to the phenotype observed from alterations of the voltage-gate sodium channel gene that limits pyrethroid binding to the translated channel protein[108–116]. While *kdr* is one of the

most prevalent resistance mechanisms, cuticle resistance is another resistance mechanism that limits the absorption of insecticides into the mosquito's body through increased cuticle thickness as well as upregulation of specific cuticle-residing proteins or enzymes, both which limit active ingredient from coming in contact with the target sites in hemoceolic nervous tissue[111,117,118]. In addition to the increase of *kdr* mutations and cuticular thickness, metabolic deactivation of insecticide classes is common, whereby metabolic detoxification genes, such as glutathione S-transferases and cytochrome P450s genes are duplicated in the genome or upregulated in transcription[89,110,111,119–123]. While the aforementioned resistance mechanisms are driven by genetic changes, some feeding prevention methods such as ITN and spatial repellents have altered the mosquito populations' feeding behaviors. For example, *An. gambiae* is a known nocturnal endophagic feeder, however, it was found that in Equatorial Guinea populations of this mosquito exhibited crepuscular exophagy following IRS treatments[124]. Cooke et al observed species level changes in feeding time behavior at a different location[125], whereby the primary malaria vectors *An. funestus* sensu lato and *An. gambiae* s.l. exhibited endophagic behaviors but the secondary malaria vectors exhibited exophagic feeding patterns[125]. Due to rising IR and alterations to mosquito feeding behavior, researchers have started to develop novel mosquito control methods. These methods should expand our control toolbox by exploring biological control techniques, new insecticide chemistries, discovering alternative ways to apply old chemistries, and using pharmacological methods which kill mosquitoes after they obtain a bloodmeal.

Current biological control strategies encompass the use of natural predators of mosquito larvae, applying insect-specific lethal fungi, releasing insects which carry a lethal dominate (RIDL) allele, or using *Wolbachia* to sterilization or reduced pathogen transmission within mosquito populations. Natural predators of mosquito larvae have been known and explored as early as the 1900's[126]. One such natural predator is *Toxorhynchites* mosquito larvae, which preys on larvae of other mosquito genera[127]. *Tx. rutilus rutilus* and *Tx. amboinensis* have been used in the US for *Ae. aegypti* and *Cx. quinquefasciatus* control in New Orleans, Louisiana[128,129]. These studies found that *Ae. aegypti and Cx. quinquefasciatus* larvae densities diminished up to 80% in some cases, indicating that *Toxorhynchities* as a biological control mechanism could be feasible[128,129]. In addition to *Toxorhynchities*, many area use fish, such as *Gambusia*, to control mosquitoes[130]. These fish prey on mosquito larvae and pupae[131]. However, it has been noted that chemical cues of the fish have been associated with reduced breeding site selection by *Culex* mosquitoes[132,133]. Furthermore, other predators of mosquito larvae include larvae of aquatic insects, such as dragonflies[134]. Acquah-Lamtey and Brandl showed that the larval stage of *Bradinopyga strachani* significantly decreased mosquito larvae in man-made water containers in Ghana[135]. However, in southern Maine, dragonfly larvae imported and used for mosquito control had no effect on mosquito larvae control[136]. While natural predators may be more attractive than synthetic control mechanisms like insecticides, these control mechanisms can also be invasive species themselves[136,137]. In addition to Bti, some researchers are investigating the use of insect-specific fungi as a mosquito control tool[138–141]. Clark et al observed in 1967 that the fungus *Beauveria bassiana* was pathogenic against adult *Culex*,

Anopheles, and *Aedes* while the larvae of *Aedes* were seemingly resistant to the pathogenic effects that the *Culex* and *Anopheles* larvae succumbed to, suggesting that fungi may be a practical tool for mosquito control[141]. Then, in 2016, Jaber et al isolated *Aspergillus nomius* spores from a dead coleoptera and found that the fungus was pathogenic to *Ae. albopictus* when applied via microinjection and killed both *Ae. albopictus* and *Cx. pipiens* when applying the spores via spraying[138]. It was also found that *Metarhizium pinghaense* exhibited pathogenicity against *An. coluzzii* contained in a Mosquitosphere outdoor mesocosm simulating field conditions in Burkina Faso[139]. These mosquitoes were exposed to a wild type *M. pinghaense* and a transgenic *M. pinghaense* which expresses two US-EPA approved neuron blockers[139]. It was found that when applying the fungal spores via sesame oil suspension on black cotton sheets, the pyrethroid-resistant mosquitoes from Burkina Faso were susceptible to both the wild type and hybrid fungi[139]. The study showed that the fungi, while exhibiting a kill effect, also affected the fecundity of the mosquitoes in subsequent generations, with the hybrid having the most pronounced effect on fecundity and generational numbers indicating the fungi can be transmitted vertically to the female's offspring[139]. Furthermore, researchers have created transgenic *M. anisopliae* which expresses a novel peptide called SM1 and scorpine, an antimicrobial agent. This transgenic organism blocks the *Plasmodium* sporozoites in *An. gambiae* from attaching to the salivary glands[142].

While first demonstrated in *Drosophila melanogaster*, release of insects carrying a dominant lethal (RIDL) has been an effective tool for mosquito control[143]. RIDL aims to replace the wild-type males with ones which carry a lethal allele in their female offspring[144]. One of the first instances of RIDL use in mosquitoes was the creation of

female-specific flightless phenotypes of *Ae. aegypti*[145]. Fu et al. described their construct as effectively sterile, as the female mosquitoes cannot attract males due to the lack of flying ability[145]. Furthermore, Wise de Valez et al. found that target populations could be eliminated in 10-20 weeks by introducing the RIDL males into lab colonies, however cage size and colony longevity could have been an factor[146]. Researchers then examined the ability of the RIDL males to mate with wild-type females caught in the Grand Caymen in lab assays, before releasing the transgenic males into the environment[147,148]. This field trial found success, with a 10% ovitrap index, or the proportion of oviposition traps with one or more eggs in a week, when compared to the untreated areas which exhibited a 49% mean ovitrap index, suggesting that RIDL can significantly reduce wild *Ae. aegypti* populations[148]. Furthermore, RIDL was used to suppress wild *Ae. aegypti* populations in Brazil, and found that the release reduced the wild population by 80-95%[149]. In addition to RIDL, precision-guided sterile insect technique (pgSIT) is another genetic control mechanism in which mosquito strains are generated to pass along female killing genes using the CRISPR/Cas9 system, which use guide RNAs to precisely target Cas9-driven insertions and deletions in genes vital for spermatogenesis and fertility[150]. PgSIT has been utilized to suppress *Ae. aegypti* and *An. gambiae* populations in the lab[151,152]. Li et al. used pgSIT on *Ae. aegypti* Liverpool strain to assess the genetic load's dissemination through a caged population and modeled its ability to use the technique for mosquito control[152]. They found that the pgSIT technology could produce flightless females from the offspring of pgSIT males mated with normal females, which resulted in subsequent populations of mosquitoes with diminished survival, fertility, and blood feeding rates[152]. Furthermore, pgSIT was

developed for *An. gambiae* (G3 strain) in the lab and when targeting the *fle* gene, the result was all F1 females dying, indicating that this control mechanism maybe accessible for these two species[151]. A company named Oxitec Ldt. has released RIDL *Ae. aegypti* as a control tool for populations in Florida after an initial field test in Brazil[153,154].

Researchers have also developed mosquito control tools which use Wolbachia, an endosymbiont bacterium, to reduce the fitness and transmissibility of pathogens by *Aedes* and *Culex* populations. *Wolbachia,* can induce sterility in infected females and drive its transmission into subsequent generations through a phenomenon called cytoplasmic incompatibility[155]. This control methods involves introducing a *Wolbachia* strain that induces cytoplasmic incompatibility into mosquitoes in the lab and releasing infected males to mate with wild type females in the field. It was found that the *w*Mel strain significantly reduced the proportion of eggs hatching, suggesting that this strain could be a valuable mosquito control tool[155]. A field trial in Australia sought to use the *w*Alb, originally isolated from *Ae. albopictus*, to observe a reduction in areas which already contained wild type and *w*Mel infected mosquitoes[156]. It was found that the areas which all three types of mosquitoes resided saw an 80% reduction in the mosquito populations which extended past the trial period, suggesting that the release of multiple incompatible *Wolbachia* strains would be a valuable control technique[156]. In addition to inducing reduced fitness of *Ae. aegypti, w*Mel has exhibited the ability to inhibit ZIKV and DENV transmission from surviving mosquitoes, demonstrating not only mosquito control, but mosquito-borne virus control as well[155,157,158]. In addition to *Aedes* mosquitoes, *Wolbachia* cytoplasmic incompatibility has had success in *Culex*

quinquefasciatus[159–161]. However, in contrast to *Ae. aegypti* reduction in the dissemination of ZIKV and DENV, *w*AlbB infected *Cx. tarsalis* exhibited an increased in WNV dissemination, suggesting differing results depending mosquito and virus species tested[162]. While the use of genetic control strategies remains controversial, IR is an issue that needs to be addressed[163,164]. Insecticide based control strategies are changing, resulting in new chemistries and products that contain more than one mode of action.

New formulations of IRS, including combined AIs, are being tested to maintain IRS efficacy considering the rising IR issues. For example, in 2016, a mixture of clothianidin, a neonicotinoid which targets nicotinic acetylcholine receptors, and deltamethrin, a pyrethroid, was sprayed inside homes in southern Benin, which resulted in extended mosquito mortality when compared to deltamethrin alone[99]. While mosquito blood feeding rates remained constant, 12-months post application, the mosquito mortality in the sprayed homes with deltamethrin was over 30% and the mixture yielded a mortality of over 51% depending on the material the product was applied to, suggesting that the addition of clothianidin can assist pyrethroids in overcoming pyrethroid-resistance[99]. Another, a new product, named Pirikool® 300CS, is a pirimiphos-methyl organophosphate that exhibited mosquitocidal activity against pyrethroid-resistant *An. gambiae* s.l. in the lab and in Benin for up to 12 months post application[165]. When Actellic®300CS, another pirimiphos-methyl product, was used in Burkina Faso, they observed a significant decrease in mosquito survival when compared to DDT, pyrethroids and bendiocarb[113]. A new active ingredient called meta-diamide is the basis of a new IRS product named VECTRON™T500, that was tested in

Benin between 2019 and 2021 and indicated mosquitocidal activity up to 18 months in a wall cone bioassay, and indicate an increased mortality rate at 12 months when compared to Actellic®300CS at the same time point[166]. Finally, when VECTRON™T500 was examined in Burkina Faso, in addition to the strong killing effect, the insecticide reduced blood feeding rates in *An. gambiae* s.l. to 4.43% when compared to the control which had a blood feeding rate of 12.33%, and no adverse events were found when surveying the inhabitants of the house where VECTRON™T500 was applied, suggesting the meta-diamide is efficacious and well-tolerated[167].

Dual-chemistry ITNs contain at least two different insecticides, using two different modes of action to reduce the likelihood of resistance developing. There are a few products available now, one being the Interceptor®G2 (IG2®) net. The IG2® net contains a mixture of chlorfenapyr and alpha-cypermethrin and underwent phase II evaluations in Benin which involved examining the efficacy of the nets over their lifetime, including after being washed[168,169]. The wild *An. gambiae* s.l. population in Benin was examined for alpha-cypermethrin resistance using CDC bottle bioassays and WHO cylinder test and were compared to *An. gambiae* Kisumu strain, a pyrethroid susceptible stain[169]. It was found that compared to the lab strain, the lethal concentration where 50% of the mosquitoes would die (LC_{50}) was 200 fold higher in the resistant wild mosquitoes compared to the susceptible strain[169]. Despite this high insecticide resistance, testing of the nets in experimental hut trials demonstrated that the IG2® nets retained their blood feeding inhibition and exceeded 72-hour mortality effects against wild mosquitoes when compared to the first-generation Interceptor® nets containing only pyrethroid, even after 20 washes[169]. During the Repeat Ivermectin Mass

Drug Administration for MALaria Control II (RIMDAMAL II) phase 3 clinical trial, the IG2® nets were distributed to households in both the control and intervention arms of the trial in at the end of the first season of the trial where the wild *An. gambiae* s.l. populations in this region are known to be pyrethroid resistant[113,170]. It was found that the malaria incidence rates in both treatment and control arms were lower after the introduction of the IG2® nets, which was associated with > 50% reduction in the human biting rate and a reduction in the number of vector anophelines captured in 2020 (*n* =2115) compared to 2019 (*n* = 5827), including a near absence of *An. funestus* in 2020 despite similar rainfall and temperatures over the two trial years, as well as a >50% reduction in the survival rate of blood fed mosquitoes captured in the control arm houses from 2019 to 2020[170]. While these new chemistries and novel approaches of re-purposed chemistries are advancing the efficacy of our control tools, the intelligent management of these tools are necessary to ensure resistance development is kept at a minimum.

Integrated mosquito management (IMM) is a concept which brings together the community, government, and control professionals to reduce both vectors and nuisance biting mosquitoes[171]. These approaches aim to educate the public in their role in mosquito control, such as removing breeding sites from around homes and closing gaps to prevent mosquitoes from entering homes[172]. IMM's main goal is to reduce the use of insecticides until absolutely necessary to prevent human disease through the use of surveillance tools such as VI[171,172]. However, while IMM aims to reduce disease prevalence and incidence within the community, new control tools need to be investigated.

Endectocides are established drugs used in veterinary medicine and have wide use in human health[173–176]. Many of these drugs are systemic insecticides, or drugs that circulate systemically in treated animals which make the blood toxic to hematophagous insects without harming the host. Endectocides of the avermectin drug class are used regularly in human health for their ability to treat endoparasitic infections such as microfilariaemia with *Wuchereria bancrofti* and *Oncocera volvulis,* but are now being explored for their ability to kill mosquitoes and thus limit transmission of mosquito-borne diseases[177]. The drawback to these drugs, however, resides in the limited number of drugs approved for human use and that humans would be exposed to any transmitted pathogens as the mosquitoes need to feed on treated humans to be exposed.

Novel control techniques have their own advantages, such as overcoming IR using dual chemistry products, long-lasting in the case of ITNs, self-propagating by use of autodissemination, and eco-friendly by using naturally occurring predators. These control techniques also have their own issues whether it be costly to implement, community resistance such as releasing genetically modified organisms, or resistance developing if used without rotation. The use of endectocides, however, are unique among these control tools, as they are widely accepted by communities, resistance to target mosquitoes has not been characterized, and the use of them preferentially targets only hematophagous insects.

1.5 Exploring endectocides for mosquito control

Endectocides are drugs which are efficacious against endo- and ectoparasites. The most successful endectocide, ivermectin, was discovered by Satoshi Ōmura and William Campbell in 1973, and is derived from a fermentation byproduct of

Streptomyces avermectinius that was isolated from a soil sample collected near a golf course in Japan[175]. The avermectin and milbemycin macrocyclic lactone class of drugs exhibited broad spectrum activity against parasites and arthropods alike, opening up treatment options for both veterinary and human diseases of which few drugs existed previously. Endectocides work by targeting specific nerve channels in endo- and ectoparasites, some of which may be absent from humans and other vertebrate animals. Alternatively, neuronal channels in invertebrate neurons can be or are far more sensitive to the drug compared to those in vertebrates. These characteristics make endectocides an epidemiologically unique drug by having the ability to treat not only hematophagous ectoparasites, but filarial, round, and hookworm infections in the gastrointestinal tracts and circulatory system[178–182].

The most commonly used endectocidal drug come from several different chemical groups, the macrocyclic lactone milbemycins and avermectins and their semi –synthetic derivatives, the isoxazolines, the neonicotinoids, and the phenylpyrazoles. Avermectins, such as ivermectin (IVM), target the glutamate-gated chloride channels, responsible for signaling the relaxation pathways of muscles in mosquitoes. The drugs force the channel open, causing the mosquito to die by flaccid paralysis[178,179]. IVM was first studied for mosquito control as early as 1985 when MK-933 (IVM) in saline was subcutaneously injected into mice, and shown to be effective at killing *An. stephensi*, *Cx. pipiens*, and to a lesser degree *Ae. aegypti* that blood fed on the treated animals[183]. After several similar studies, IVM's efficacy on mosquitoes from the field was first observed by research groups using IVM for filariasis control, where they observed IVM-based mosquitocidal effects on mosquitoes like *An. punctulatus* that were captured in

the houses of treated people[184]. Isoxazoline-based drugs, such as fluralaner, act as gamma-aminobutyric acid (GABA) channel antagonists, forcing closure of the mosquito's GABA channels, which are responsible for inhibiting excitatory signals to the muscles, and causing the mosquito to die via rigid paralysis[185]. Additionally, phenylpyrazoles, such as fipronil, also target the GABA channels, however fipronil targets the same area of the GABA channel targeted by dieldrin, an organochlorine insecticide, and cross-resistance has been suggested in *An. stephensi*[186]. The cross-resistance issue of fipronil as well as safety concerns have so far limited phenylpyrazoles use as endectocides, and similar issues have been observed with isoxolazines like fluralaner, which has been linked to neurological toxicity in mammals. Neonicotinoids, such as imidacloprid, are nicotinic acetylcholine receptor agonists, causing paralysis in mosquitoes, leading to death[187]. These insecticides have exhibited safety in mammals, indicating selectivity for insect nicotinic receptors over mammalian ones[188]. Additionally, neonicotinoids, such as clothianidin, have been added to IRS chemistries to enhance their mosquitocidal properties[99]. On the other hand, IVM's approval and widespread use in human medicine for controlling diseases such as lymphatic filariasis, onchocerciasis and scabies, has facilitated its testing as a first-in-class endectocidal drug for targeting adult mosquitoes via their blood feeding habit to limit malaria and arbovirus transmission[177,189–191]. It may be expected that other developing endectocides could follow similar testing. A new isoxazoline, lotilaner, has recently been approved for the treatment of *Demodex* mite infestations in human eyelashes[174]. Lotilaner, then is a first-in-class human medication which has been

approved by the FDA, perhaps opening the door for mass drug administrations of the drug to control pathogens transmitted by mosquitoes or other blood feeding arthropods.

In addition to MDAs, researchers have developed novel applications of endectocides in forms other than systemic drugs. Tenywa et al described a novel application of IVM in an ATSB, targeting *An. arabiensis*, a mosquito which is a member of the *An. gambiae* s.l. complex[105]. They found that the ATSBs were more likely to attract mosquitoes if they were located outside, next to vegetation as opposed to inside a home, however, mosquitoes still visited the ATSBs inside when people were sleeping under a bed net[105]. The IVM concentration in the ATSB, 0.01%, was enough to illicit a 95% killing effect in wild type *An. arabiensis*[105]. In addition to the ATSBs, industry has developed both abamectin, an avermectin derivative, and an isoxazoline for use in ULV and IRS applications, respectively[192,193]. ReMoa-Tri® is a novel triple-action insecticide developed by Valent Bioscience containing abamectin, fenpropathrin, and a fatty acid, and applied via ULV spraying [192,194]. The application of this novel insecticide resulted in up to 100% mortality of pyrethroid-resistant *Cx. quinquefasciatus* Collier strain and 89.82% mortality of pyrethroid-resistant *Ae. aegypti* Collier strain after 24-hours post-application [192,195]. Syngenta also has recently released an isoxazoline-based product for use in IRS[193,196]. While little information has been shared, the company states it has submitted the product to the WHO Pre-qualification program[193]. Currently, IVM MDA is not approved for individuals who are pregnant, or breast feeding an infant younger than one week old, or children under 15kg. By utilizing the IRS or the ULV application of endectocides, those individuals would be protected. However, the continued use of endectocides without providing a rotation of products which contain active ingredients

with different modes of action could result in resistance developing within the population. But these distribution methods of endectocides can fill a gap where the traditional method of application, MDA, tends to fall short, however they also run the risk fostering resistance to critical drugs used in human and veterinary medicine. Importantly, researchers have identified a potential resistance mechanism to IVM in *An. gambiae* and mutations to the glutamate-gated chloride channel was described in *Pediculus humanus capitis* in Iran in 2025, bringing the question if IVM resistance development is a distant or current issue[197,198].

Currently, IVM-based endectocide approaches are being tested for their ability to lower malaria prevalence or incidence by targeting local *Anopheles* populations across Africa and southeast Asia to reduce parasite transmission[170,191,199–208]. Our current understanding of IVM effectiveness against *An. gambiae* has been well documented and studies show it is extremely susceptible to IVM concentrations easily achieved in the blood given typical dosing schedules, with a reported seven day LC_{50} as low as 3.4 ng/mL[204]. However, many of these studies relied on membrane feeding assays of mosquitoes with IVM dissolved in dimethylsulfoxide (DMSO) then added to blood, rather that feeding blood from treated patients[204,209–211]. With the promising PKPD results from the studies testing different IVM doses and feeding mosquitoes directly on participant blood, several clinical trials where initiated to elucidate MDA safety and efficacy for lowering malaria incidence or prevalence in treated communities[170,199,204–207].

The RIMDAMAL clinical trial was small, cluster-randomized control trial performed in villages of southwestern Burkina Faso. Foy et al observed a significant decrease in malaria incidence rates in the intervention arm when compared to the

control arm using repeated MDAs with a single 150-200μg/kg dose of IVM over the course of one rainy season. The intervention arm MDAs were repeated every 3 weeks for a total of 18 weeks, and the first MDA, which was given to both the intervention and control arm, was paired with albendazole, an anthelmintic drug[199]. [212,213].

In the IVERMAL clinic-based trial conducted in Kisumu, Kenya, a 300 or 600μg/kg dose of IVM for three days was paired with the standard three-day course of dihydroartemisinin-piperaquine (DHA-P). This was a combination treatment regimen for adult participants who were experiencing uncomplicated malaria with the primary goal of testing the safety and mosquitocidal properties over the three-day course while co-administered with malaria treatment[204,214]. Participants' whole blood was obtained at various time points up to 28-days post treatment, and *An. gambiae* (Kisumu strain) were offered the treated blood via standard membrane feeds[204]. Mosquitoes were observed every 24 hours post feed for 28 days and mortality was recorded to assess the mosquitocidal activity of the paired drug mixture[204]. Smit et al found that more non severe adverse events were associated with the 600μg/kg dose of IVM when compared to the placebo and the 300μg/kg dose, but mosquitocidal activity in the 600μg/kg was more pronounced using participants' blood obtained 14-days post-treatment than the 300μg/kg dose[204]. A pharmacokinetics model of the 300μg/kg for three days dosing procedure was then constructed, and further verified, which suggested the dose allowed for a longer IVM venous concentration than the traditional one-time 400μg/kg of IVM treatment[214,215].

Elements of the IVERMAL clinical trial were then used in The Gambiae in a field-based clinical trial dubbed MASSIV[205,216], which similarly used 300μg/kg IVM paired

with DHA-P but given to thousands of villagers to test the primary hypothesis that this MDA strategy could reduce malaria prevalence in the treated communities relative to controls[205]. Secondary entomology outcomes were to analyze the difference in *An. gambiae* parity rates and sporozoite rates between the control and intervention villages[205,216]. Investigators found there was a significant decrease of malaria prevalence in the intervention arm when compared to the control arm of the trial, but the control arm neither received IVM nor DHA-P, so it was not clear if the effect was due to the endectocide or the antimalarial drugs[205]. The sporozoite rates within *An. gambiae* s.l. were similar between arms, however the entomological inoculation rate was significantly lower in the intervention arm when compared to the control arm and the parity rate was unaffected in both arms, contrary to former studies[205,209,217,218]. It should be noted that field-based clinical trials such as RIMDAMAL and MASSIV provide more realistic results of an intervention as it is given in a community with few exclusions and limitations asked of the populace, but inherently have many confounders too, for example, the wild mosquitoes have access to any bloodmeal source in the community. Mosquitoes which were considered parous could have taken meals from animals or humans which did not get treatment, which would add parity bias to the population as IVM is known to have mosquitocidal effects, killing off mosquitoes which may have been nulliparous.

The Broad One Health Endectocide-based Malaria Intervention in Africa (BOHEMIA) was another field-based clinical trial aiming to treat both humans and livestock with IVM alone in both Mozambique and Kenya[206]. Currently, no outcomes have been published, however the primary objectives, inclusion, and exclusion criteria

have been reported[206]. Similarly, the MATAMAL field-based clinical trial aimed to reduce malaria prevalence in communities by combining the 300μg/kg for three-days IVM MDA dose with DHA-P MDA in islands of the Bijagos Archipeligo of Guinea-Bissau. Thus, this trial was similar to the MASSIV trial, but with the control arm receiving IVM MDA only, so it allowed for discernment of the effects of IVM MDA from the DHA-P MDA on the primary outcome. The main entomological outcome was *Anopheles* parity rates however, the entomological survey only occurred once during the clinical trial, occurring between one- to two-weeks after the last MDA[207]. This clinical trial found that combining IVM MDA to DHA-P MDA did not result in lowered malaria prevalence compared to IVM MDA alone[207]. Additionally, *Anopheles* parity was not significantly different between the treatment and control arms[207]. A major confounder of both the BOHEMIA and MATAMAL trials that likely influenced the results were the timing of each MDA, which were not tightly controlled between people and clusters in the arms in a limited space of days but rather took weeks to complete. This meant that many people in the same arm were treated early in each MDA round and many treated late in each round, and so relatively few people in each cluster and arm had maximum concentrations of drug in their bodies at any one time over each MDA, which limited the probability of a mosquito to ingest a lethal blood meal on any given day.

The RIMDAMAL II field-based clinical trial was the only phase III study that aimed to reduce malaria incidence rates, with a focus on children ten-years-old and younger. Furthermore, the trial was designed to integrate the 300μg/kg for three-days IVM MDA dosing strategy with government-led monthly SMC distributions to children 3-59 months[170,219]. In addition to the primary outcome, secondary outcomes including the

force of infection, mosquito anti-saliva antibody concentration in participants, mosquito population calendar age, and the pharmacokinetics and pharmacodynamics of human processed IVM[170,219]. Entomological collections occurred twice during each MDA period, seven- and 21-days post MDA, using both CDC light traps and aspiration of mosquitoes residing inside homes[170,219].

The trial found that the malaria incidence rates in children remained the same between both arms, however malaria incidence rates and mosquito captures in both arms were significantly reduced in year two when compared to year one[170]. The reduction in these numbers were likely due to the introduction and distribution of the IG2® bed nets in communities of both arms, which were developed to combat the rising IR found within *An. gambiae*[169,170]*.* Mosquito survivorship of fully engorged females captured via house aspiration was examined and it was found that the mosquitocidal activity of IVM waned after 21-days, contrasting to what was reported from the IVERMAL and MASSIV trials [170,204,216]. The RIMDAMAL II study additionally observed a novel concept in the mosquito-*Plasmodium* relationship whereby differences were observed in the type of *Plasmodium* species successfully developing in *An. gambiae* vs. *An. funestus*, a secondary vector in Burkina Faso[220]*.* In short, Lado et al found that *P. falciparum* was more prevalent in the salivary glands in *An. gambiae* s.l. populations while *P. ovale* was significantly more prevalent in *An. funestus,* despite that the midguts of both complexes had similar exposure to the same parasites in their bloomeals[220]*.* This suggests that the two mosquito species may have differential vector competence for different species of the parasite [220].

While IVM has been mainly investigated as a malaria control tool, our lab have also been researching its potential to control WNV transmission in the United States[221–223]. It was found that the LC_{50} of IVM dissolved in DMSO and then added blood for *Cx. tarsalis* was 49.94ng/mL, when compared to the 20ng/mL for *An. gambiae*, suggesting that while *Cx. tarsalis* are not as susceptible to IVM as *An. gambiae,* this concentration is in the range that may be achieved with safe treatment doses for avian hosts which are the primary blood sources for this species[204,223]. When *Cx. tarsalis* was fed on chickens which had consumed 200mg/kg of IVM in their feed, mosquito mortality reached 95%, with no adverse effects noted for the chickens[223]. This trend was replicated when the mosquitoes were directly fed on wild caught Eurasian Collared Doves which also had consumed the 200mg/kg of IVM in feed, suggesting that the treatment of wild birds of IVM may be possible to lower WNV transmission rates[223]. A model was then created which indicated that IVM-treated birdseed in feeders may be able reduce WNV transmission during the season if certain parameters of coverage and mosquito killing are met, thereby reducing the human infections[222]. With these data, our lab paired with colleagues at University of California – Davis and have initiated field trials of IVM coated birdseed with the primary objective of lowering the WNV vector index around households where IVM-treated birdseed is supplied throughout the mid to late summer weeks in bird feeders. Several entomological outcomes are being assessed in this trial, including measures of *Cx. tarsalis* age using a novel mosquito population age-grading technique.

1.6 Mosquito population age-grading

A mosquito's age directly influences the probability of its ability to be infectious due to the EIP of mosquito-borne pathogens. As stated previously, the EIP is a range that is different for every pathogen and mosquito species but is governed by the time a pathogen needs to either escape from or mature in the mosquito midgut and then invade the salivary glands where it can be transmitted via the saliva upon a subsequent bite from the mosquito. Thus, the older a mosquito is, the higher the risk is for its ability to transmit a pathogen, should it be infected to begin with. In 1912, Perry observed that *Anopheles* which had more wing wear were more likely to have sporozoites within their salivary glands[224]. This discovery started the idea of simple age-grading of mosquitoes to quantify pathogen transmission risk by placing the mosquitoes into morphological bins estimating their age[224]. Perry's method however fell out of favor, in lieu of the technique first described by Detinova for measuring mosquito parity rates by characterizing the state of the tracheoles on ovarioles of each ovary, which are tightly coiled if the mosquito has never produced a batch of eggs or uncoiled and extended, indicating she has likely blood fed and undergone at least one gonotrophic cycle[225]. This method, however, is qualitative, only placing mosquitoes into parous or nulliparous states, and so does not allow for accurate estimations of a mosquito's calendar age nor the infectiousness of the mosquito population. It is also highly technical, requiring the user to dissect ovaries and observe them under magnification. The qualitative nature of the Dentinova technique was somewhat mitigated by the Polovodova technique, which can determine the number of previous gonotrophic cycles by counting dilatations, or the number of egg sac stage relics, on the ovarioles[226]. However, this method is even more

technical and time consuming to perform. Additionally, these methods cannot be used on some mosquito species as they can be autogenous, having the ability to produce a clutch of eggs without imbibing a blood meal[49,51]. Thus, novel, quantitative age-grading techniques are needed to better understand mosquito population age dynamics.

In 1986, a novel method of age-grading insects was described by analyzing the accumulation of pteridines on *Stomoxys calcitrans*[227]. It was found that this method may be useful in age-grading *An. gambiae* and *An. stephensi*, however, it was found that pteridine fluorescence levels in *Ae. polynesiensis* and *Cx. quinquefasciatus* were below the level of quantification when using a spectrofluorometer[228,229]. In lieu of the pteridine method, researchers started to evaluate the use of cuticular hydrocarbons via gas chromatography[230,231]. Cuticular hydrocarbons are responsible for preventing water loss and they could be associated with an increase in age[232]. This method was able to predict age of *Aedes* mosquitoes up to 15 days, after which the robustness of the method faltered[230,231]. However such biochemical analysis methods are not practical for age grading mosquito populations due to their high cost per sample or lack of sensitivity[54].

With the advent of reverse transcription quantitative PCR (RT-qPCR), genomic age-grading techniques have also been explored[233–235]. Cook et al. observed an age-related increase in gene expression in *Sarcoplasmic calcium binding protein 1* (*SCP-1*) in lab reared *Ae. aegypti* Cairns strain, and then tested wild, field collected eggs that were allowed to hatch then held in outdoor mesocosms where mosquitoes were collected every four days[233]. It was found that by combining the quantification of transcripts of the *SCP-1* gene with three others, wild *Ae. aegypti* age interpolations

could occur up to 20 days[233]. It was found that ambient temperature, however, can influence transcription of the *SCP-1* gene, suggesting that environmental factors will lead to inaccurate interpolation of wild mosquitoes unless a model was developed at the same temperature ranges that wild mosquitoes experienced[234]. It was then proposed to use a season-specific model to circumvent the ambient temperature issues[236]. However, current models could shift due to local climates and a model would need to be developed for every climate, and species-specific models where mosquito populations are located. This, plus the cost of RNA extractions and molecular testing per mosquito could be an expensive and impractical solution for end users such as mosquito control districts who would need to reevaluate their model every few years.

Since biochemical and genomic approaches to mosquito age-grading have fallen out of favor, researchers have started to investigate using near-infrared (NIRS) and mid-infrared (MIRS) spectroscopy as rapid chemometric methods for age-grading[237–240]. NIRS was found to accurately estimate if *An. arabiensis (89%)* and *An. gambiae* (78%) were less than seven or greater than seven days old while wild *An. gambiae* s.l. could be predicted with 90% accuracy, however this method showed a high individual mosquito error[238]. Additionally, Liebman et al. found that larval and adult diets in *Ae. aegypti* influenced NIRS output, suggesting that a developed model may only be useful for one breeding site due to changes in larval food type and availability[241]. Nonetheless, researchers are attempting to refine their models using machine learning methods to provide an unbiased estimate of the NIRS and MIR output[239]. as well as be a tool for rapid speciation of the scanned mosquitoes[240,242]. One MIRS study found that *Ae. aegypti* could accurately (95-97%) be placed into two and ten day old bins, however the

researchers only examined mosquitoes which were two and ten days old, possibly introducing bias into their study, but this provided proof of concept[240]. Interestingly another group investigated MIRS' ability to speciate *An. gambiae* s.s, and *An. arabiensis*, both of which belong to the *An. gambiae* s.l. complex due to being morphologically identical[242]. They found that MIRS could accurately speciate *An. gambiae* s.s. and *An. arabiensis* 76.8 and 76.6% of the time, respectively[242]. However, when using MIRS to interpolate age, it was found that the method was only accurate at describing young (one day) and old (15 day) mosquitoes, but the models were not accurate when describing the intermediate ages[242]. While NIRS and MIRS are promising methods, it has been shown that they can be skewed depending on mosquito age and diet[241,242]. Additionally, chemometric based age-grading method outputs are currently binary, placing mosquitoes into young or old categories, which will result in potentially infectious mosquitoes being missed. To re-simplify this field, we envision a reimagining of Perry's method of analyzing wing wear so that it could have the potential to rapidly and better interpolate mosquito population age for assessing mosquito borne disease risk for researchers and mosquito control districts.

To this end, Gray et al first quantified Perry's qualitative method of identifying older mosquitoes based on wing wear by taking wing micrographs from different-aged adult female *An. gambiae* and counting the long wing scales remaining on the wing fringe[243]. These initial experiments were conducted on mosquitoes of known age, and it was found that the long wing scale loss was associated with age and mosquito populations. Furthermore, the technique could distinguish age groupings of mosquitoes better than parity analysis and was able to distinguish continuously maintained lab

populations that were fed a sublethal dose of IVM compared to untreated controls. The treated population had more of these long wing scales than the control mosquito population, suggesting that the IVM treated population was younger than the control population[243]. Nonetheless, the method of human counting wing scales on many wing photos was tedious and human-error prone, so we investigated computer vision algorithms to better perform this method. The most accurate algorithm analyzed the pixels on each wing photo and gave each pixel an intensity value from black to white. As the mosquito flies during aging, the dark scales relative to the clear wing are lost and the summary score of the wing picture pixel intensity become whiter. By analyzing the pixel intensity values, models were able to accurately predict a pixel intensity cut off in which an individual mosquito could be above or below the known malaria EIP, approximately ten days[243].

1.7 Summary

This chapter reviews the transmission of mosquito borne disease, while focusing on malaria transmission in West Africa and WNV transmission in the US, key epidemiological methods on mosquito-borne disease transmission, mosquito surveillance methods, mosquito control techniques and their evolution amidst rising IR issues, and how age-grading can enhance mosquito surveillance and mosquito-borne pathogen transmission.

However, the current literature is lacking in understanding of the mosquitocidal properties of only human processed IVM. The IVERMAL, MASSIV, and MATAMAL clinical trials paired IVM with DHA-P. While IVERMAL measured their entomological outcomes with mosquito mortality, they did so in the presence of DHA-P. Additionally,

the MASSIV and MATAMAL trial measured their entomological impacts in the form of parity, not mosquito mortality, and IVM has been reported to reduce parity in *An. gambiae* s.l.[244].

The field is also lacking in the development of a consistent, high-throughput, and simple age-grading tool which can be used by researchers and mosquito control experts alike. Current age-grading techniques can only accurately distinguish between old and young mosquitoes, which resemble the Detinova parity method. New methods are being examined which pair machine learning techniques with MIRS, resulting in exceptional accuracy, however, these methods would leave out those who do not have access spectrometers or advanced processing systems[245].

Understanding the pharmacodynamics of human processed IVM, without DHA-P, is necessary to understand if the endectocide treatment is a valid control method, which could result in a novel approach to mosquito control. Furthermore, while Perry's method of wing degradation was a qualitative approach, identifying wing degradation and wing scale loss over time would be a quantitative approach to develop a novel age-grading method, which would be accessible to mosquito control experts and academics alike. These areas of research will broaden our knowledge of mosquito control efforts, in both the development of novel control tools and the development of better ways to interpolate the age of wild mosquitoes.

CHAPTER 2: PHARMACOKINETICS AND FEEDING EFFECTS OF HUMAN PROCESSED IVERMECTIN ON *ANOPHELES GAMBIAE* G3

2.1 Introduction

The global burden of malaria in 2023 was estimated to be 263 million infections and 597,000 deaths, with most cases and deaths occurring in sub-Saharan Africa[31]. The predominant vectors within the continent are the *Anopheles gambiae* complex, *An. funestus,* and the invasive *An. stephensi*[8,246,247]*.* Current "gold-standard" control methods rely on indoor residual spraying (IRS) of pyrethroids, while simultaneously using insecticide treated bed nets (ITNs), preventing an estimated 663 million cases between 2000 and 2015[168,248–252]. However extended use of these methods over the last 25 years has resulted in insecticide resistance and population behavior changes, such as altered feeding locations and time, whereby many vector populations have shifted their blood feeding to outside of the home or during crepuscular periods when individuals are not sleeping[115,124,253,254]. To counter insecticide resistance (IR), new IRS and ITN chemistries have been developed, as well as new formulations with combinations of two different insecticides with different modes of actions or insecticide paired with a synergist. The development and implementation of dual chemistry ITNs, using two different active ingredients with different modes of action has been proven to be effective in affecting IR mosquito populations and reducing malaria infection rates in many situations[169,249–251]. For new IRS chemistries, some applications have had a positive effect while others have resulted in the rise of transmission by resistant populations. For example, when new IRS chemistries based on clothianidin were used

in southeast Uganda following years of using organophosphate-based IRS, the region experienced a dramatic rebound of malaria due to clothianidin-resistant *An. funestus*[255,256]. Given the uncertainty of success of simply using older control tools with new formulations, entire new control mechanisms need to be developed and researched to maintain or improve current malaria control efforts.

Endectocides such as avermectins and isoxazolines could be one of these new control mechanisms. These are mosquitocidal drugs that can be administered safely to animals and humans and are directly ingested by mosquitoes during blood feeding on the treated host, so they do not rely on contact and absorption through the cuticle. Endectocides also can have different targets or modes of action from current approved insecticides used for IRS and on ITNs, so they may be able to circumvent insecticide resistance issues the region faces[178,191,257]. Ivermectin (IVM), an avermectin derivative, is the primary anthelmintic drug used to control filarial worms in humans and has been shown to be particularly efficacious against anophelines[201]. IVM exhibits mosquitocidal effects in the range of nanograms per milliliter of blood ingested, while also reducing fecundity and blood feeding frequency of mosquitoes that imbibe a sublethal dose[210,258,259]. Furthermore, IVM has been utilized for decades in mass drug administrations (MDAs) as an antihelminth drug for many of the same rural African populations that are also afflicted with malaria, and so is known and accepted by the these communities as a drug that benefits their health[260,261]. For these reasons, IVM is being studied as the first-in-class endectocidal drug for malaria control[261].

Initially, *in vitro* studies relied on dissolving powdered IVM into dimethylsulfoxide, mixing it into blood, then offering the drug and blood mixture to mosquitoes using

artificial blood feeding devices[262,263]. These studies indicated that IVM was a valuable candidate for mosquito control and subsequently moved from *in vitro* to *in vivo* studies, first with treated animals and then with treated humans, such as the IVERMAL trial which demonstrated human processed IVM is as or more effective as the in vitro studies[264,265]. Recently, clinical trials of differing designs have been conducted across Africa to elucidate the effectiveness of IVM on a population-level scale. These studies include IVM plus an antimalarial treatment (MASSIV), IVM coupled with seasonal malaria chemoprevention distributions to children (RIMDAMAL II), and IVM treatment of both humans and livestock (BOHEMIA),[170,199,206,216].

IVM has a relatively short half-life in human plasma post-treatment, thus modifications to the dosing or formulation are necessary to increase the duration of the drug or its mosquitocidal metabolites within the blood of treated individuals so that the mosquitocidal effect is long-lasting and might have maximum efficacy against the population of biting mosquitoes. In 2020, Slater et al. modeled the difference between a dosing regimen of one 400 μg/kg treatment and 300 μg/kg per day for three days from data collected in the IVERMAL trial and found that the 300 μg/kg taken sequentially for three days would retain its mosquitocidal effects for up to 28 days[215]. This dosing regimen was utilized for the RIMDAMAL II clinical trial, which had a primary outcome of lowering the malaria incidence rates within children[170]. In the RIMDAMAL II trial, 14 clusters (villages) in southwestern Burkina Faso were recruited, randomized, and allocated into two arms (placebo and intervention). The trial was conducted during sequential wet seasons (from July to November) in 2019 and 2020 where four MDAs were administered each season (eight total MDAs). Entomological testing occurred in

six of the 14 villages. During the final MDA period in 2020, 178 participants from six villages (three placebo; three intervention) were recruited for serial plasma collection before, during, and after the MDA took place on days 0, 2, 4, 7, 14, and 28. The goal of these plasma collections was to understand population-level differences in the pharmacokinetics of IVM in study participants, and compare it to the pharmacodynamics of the drug on mosquitoes. For this latter goal, we fed lab-reared *An. gambiae* (G3 strain) mosquitoes participant plasma mixed with red blood cells via artificial membrane feeders.

2.2 Results

2.2.1 Pharmacodynamics of ivermectin from RIMDAMAL II participants on An. gambiae

Our first experiments were designed to discern mosquito survival for 15 days following ingestion of plasma collected from 9 different participants across all time periods. Grouping all participant data together by time periods, *An. gambiae* (G3 strain) mosquitoes which fed on bloodmeals containing participant plasma exhibited significant mortality relative to controls when fed on plasma collected at 2-, 4-, and 7-days post IVM treatment. By day 11, all mosquitoes (n=269) which imbibed the day-2 plasma died, with the most pronounced effect occurring by day 3 where only 5.2% (14/269) were still alive. Additionally, mosquitoes which fed on plasma collected on days 4 and 7 exhibited survival rates of 18.7% (52/278) and 43.1% (175/406) by day 3 and 6.5% (18/278) and 3.9% (16/406) survival rates by day 15, respectively (Figure 2.1). Finally, mosquitoes which fed on plasma collected on days 14, and 28 had 3-day survival rates of 73.9%

(193/261) and 83.1% (256/308) and 15-day survival rates of 22.6% (59/261) and 18.5% (57/308) respectively (Table 2.1, Figure 2.1).

Table 2.1: Mosquito survival on day 3 and 15 post-bloodmeal		
Plasma	**Day 3 survival %**	**Day 15 survival %**
Placebo[1]	76.3 (316/414)	17.4 (72/414)
D0	87.5 (259/296)	34.1 (101/296)
D2	5.2 (14/269)	0 (0/269)
D4	18.7 (52/278)	6.5 (18/278)
D7	43.1 (175/406)	3.9 (16/406)
D14	73.9 (193/261)	22.6 (59/261)
D28	83.1 (256/308)	18.5 (57/308)
[1]Placebo participants' (n=9) D0 plasma was tested alongside plasma from intervention arm participants. One placebo participant was examined per intervention participant, which was age and sex matched.		

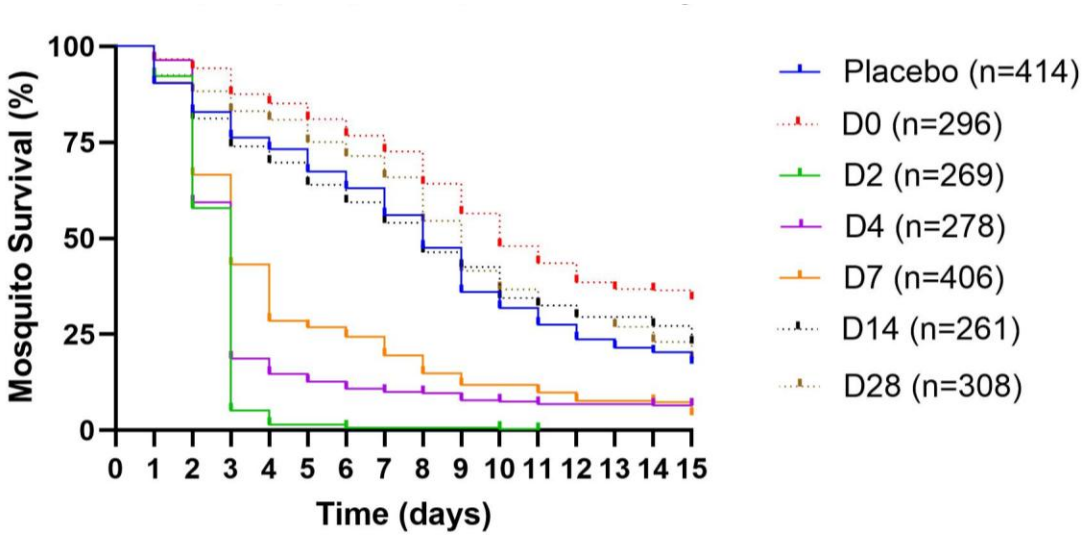

Figure 2.1: Mosquito survival over time after consumption of IVM in blood plasma. Mosquito mortality of all participants (n = 9) of the IVM MDAs. Placebo participants (*n* = 9) were those given placebo IVM MDA and plasma was collected on day 0.

When compared to the placebo arm controls, there was a modestly higher, but significant, mosquito survivorship when mosquitoes fed on plasma obtained from participants on days 0 and 28, but a significant decrease in survivorship from feeding on

plasma collected on days 2, 4, and 7, with day 14 timepoint showing no significant difference at 15 days (Table 2.2). However, when comparing the treatment arm controls (day 0) to all other treatment times, there was a significant decrease in mosquito survivorship at 15 days (Table 2.2).

We then conducted an analysis of mosquito hazard ratios (HR) from groups that imbibed participant plasma collected at the set timepoints post-IVM treatment relative to plasma taken from the participants prior to ingesting the first treatment (Figure 2.2). The highest HR was observed at 2-days post-IVM treatment (HR = 13.17 [95% CI: 10.1-17.17]). HRs on day 4 (HR = 4.88 [95% CI: 3.88-6.15]) and day 7 (HR = 3.12 [95% CI: 2.59-3.75]) continued to show a strong mortality effect of the drug from participant plasma. Participant plasma obtained on days 14 (HR = 1.40 [95% CI: 1.14-1.72]) and 28 (HR = 1.45 [95% CI: 1.07-1.36]) post-treatment showed a very modest but significant mosquitocidal effect from the remaining drug in participants' plasma (Table 2.2)

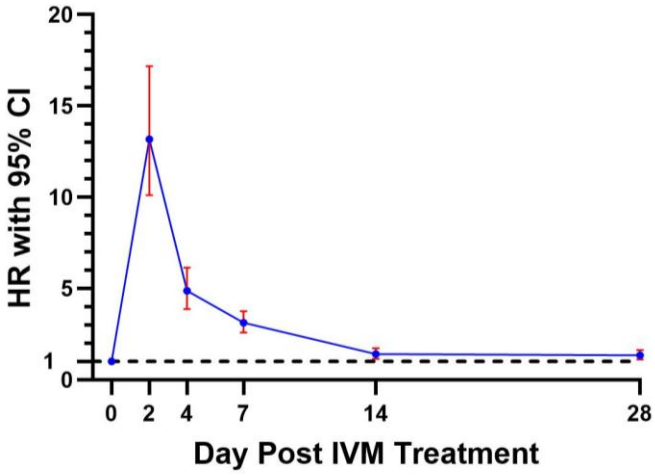

Figure 2.2: Blood Plasma Hazard Ratio. Mosquitoes which fed on blood plasma post IVM treatment in relation to mosquitoes which fed on plasma collected prior to IVM treatment. HR w/95% CI were calculated using Mantel-Haenszel.

Table 2.2: Mosquito survival curve comparisons.						
Comparison	***p-value***	**Change[1]**		**Comparison**	***p-value***	**Change[1]**
Placebo vs D0	<0.0001	Increased				
Placebo vs D2	<0.0001	Decreased		D0 vs D2	<0.0001	Decreased
Placebo vs D4	<0.0001	Decreased		D0 vs D4	<0.0001	Decreased
Placebo vs D7	<0.0001	Decreased		D0 vs D7	<0.0001	Decreased
Placebo vs D14	0.4696	None		D0 vs D14	<0.0001	Decreased
Placebo vs D28	0.0205	Increased		D0 vs D28	<0.0001	Decreased
(DX = Day); Gehan-Breslow-Wilcoxon test used to analyze survival curves; [1]The relationship between the survivorship of DX relative to D0						

2.2.2 Pharmacodynamic differences between participant sex and age

Mosquito survival was then grouped by participant sex and age brackets (5-10, 10-18, and ≥ 19) to identify if these demographic strata altered the pharmacodynamics of IVM.

Female participants' plasma collected up to 7 days post-treatment caused significant mosquitocidal activity over 15 days after the bloodmeal when compared to female participants' plasma taken at day 0, before the intervention occurred (table 2.3). The most pronounced effects of the drug on the mosquitoes occurred 3 days after the blood-meal with a survival rate of 5.4% (8/149) for mosquitoes which fed on plasma collected 2-days post-treatment. Mosquito survival rates 3 days post bloodmeal from female participants' plasma collected on days 4 and 7 were 24.2% (43/178) and 39.8% (117/294), respectively (figure 2.3A).

Male participants' plasma exhibited significant mosquitocidal activity for all time points which plasma was drawn when compared to male participants' plasma taken at day 0 (Table 2.3B). The most pronounced effect on mosquito survivability occurred three

days post-bloodmeal when mosquitoes fed upon plasma collected on days 2, 4, and 7 post-treatment, with 5.0% (6/120), 9.0% (9/100) and 51.8% (58/112) survival, respectively (Figure 2.3B).

Table 2.3: Sex differences of participants' plasma on mosquito survivorship

	Male[1]		Female[2]	
Comparison	***p-value***	**Change[3]**	***p-value***	**Change[3]**
D0 vs D2	<0.0001	Decreased	<0.0001	Decreased
D0 vs D4	<0.0001	Decreased	<0.0001	Decreased
D0 vs D7	<0.0001	Decreased	<0.0001	Decreased
D0 vs D14	<0.0001	Decreased	0.1824	None
D0 vs D28	<0.0001	Decreased	0.4125	None

[1] *n = 4;* [2] *n = 5;* [3]The relationship between the survivorship of DX relative to D0

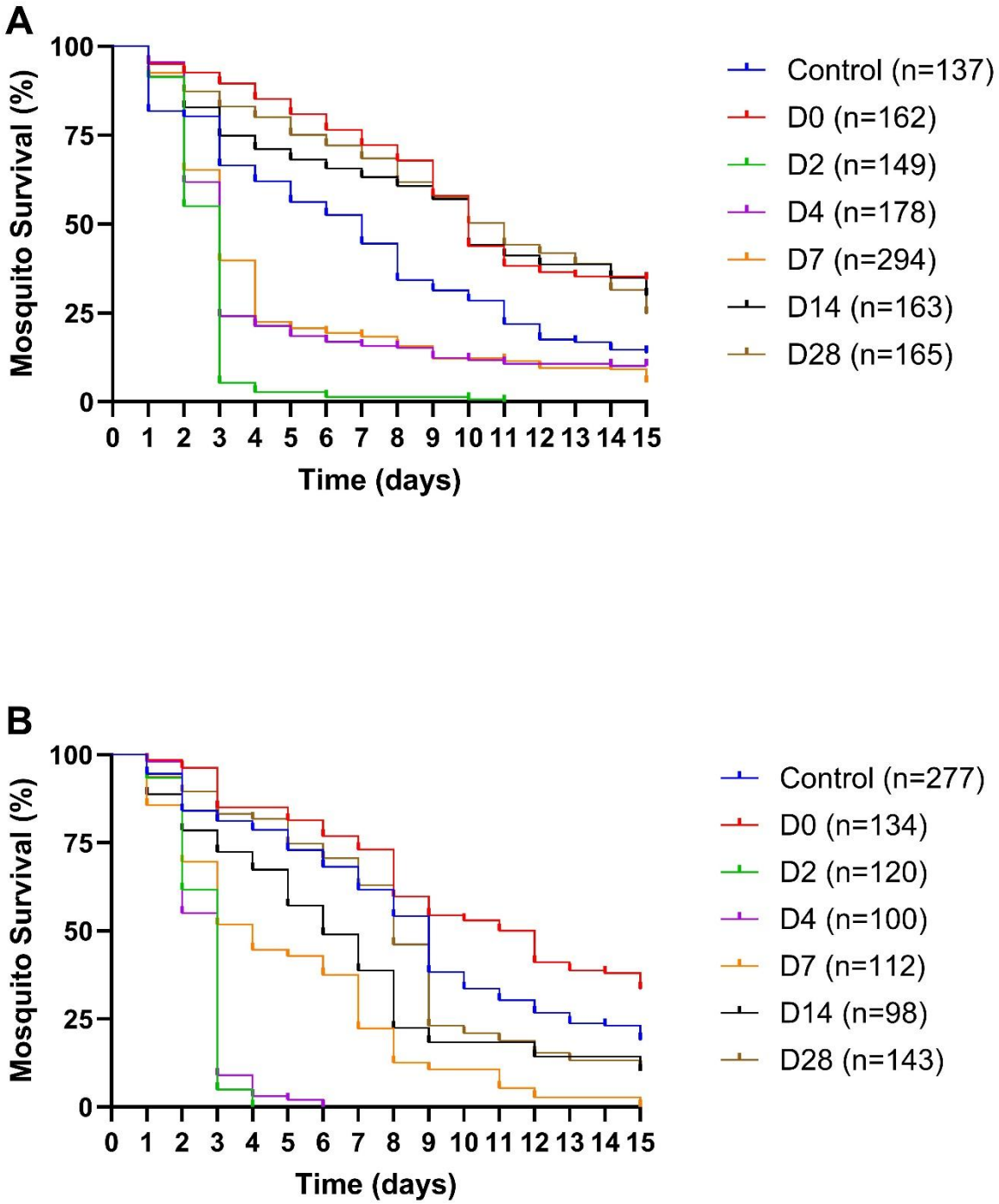

Figure 2.3: Mosquito survival stratified by participant sex. (A) Plasma from participants who are biologically female (*n* = 5). (B) Plasma from participants biological males (*n* = 4).

We then analyzed mosquito survivorship based on plasma from participants grouped in age brackets (5-10, 10-18, and ≥ 19) regardless of sex and identified a significant decrease in mosquito survival in all comparisons against plasma drawn on day 0 except for 5–10-year-olds' plasma from day 14 post-treatment and ≥19-year-olds' plasma from day 28 post-treatment (Table 2.4). Similar with all other analyses, mosquitoes which fed on plasma obtained 2 days post-treatment were associated with the most noticeable decrease in survival rates in all age groups, 10.9% (10/92) for 5-10-year-olds, 2.4% (3/127) for 11-18-year-olds, and 3.8% (3/78) for ≥19-year-olds (Figure 2.4).

Table 2.4: Age differences of participants' plasma on mosquito survivorship

	5-10[1]		**11-18[2]**		**≥19[3]**	
Comparison	*p-value*	Change[4]	*p-value*	Change	*p-value*	Change
D0 vs D2	<0.0001	Decreased	<0.0001	Decreased	<0.0001	Decreased
D0 vs D4	<0.0001	Decreased	<0.0001	Decreased	<0.0001	Decreased
D0 vs D7	0.0207	Decreased	<0.0001	Decreased	<0.0001	Decreased
D0 vs D14	0.6592	None	<0.0001	Decreased	<0.0001	Decreased
D0 vs D28	0.0057	Decreased	<0.0001	Decreased	0.1569	None

[1] *n = 3;* [2] *n = 2;* [3] *n = 4;* [4]The relationship between the survivorship of DX relative to D0

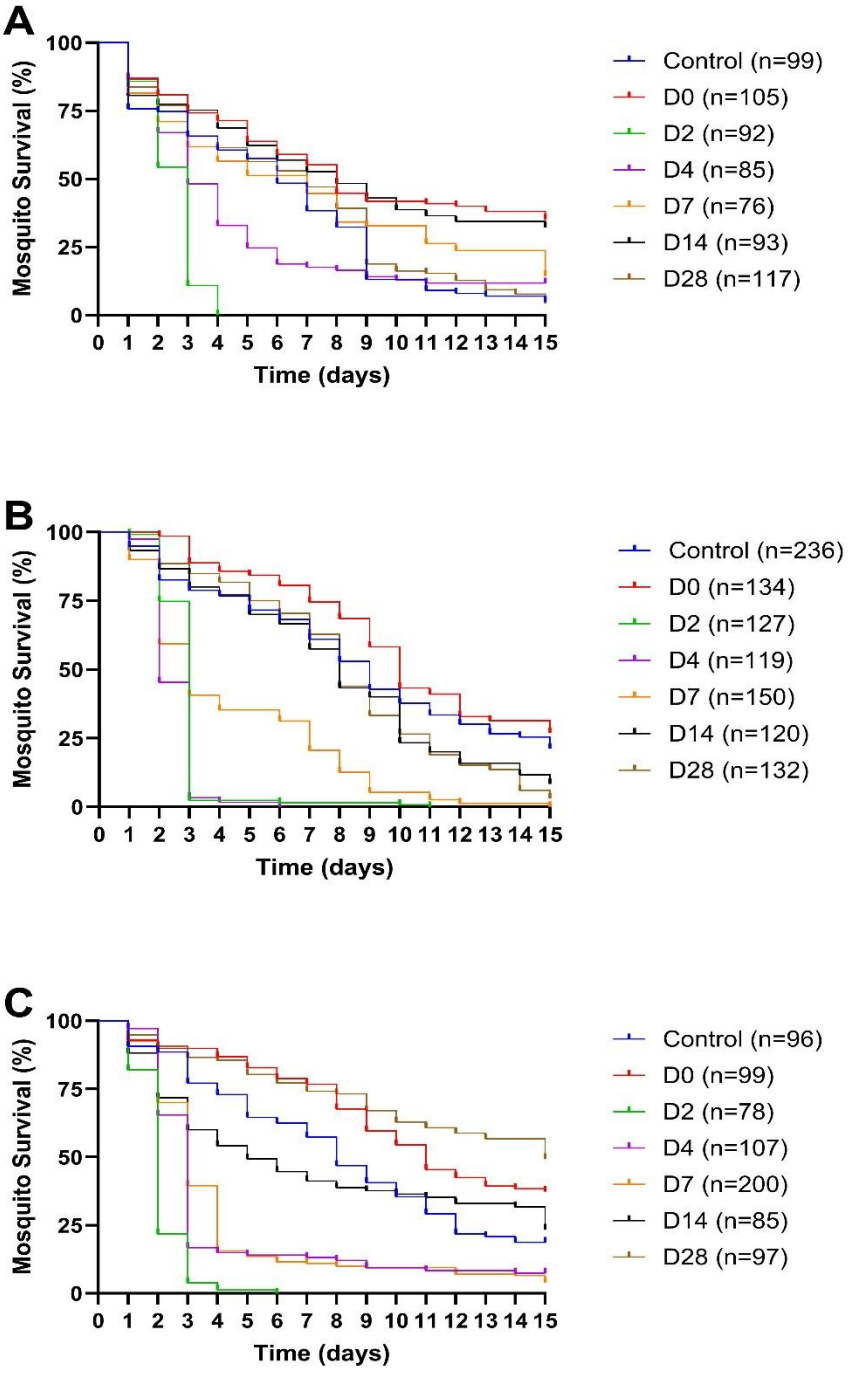

Figure 2.4: Mosquito survival stratified by participant age. (A) Participants who were between the ages of 5-10 (*n* = 3). (B) Participants between the ages of 11 and 18 (*n* = 2). (C) Participants 19 and older (*n* = 4).

2.2.3 Comparisons of pharmacokinetics and pharmacodynamics

Analysis of mosquito survival figures over time showed a trend where mosquitocidal activity shifted with participant age. With participants who were 5-10 years old, we observed mosquitocidal activity from their plasma only through day 4 post-treatment. However, with participants who were 11-18 years old, mosquitocidal activity from their plasma was maintained through day 7 post-treatment and among participants ≥ 19 years old, mosquitocidal activity was maintained through day 14 (Figure 2.4). To better understand this relationship, we investigated the participants' IVM pharmacokinetics. All participants' plasma tested had a venous IVM concentration that elicited a mosquitocidal effect on *An. gambiae* which fed on the plasma obtained on days 2 and 4 (Table 2.5). It was observed that IVM concentrations in plasma obtained on day 7 started to wane when the tested participants were between the ages of 5-18, yet levels still provided an observable effect (Table 2.5). However, venous IVM levels in plasma were below the limit of quantification (BLQ) (0.400 ng/mL) using liquid chromatography tandem mass spectrometry at 14 days post-treatment in participants in the 5–18-year-old bracket (Table 2.5). Furthermore, if the participant was ≥ 19 years old, IVM could be detected at least to day 14 and had a range of 1.361-15.899 ng/mL (Table 2.5). It was found that except for 2 adult participants, venous IVM plasma concentrations were BLQ by day 28.

Table 2.5: Tested participants venous ivermectin plasma concentration.							
Sex	**Age**	**Day 0 PK (ng/mL)**	**Day 2 PK (ng/mL)**	**Day 4 PK (ng/mL)**	**Day 7 PK (ng/mL)**	**Day 14 PK (ng/mL)**	**Day 28 PK (ng/mL)**
F	7	BLQ	78.124	8.831	1.902	BLQ	BLQ
F	13	NA	8.084	39.867	16.367	BLQ	BLQ
F	31	NA	172.297	27.083	174.843	9.372	BLQ
F	41	0.467	78.012	31.637	17.127	4.147	0.455
F	59	BLQ	96.822	13.009	7.084	1.361	BLQ
M	6	BLQ	37.155	5.566	1.159	BLQ	BLQ
M	7	NA	44.887	7.345	2.133	BLQ	BLQ
M	18	NA	60.770	18.358	3.283	BLQ	BLQ
M	29	BLQ	277.73	118.285	75.303	15.899	1.251
n = 9; (NA = Not Assayed, BLQ = Below the Limit of Quantification)							

While comparing pharmacokinetics to pharmacodynamics using a mixed effects Cox proportional hazards model, it was determined that IVM blood concentration was a significant predictor of mosquito mortality. For every 1ng/mL increase in venous IVM concentration, the hazard ratio increased by 1.02 ([95% CI: 1.01-1.02], $p < 0.0001$). Additionally, it was found that as the age of the participant increased, there was a significant decrease in mosquito survivability ([HR: 0.993, 95% CI: 990-.996] p < 0.0001). Finally, when mosquitoes fed on male participants with a detectable IVM concentration, the mosquitoes had a higher rate of survival than mosquitoes which fed on female participants that had similar concentrations of venous IVM ([HR: 0.999, 95% CI: 0.995-0.999], $p = 0.0068$).

In further analyses, we conducted one-phase decay models since following the C_{max} after the last dose is administered, IVM follows a 1st order pharmacokinetics model, identifying the half-life of venous IVM concentrations within our tested population with respect to both sex and age strata. We identified trends which correlate to what the

mixed effects model identified. Males venous IVM concentrations have a half-life of 1.6 while female's half-life is 2.9, suggesting that females retain IVM concentrations in their plasma for a longer period (Figure 2.5). Furthermore, when partitioning participants by age backet, the half-life of IVM concentrations was 0.7 days, 3.2 days, and 2.6 days in 5-10-year-old, 11–18-year-old, and ≥ 19 olds, respectively (Figure 2.6). However, it should be noted that three of the four participants tested in the ≥ 19 age bracket were female, which could have influenced the trend.

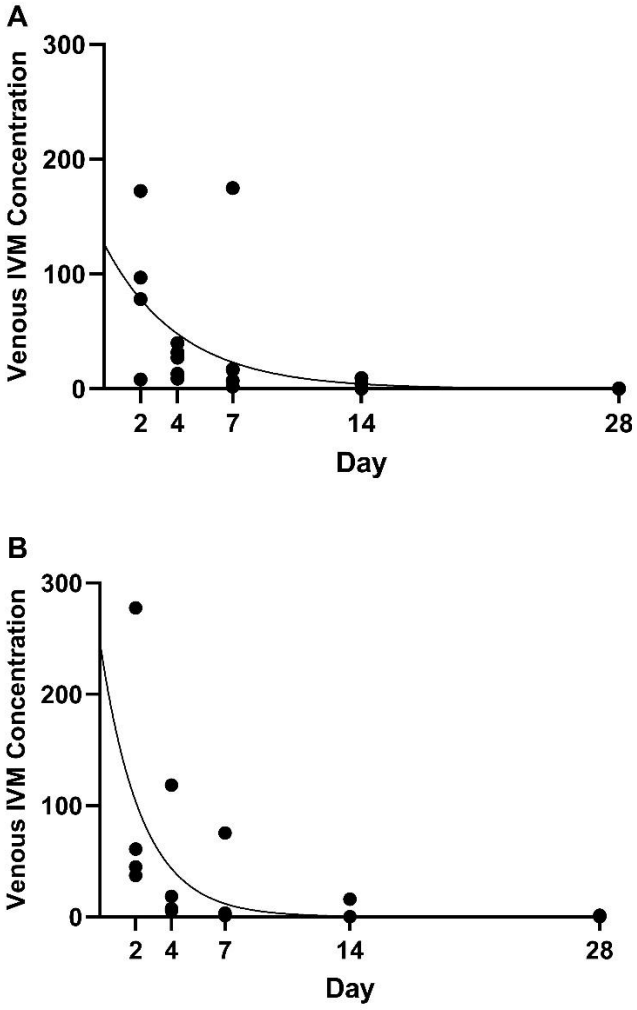

Figure 2.5: One phase decay model of IVM in participants stratified by sex. (A) Female participants IVM half-life (*n* = 5). (B) Male participants IVM half-life (*n* = 4).

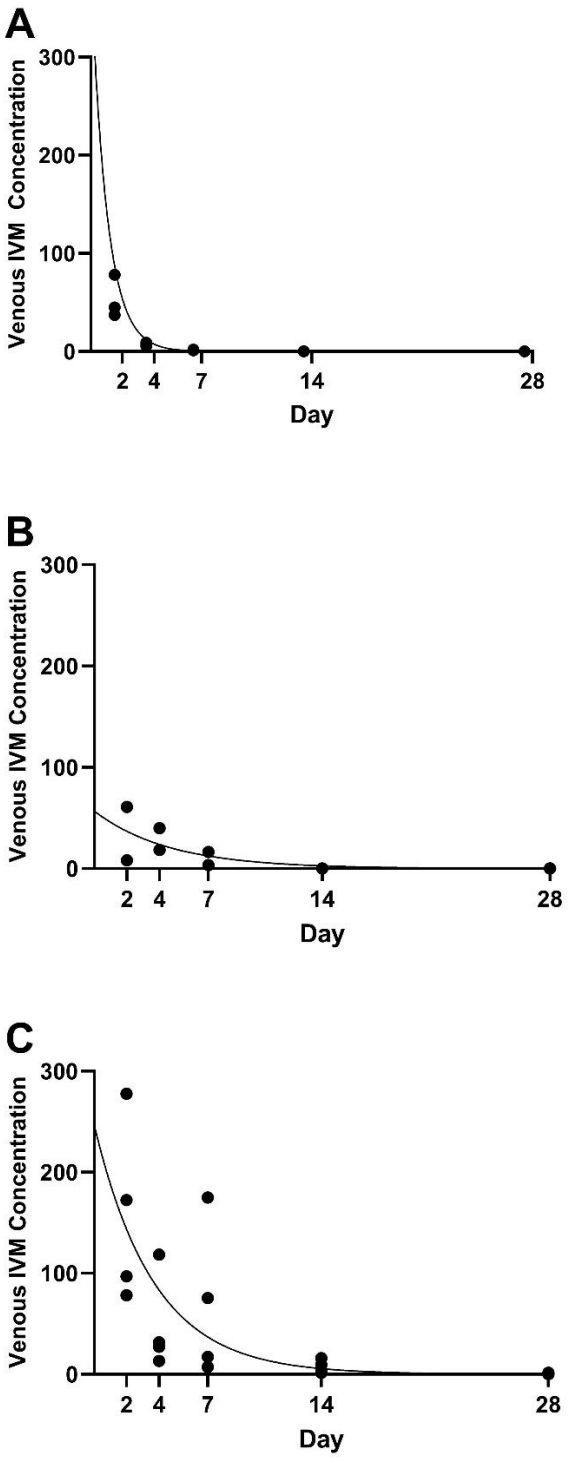

Figure 2.6: One phase decay model of IVM in participants stratified by age. (A) Participants in the 5-10 age range IVM half-life (*n* = 3). (B) Participants in the 11-18 age range IVM half-life (*n* = 2). (C) Participants 19 years and older IVM half-life (*n* = 4).

2.2.4 Identifying mosquitoes partially feeding on participant plasma

While conducting the bloodmeals, it was observed that mosquito groups which were offered the reconstituted plasma collected between days 2-14 post-intervention had a higher proportion of mosquitoes which partially fed compared to the control group. Since it is impossible to differentiate mosquitoes which probed and decided not to feed versus mosquitoes which did not probe at all, we focused on mosquitoes which partially fed while the bloodmeal was offered (Figure 2.7).

Figure 2.7: *An. gambiae* mosquito engorgement. From left to fight, mosquitoes were classified as fully fed, partially fed, and unfed.

Proportion analysis of partially engorged and fully engorged mosquitoes was conducted and significant differences were found between mosquitoes which were offered plasma collected on day 0 and mosquitoes which were offered plasma collected on day 2 ($p < 0.001$), 4 ($p = 0.001$), 7 ($p = 0.001$), and 14 ($p < 0.001$) (Figure 2.8). However, when comparing the proportion of mosquitoes which were offered plasma collected on days 0 and 28, no difference was found ($p = 0.816$) (Figure 2.8).

Furthermore, when comparing the feeding proportions with the participant pharmacokinetics, it was observed that participants have the highest IVM concentrations in day 2, 4, and 7 (Table 2.5). However, while day 14 had a significant increase in partially fed mosquitoes, most of the participants were BLQ (Table 2.5). Additionally, most of the participants had an IVM concentration BLQ on day 28 and four out of the nine participants had BLQ on day 0 (Table 2.5).

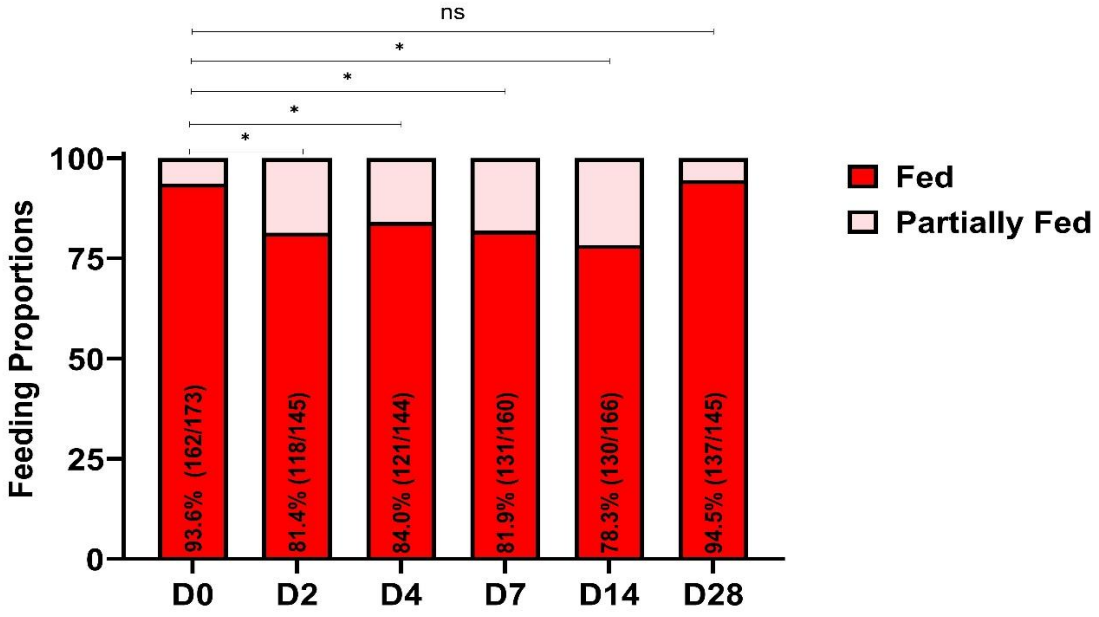

Figure 2.8: *An. gambiae* participant plasma feeding proportions. The proportion of fully fed mosquitoes offered days 2 ($p = 0.0009$), 4 ($p = 0.0098$), 7 ($p = 0.0012$), and 14 ($p < 0.0001$) were significantly reduced compared to fully fed mosquitoes offered days 0 and 28 ($p = 0.8158$) participant plasma. Fisher's exact test.

2.2.5 Bloodmeal identification of wild Anopheles gambiae sensu lato

After identifying partially fed mosquitoes in the lab, we examined the bloodmeal contents of wild *An. gambiae* sensu lato captured from Burkina Faso during the RIMDAMAL II trial to discern if the partially feeding effect observed in the lab could be inferred by the blood meal contents of wild mosquitoes captured in households during the trial. It was found that in 2019, 78.1% (278/356) of engorged mosquitoes had human only bloodmeals, while 12.6% (45/356) had a mixed bloodmeal (containing both human and animal blood) and 9.3% (33/356) had a non-human meal. Among engorged mosquitoes captured in 2020, 80.8% (270/334) contained human only meals, 9.9% (33/334) of meals were mixed, and 9.3% (31/334) were non-human meals (Figure 2.9).

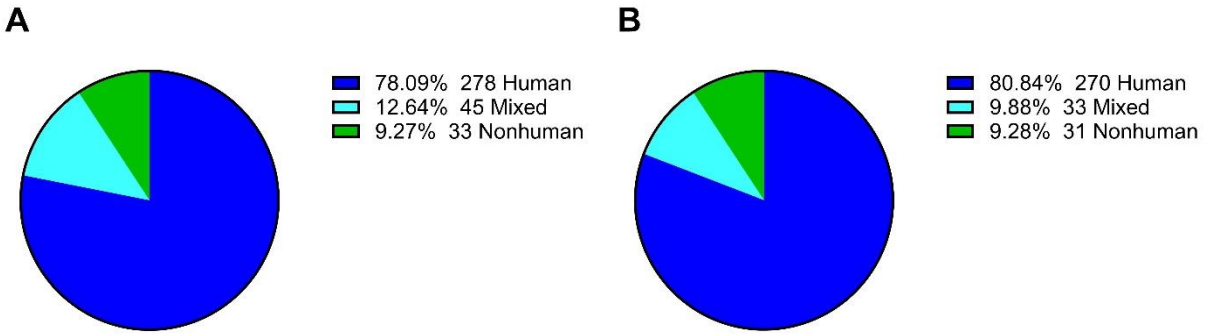

Figure 2.9: Wild *An. gambiae* bloodmeal contents during the RIMDAMAL II clinical trial. (A) Proportions of bloodmeals analyzed in 2019. (B) Proportions of bloodmeals analyzed in 2020.

We then compared blood meal proportions across years and found that proportions blood meal types were not significant between the two years. 50.73% (278/548) of human meals occurred in 2019, while 49.3% (270/548) occurred in 2020 (p = 0.76). We found a nonsignificant yet higher proportion of mixed meals in 2019 with 57.7% (45/78) while 2020 accounted for 42.3% (33/78) (p = 0.21). Finally, there were

similar proportions of non-human bloodmeals with 51.6% (33/64) and 48.4% (31/64) occurring in 2019 and 2020, respectively ($p = 0.90$).

During the trial, mosquitoes were captured twice between MDAs to assess if the IVM coverage was impacting mosquito populations over time. These collections took place one- and three-weeks post-MDA, thus these timeframes corresponded to differences in IVM present in most participants' blood due to the drug's pharmacokinetics, whereby at one-week post-MDA approximately 30 ng/mL IVM could be detected in treated participants, while at three-weeks post-MDA the drug was below the limit of quantification in most treated participants. Therefore, we examined the data based on the time the mosquitoes were captured post-MDA to discern if over time mosquito populations shifted from human only meals to mixed or non-human. We found there was no significance when comparing the total meals per collection period using a Tukey's test ($p = 0.76$). We then conducted a binomial test to determine if there was any significant difference in the number of human bloodmeals across MDAs between the placebo and treatment villages (Table 2.6). It was found that there was a significant decrease in human blood-meal proportions in MDAs 2+3 and 4+1, respectively, when comparing intervention villages to placebo villages ($p = 0.0361; 0.0004$, respectively). Furthermore, there was a significant increase in human bloodmeals in MDA 6+3 in the intervention villages when comparing them to the placebo villages ($p < 0.0001$). However, no differences were found between the intervention and placebo villages during MDAs 1+3, 6+3, and 8+1.

Table 2.6: Differences in human bloodmeals from placebo and treatment arms by MDA		
MDA	***p-value***	**Change[1]**
1+3	0.4341	None
2+3	0.0361	Decrease
4+1	0.0004	Decrease
5+3	<0.0001	Increase
6+3	0.5084	None
8+1	0.8545	None
Binomial test; Placebo villages were used as expected human bloodmeals stratified by MDA; [1]Relationship of intervention arm compared to placebo		

2.3 Discussion

Here we described the pharmacodynamics of human processed IVM with respect to the RIMDAMAL II participant population, explored the differences in sex and age strata, identified a possible aversion to bloodmeals treated with IVM both in lab and wild mosquitoes, and compared the drug's pharmacokinetics and pharmacodynamics among participants.

When discussing pharmacodynamics, it is important to consider the entire population being treated. Modeling suggests that a population treated with 300μg/kg of ivermectin delivered sequentially for three days should result in mosquitocidal activity against *An. gambiae* s.l. for up to 21 days post treatment and the highest activity at C_{max}, which occurs two days and four hours post last treatment dose[204,215]. In agreement with the modeling, we observed greater mortality effects with plasma obtained from RIMDAMAL II participants on days two and four post intervention. These data are consistent with data obtained during the IVERMAL trial, which examined the efficacy of a 300μg/kg dose over three days against 600μg/kg over three days in combination with dihydroartemisinin-piperaquine to treat uncomplicated *Plasmodium falciparum* infections in adults[204]. However, RIMDAMAL II only administered IVM and

not dihydroartemisinin-piperaquine plus IVM concurrently[170]. Our HR reported here, at two days post-intervention, is higher than what was reported in the IVERMAL trial[204]. This could be due to differences in mosquito strains, from the co-administration of dihydroartemisinin-piperaquine, or the fact that the IVERMAL trial only studied adults presenting with malaria, while the RIMDAMAL II trail studied participants aged five and up irrespective of their malaria infection status[170,204]. One, or all, of these factors could have led to the discrepancy observed between the two HR.

Furthermore, these data suggest that sex and age have an impact on the pharmacodynamics of IVM with treated females exhibiting an extended mosquitocidal period of up to seven days post treatment while treated males had a less pronounced seven-day post treatment effect when compared to the controls. Ouédraogo et al. has also reported this relationship when testing uncomplicated *P. falciparum* infected participants, treating them with artemether-lumefantrine and IVM[208]. This was associated with their female participants having a higher mean BMI than male participants[208]. Since IVM is a lipophilic drug, individuals who have a higher BMI should have longer drug half-life[266].

With respect to age, the number of participants tested in the ranges 5-10 years old (*n=3*), 10-18 years old (*n=2*), and ≥ 19 years old (*n=4*) were small, and so may not yield definitive results, but the trend was towards longer mosquitocidal activity connected to longer pharmacodynamics of the drug in older individuals. Participants who were in the 5-10 years old age bracket exhibited mosquitocidal activity up to four-days post intervention while those who were 10-18 years old showed mosquitocidal activity for up to seven-days post intervention. Finally, participants who were ≥ 19 years

old exhibited mosquitocidal activity up to 14-days post intervention. However, as stated before, of the four participants tested in the ≥ 19 bracket, three were female, which could have influenced this result. Consistent with our findings, a study conducted in Côte d'Ivoire observed the pharmacokinetics of IVM in school aged and pre-school aged children and found that children clear IVM quicker than adults which were given the same concentration per kilogram[267]. Furthermore, Brussee et al. also found that children had a higher median clearance of IVM than adults when a 200µg/kg dose was administered[268]. Before these data can be corroborated in the context of the RIMDAMAL II clinical trial, more plasma from participants, from both sexes, needs to be examined. Currently though, these data suggest that focusing treatment on older participants might be more effective for maximizing the duration of mosquitocidal activity against a village's population of mosquitoes.

Upon comparing the observed aversion to blood feeding on plasma containing IVM in mosquitoes, it was evident that they were more likely to partially feed on plasma obtained on days 2, 4, 7, and 14 post-IVM treatment relative to the day 0 collection. However, there was no aversion to blood feeding on plasma collected on day 28. This suggests that there is some IVM detection followed by premature feeding termination or IVM-related feeding inhibition by actively feeding mosquitoes leading to partial feeding taking place within the lab mosquitoes at times when IVM concentrations are typically detectable in plasma. One possible mechanism of IVM detection could be sensilla that are found in the buccal cavity. Three of these structures were first identified by Day in 1954 in *Aedes aegypti* and verified by Dapples and Lea in 1974 using a scanning electron microscope[269–271]. Day suggested these sensilla could be responsible for

detecting and determining the contents of a meal, leading to contraction or relaxation of the proventricular valve that determines whether the meal should be deposited in the ventral diverticulum (crop) if a sugar meal was ingested, or the midgut if a bloodmeal was imbibed[269]. These papillary sensilla could be responsible for sensing IVM or IVM metabolites in the blood, causing the mosquito to retract its proboscis and only imbibing a partial meal.

The future of endectocides for mosquito control depends on the use case. Currently, avermectin use in attractive toxic sugar baits (ATSB) are under development and are marketed in at least one ultra-low volume (ULV) spray product, but these products are not presently available for controlling malaria vectors in Africa[105,192]. Additionally, while no endectocides are currently approved for mass drug administration to control malaria, mass administration programs as their currently implemented leaves a sizable portion of the community without treatment due to caution in treating young children and pregnant women. However, ATSBs and ULV sprays are not without drawbacks. Both ATSB and ULV sprays are nonspecific, leading to nontarget arthropod death. Some of these issues can be circumvented by restricting sprays to night when mosquitoes are active but other arthropods may not be present.

New endectocides are being tested for mosquito control, including isoxazoline drugs such as fluralaner and lotilaner[176,272–275]. Current data shows these drugs have much longer pharmacokinetic profiles in treated animals relative to IVM[272,276–279]. Furthermore, lotilaner has been approved for use in humans as a first-in-class medication for the treatment of *Demodex* Blepharitis, a barrier which previously has made clinical trials using isoxazolines difficult to conduct[174]. Additionally, there is

currently an isoxazoline drug approved for IRS, which could provide new avenues which companies can use these insecticides without the need to treat human populations[193].

Ultimately, the future of mosquito control using endectocides would need to be a multifaceted approach. The data presented in this chapter indicates that during the RIMDAMAL II clinical trial, IVM treatment was sufficient to kill mosquitoes when compared to the control arm. Furthermore, among wild blood fed mosquitoes captured in households where participants were treated with IVM, those captured one week post-MDA had lower survivorship than those captured three weeks post-MDA when venous IVM concentrations were mostly undetectable[170]. However, the proportion of human bloodmeals fluctuated from MDA to MDA, indicating that wild *An. gambiae* was feeding on treated individuals, not avoiding them as suggested from the *in vitro* plasma assays. It is possible that the wild mosquitoes were not as deterred from imbibing IVM treated bloodmeals, potentially because IVM is used in MDA in this region for helminth control or the wild mosquitoes were insensitive to IVM due to documented IR[170].

Importantly, malaria and entomological inoculation rates (number of infectious bites per person per night) remained the same between the RIMDAMAL II trial arms[170]. This suggests that MDAs containing endectocides alone may not be enough to reduce malaria transmission unless the half-life of the drug can be increased, such as with the development of long-lasting injectable formulations for both animals and people[280]. Other new products that are being developed for use in areas outside of the home might also enhance IVM's effect on outdoor biting mosquitoes, such as those using highly volatile pyrethroids (e.g. transfluthrin), as spatial repellents.

One use case may be to combine endectocide MDAs, ATSB to target sugar feeding, or measures inside the home (IRS, ITNs, and spatial repellents), as a multi-targeted control tool to achieve desirable outcomes, such as a decline in malaria incidence. Additionally, we observed a decline in total mosquito numbers throughout 2020 during the RIMDAMAL II clinical trial, which coincided to the use of the dual-chemistry IG2® ITN's[170]. The use of control mechanisms that contain different active ingredients which have different modes of action can also prevent resistance development, an issue which has plagued west Africa.

Using just one or two of these control tools is not enough to result in a desirable change, and what works for one community might not work for others. However, using these tools together may result in outcomes which are favorable to reduce malaria transmission rates. Deployment of these tools together will require stronger surveillance efforts, including human-landing captures, identifying mosquito infection rates, understanding the extrinsic incubation period of different *Plasmodium* species, and better measures of mosquito population age structures.

2.4 Methods and materials

2.4.1 Blood Plasma Collection

Human venous blood was collected from a subset of participants (*n = 178*) in both intervention and placebo arms enrolled in the RIMDAMAL II clinical trial at set intervals following the last study MDA at days 0, 2, 4, 7, 14, and 28 post-ivermectin intervention (Table 2.7 & Figure 2.10). Blood samples were then centrifuged, plasma was placed in new containers and transported back to the laboratories of the Institute de

Recherche en Sciences de la Santé in Burkina Faso where they were stored at –80°C. They were eventually shipped to Yale University on dry ice for pharmacokinetics analysis, and then shipped to Colorado State University for pharmacodynamics analysis. Tested participants were chosen based age, sex, village, complete plasma panel, and quantity of plasma to ensure an even distribution across villages, age brackets, and sex.

Figure 2.7: Participants' plasma draws

Village	# of samples	Sex breakdown	Age Breakdown
BG*	31	Female = 19	5 – 10; (n = 9)
		Male = 12	11 - 18; (n = 10)
			≥19; (n = 12)
MT	34	Female = 15	5 - 10; (n = 11)
		Male = 19	11 - 18; (n = 11)
			≥19; (n = 12)
DL	28	Female = 17	5 - 10; (n = 7)
		Male = 11	11 - 18; (n = 10)
			≥19; (n = 11)
NV	18	Female = 10	5 - 10; (n = 5)
		Male = 8	11 - 18; (n = 3)
			≥19; (n = 10)
GB*	36	Female = 17	5 - 10; (n = 11)
		Male = 19	11 - 18; (n = 10)
			≥19; (n = 15)
KP*	31	Female = 15	5 - 10; (n = 9)
		Male = 16	11 - 18; (n = 9)
			≥19; (n = 13)

*Treatment villages; *n = 178*

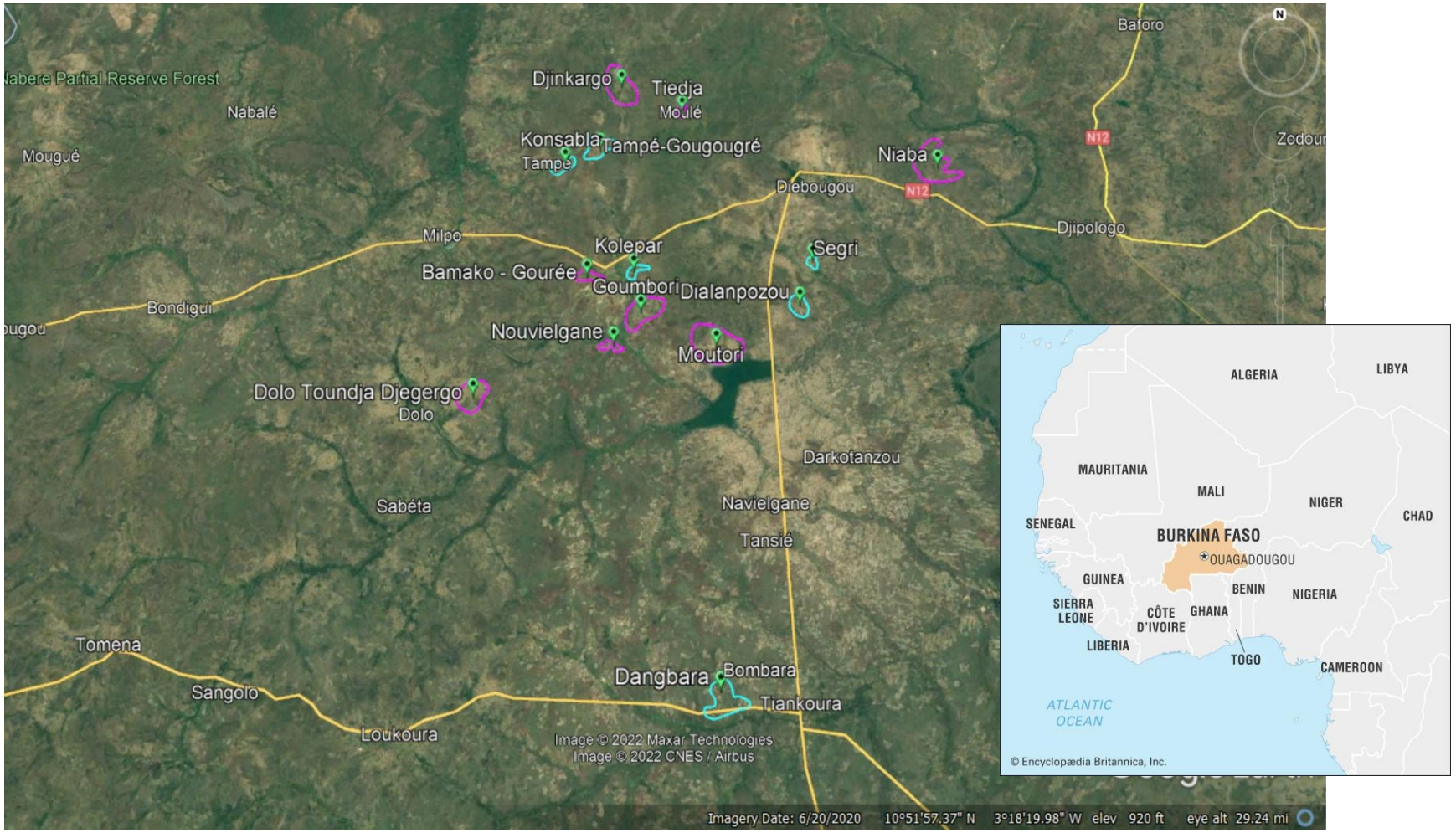

Figure 2.10: Google earth map showing the villages where the RIMDAMAL II clinical trial took place in Burkina Faso.

2.4.2 Mosquitoes

Anopheles gambiae G3 strain were reared in standard insectary conditions (12:12 light:dark, 28°C, and 75% relative humidity), housed at Colorado State University's Center for Vector-borne Infectious Diseases. Larvae we given ground Tetramin® fish food and adults were provided with a constant supply of fresh water and sugar cubes.

2.4.3 Reconstituting blood plasma, blood fed, and sorting

Defibrinated calf blood was chosen for this analysis as lab mosquitoes readily imbibe bovine bloodmeals. Additionally, since the blood types of our participants are unknown, this could have led to unwanted consequences of using human red blood cells (RBC) with unpaired plasma.

Before blood feeding mosquitoes, 500µL of defibrinated calf blood (Colorado Serum Company) was centrifuged (Eppendorf 5430R) at 2500rcf for 1.5 minutes at 4°C to separate RBC from the plasma. Bovine plasma supernatant was pipetted and discarded. 100µL of bovine RBC pellet was transferred into a 1.5mL tube and 100µL of participant human blood plasma was added to create a 50/50 mixture of plasma to RBCs. The bovine RBC and human plasma mixture was then vortexed for five seconds and placed into a desktop microcentrifuge (USA Scientific) for one second to make the bloodmeal.

Three-to five-day old *An. gambiae* mosquitoes were separated and retained in seven half gallon plastic bins, one bin for each of the intervention participants collected plasma (0, 2, 4, 7, 14, 28 days) and one bin was fed day 0 plasma from a participant

from a placebo village. The placebo participant was age and sex matched to the intervention participant. The placebo participant day zero plasma acted as a control to our intervention participants' day zero plasma, in case our intervention participants' plasma still contained trace amounts of IVM, which was the case for one participant.

Mosquitoes were starved of sugar and water for four hours prior to starting the bloodmeal. Mini glass feeders (Lillie Glassblowers, Smyrna, Georgia) were connected to a recirculating heated water bath (Fisherbrand Isotemp 4100), heated to 37°C, and feeders were filled with 200µL of the reconstituted blood. Mosquitoes were allowed to feed for one hour and then cold anesthetized for 1.5 minutes. Fully engorged females were sorted, counted, and retained in pint-sized paper ice cream containers. Partially and non-fed females were counted and discarded. Mosquitoes which were identified as non-feds were not utilized for any analysis as it is impossible to determine why the non-feds did not imbibe blood. Retained mosquitoes were maintained at standard insectary conditions mentioned above with constant access to sugar cubes and water. Mosquitoes were observed every 24 hours where mortality was counted and recorded for 15 days.

2.4.4 Bloodmeal analysis

Blood engorged *An. gambiae* s.l. were collected via aspiration from inside homes located in villages participating in the RIMDAMAL II clinical trial, 1 and 3 weeks after each IVM MDAs took place. Mosquitoes were selected at random from across six MDAs (3 occurring in 2019, and 3 occurring 2020) for blood-meal identification. Bloodmeal analysis followed the methods described by Kent and Norris[48]. Briefly, mosquitoes with

fully fed abdomens were homogenized and centrifuged. DNA was then extracted and purified using a Kingfisher Flex (ThermoFisher Scientific Inc.). Finally, a multiplex PCR amplified the cytochrome b mitochondrial gene within the bloodmeal. PCR products were then subjected to electrophoresis in a 1.5% gel to identify the host bloodmeal within the mosquito midgut. Gel electrophoresis ran at 90 volts for 45 minutes and was imaged on a BIO-RAD ChemiDoc MP Imaging System to identify the separate bands, which identifies if the bloodmeal originated from a human, dog, cow, pig, or goat host.

2.4.5 Statistical Analysis

The following analysis was conducted on Prism 10 (GraphPad version 10.10): Hazard ratios were calculated using a Mantel-Haenszel test as the assumption of proportional hazards was questionable due to the individual IVM concentrations within the participants and IVM effects at earlier time points. Gehan-Breslow-Wilcoxon test were used to test if the Mantel-Haenszel HR were significant, as well as the survival curve significance. The Gehan-Breslow-Wilcoxon test was chosen due to its ability to give more weight to earlier death timepoints, rather than all deaths across the 15-day experiments. Mosquito feeding proportions were tested using Fishers Exact test with Bonferroni-adjusted *p-values.* Chi-square test for goodness of fit were used to understand the differences between human-only blood-meals versus mixed and non-human blood-meals from intervention and placebo villages. A one-phase decay model using only samples collected on or after Day 2 post last dose was used to determine the half-life of IVM concentrations since IVM follows a 1^{st} order pharmacokinetics model

following the C_{max}. A constant plateau of 0 was decided on as participants could not have lower than 0 venous IVM concentrations.

Rstudio (R.4.3.2) was used to run a mixed effects Cox proportional hazards model against mosquito mortality using the following packages: survival, coxme, ggsurvfit, tidyverse.

CHAPTER 3: USING PIXEL INTENSITY TO AGE WILD *ANOPHELES GAMBIAE* SENSU LATO POPULATIONS IN BURKINA FASO[1]

3.1 Introduction

An adult female mosquito's age is a key factor in its ability to blood feed, lay eggs and transmit pathogens. Anthropophilic species like *Anopheles gambiae* typically obtain their first bloodmeal three to five days post-eclosion[281]. The extrinsic incubation period (EIP), defines the time it takes for a vector-borne pathogen ingested in a competent mosquito's blood meal to infect or penetrate the mosquito's tissues, undergo development (in the case of *Plasmodium* parasites or filarial worms) and disseminate to tissues from where it can be transmitted to the next vertebrate host (e.g. salivary glands or thoracic flight muscles). For *Plasmodium falciparum* in African *Anopheles* spp., the EIP is approximately between nine and 16 days depending on temperature and species[282,283], while the typical lifespan of an *Anopheles* mosquito in the wild is roughly 15-20 days[283–285]. Thus, very few mosquitoes in populations ever become infectious and large sample sizes are required to reliably estimate transmission intensity. However, much effort, time and costs can be expended to capture and test for infectious mosquitoes from these large collections. As such, the ability to rapidly and accurately age-grade mosquitoes captured from a population could allow for simple and less resource-intensive estimates of transmission risk and help better evaluate the efficacy of vector control interventions that often occur before periods of high pathogen transmission.

[1] "Pixel intensity of wing photos used to predict age of *Anopheles gambiae* sensu lato captured during the RIMDAMAL II Clinical Trial." Pugh G., Sougué E., Burton T.A., Yoe R., Gray L.I., Hephaestus B., Somé A., Asay B., Somé A.F., Dabiré R.K., Parikh S., Foy B.D., Preprint in bioRxiv, *In Review at Sci. Reports*

Original mosquito age-grading techniques were qualitative, such as classifying wing degradation, assessing the presence of mites on mosquitoes, or meconium in midguts[224,286,287]. Eventually evaluating parity by assessing ovary tracheole skeins on dissected ovaries became the gold standard age grading technique, which was further refined and quantified by counting ovariole dilatations from dissected ovaries[225,226,288]. However, these techniques can be imprecise, they only provide physiological age rather than calendar age, and it can be difficult and time-consuming to process many mosquitoes per field collection with the dissection techniques required. New age-grading techniques have been investigated, including biochemical, gene and protein profiling, and spectroscopy methods[233,235,238,239,242,245,289–296]. While these methods are quickly reinvigorating mosquito age-grading processes, there remain challenges towards practical implementation in the field. These challenges include the need for expensive equipment which can be difficult to use in a field setting, or shipment of specimens for analysis by this equipment outside of the field site, as well as destructive testing of the samples. Furthermore, these techniques may require recalibration of age models at each field site and/or timepoint the samples are collected, and they can involve advanced technical and statistical expertise to run samples and analyze the data produced[294,297].

We previously developed a simple, low-cost, high-throughput, and nondestructive method of age-grading lab-reared *Anopheles gambiae* populations by calculating the pixel intensity (PI) of wing photos, which analyzes the white intensity of the pixels of a mosquito wing photo in grayscale[243]. This method can quantitatively assess wing scale loss over time due to flying because a mosquito's wing scales are often darker than the

underlying membranous wing. In the study, we demonstrated this method's ability to distinguish the age structure of two mosquito populations reared in different mesocosms, whereby one was regularly treated with blood meals that contained the mosquitocidal drug ivermectin, and the other control mesocosm was only provided regular blood meals. However, it was unclear if this method could be extended to field mosquitoes. Here, we have refined our techniques for PI analysis of wings, applied our lab-reared *An. gambiae* age-model to estimate ages of wild caught *An. gambiae* s.l. captured during a clinical trial conducted in Burkina Faso called RIMDAMAL II (which tested the effect of ivermectin mass drug administrations (MDA) on malaria incidence)[170], and demonstrate how this technique can be used to infer the efficacy of vector control interventions that occurred during the trial.

3.2 Results

3.2.1 Total Pixel Intensity vs Mean Pixel Intensity

Our previously published PI analyses calculated the total PI of each wing photo (left- and right-wing photos) per female mosquito and used these values to calculate the mean of the total PI per mosquito[243]. However, this analysis yielded highly variable results of the mean total PI from some mosquitoes caught and processed during the RIMDAMAL II trial, which we determined were due to differences in file sizes, photo resolution, and relative photo brightness. Independently analyzing the mean PI of each wing photo normalized the PI output regardless of file size and other parameters. A mean PI per mosquito was then calculated using the mean PI of each wing, which allowed for normalized comparisons across groups of mosquitoes processed during the

trial. Overall, the prior published analysis of total PI gave ranges from $2.4x10^8$-$6.6x10^8$ while our updated analysis of mean PI gave ranges from 127.85-133.08.

3.2.2 PI Standard Deviation Among Mosquito Wings

We then calculated the standard deviation (SD) of the mean PI between the two wings per mosquito to understand how the variance between wings may be associated with the mean PI and thus potentially influence a mosquito's predicted age. Among the lab mosquitoes aged in a mesocosm, the mean SD was 0.13 (Range: 0.00-0.76) and among the wild mosquitoes, the mean SD was 0.08 (Range: 0.0004-3.34), however, comparisons of SD of both mosquito populations relative to mean PI or age suggested the SD of the PI between mosquitoes' wings has only a modest effect on the overall estimated age distribution of the analyzed mosquito population (Figure 3.1). Overall, among wild mosquitoes where the SD between wings was less than 0.5, the mean PI was 128.51 (Range: 127.82-133.15) while those where the SD between wings was greater than 0.5 had a mean PI of 130.72 (Range: 128.44-133.07), suggesting that as a mosquito ages and loses more scales through more flying, there is a modestly higher likelihood of having one wing that has significantly fewer scales than the other. A similar trend is observed in the lab mosquitoes. Finally, analysis of each pair of wings suggests there is no favoritism between left and right wing. 51.69% (95% 49.42 – 53.96%) of left wings had a higher PI while 48.31% (95% CI: 46.04 – 50.58%) right wings had a higher PI (Figure 3.2).

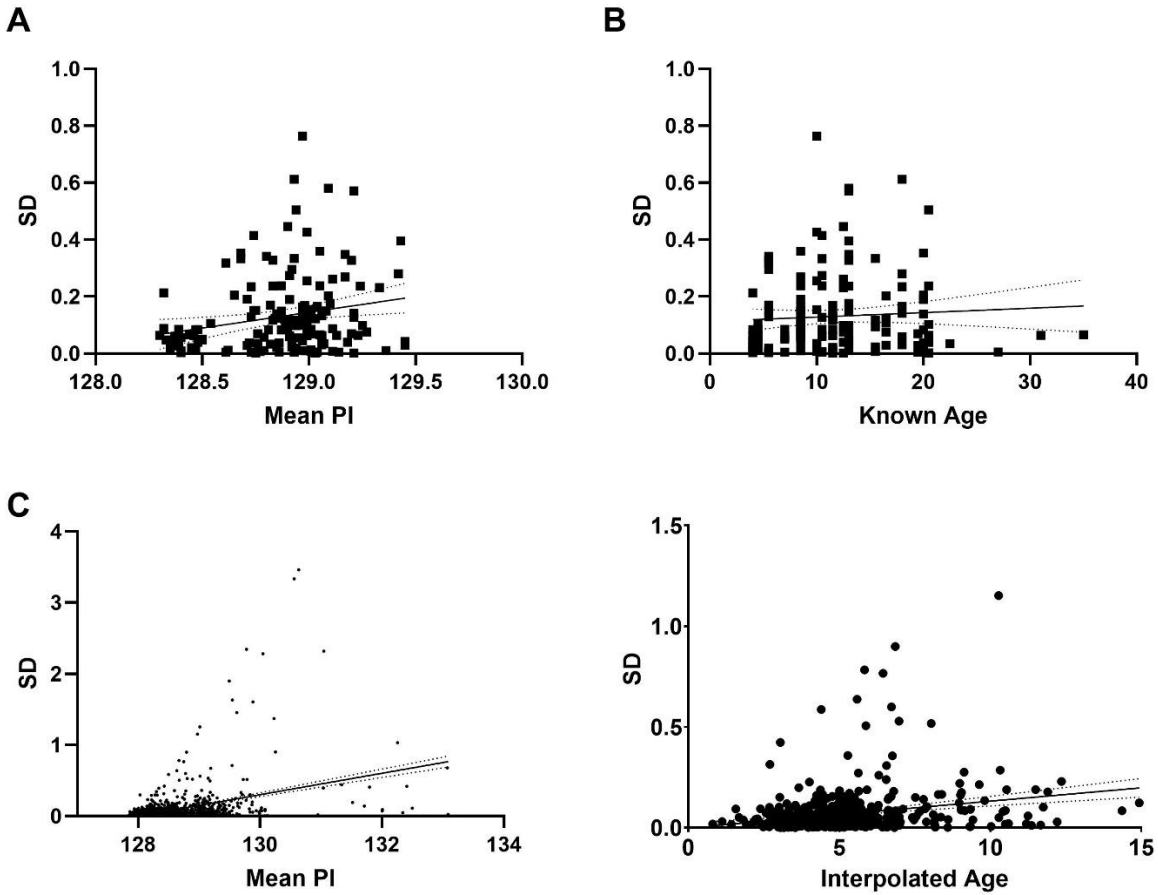

Figure 3.1. The standard deviation of the mean pixel intensity values for each set of a mosquito's wings is modestly correlated with increasing mean pixel intensity (PI) or mosquito age. Each dot represents data from a set of a mosquito's wings. Top panels: laboratory-reared *An. gambiae* aged in a mesocosm (n=149 in both A and B). Bottom panels: *An. gambiae* s.l. captured during the RIMDAMAL II trial (C; n =1861), (D; n = 549). Regression line slopes in panels A, C, and D are significantly different from zero (panel A, $P = 0.008$, $r^2 = 0.045$; panel C, $P < 0.0001$, $r^2 = 0.1474$; panel D, $P < 0.0001$, $r^2 = 0.054$)

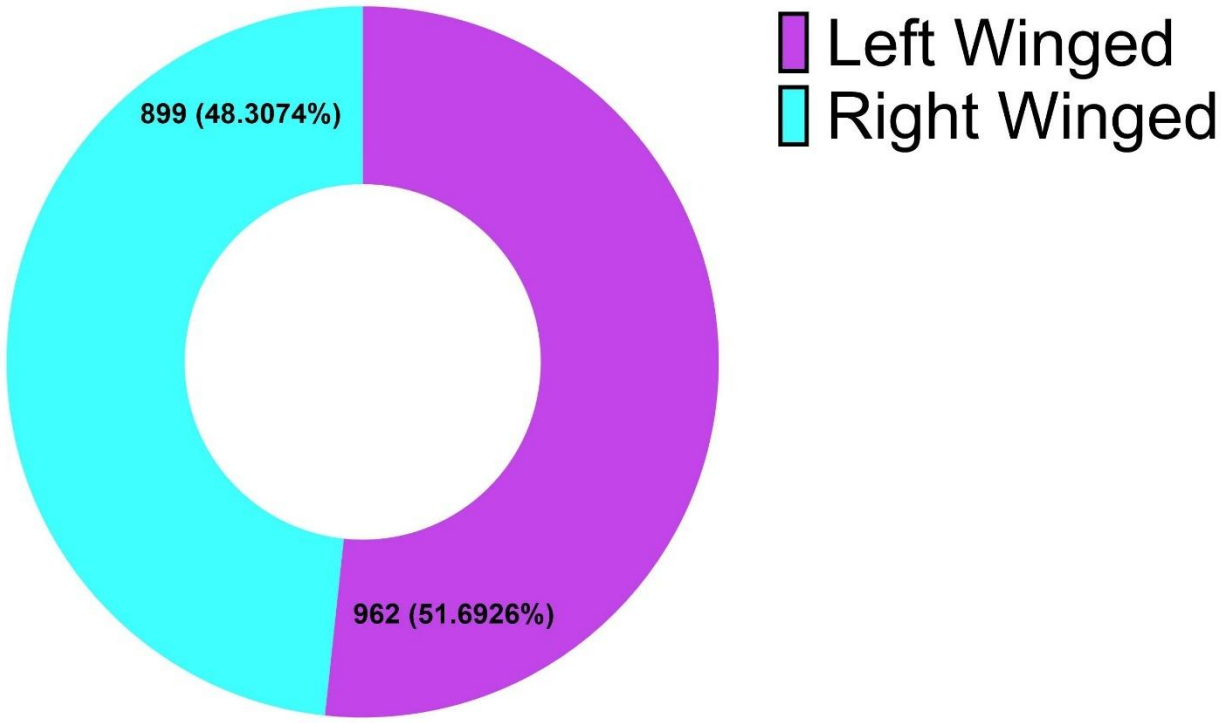

Figure 3.2. Mosquito populations do not have a favored wing. The difference between the left and right pixel intensities were calculated. A positive difference resulted in a higher left-wing PI and a negative difference resulted in a higher right-wing PI. A binomial test found there was no significance (p = 0.1506) between the two populations with the assumption that wing favorability would be evenly split within the population.

3.2.3 Individual and binned pixel intensity of mosquito populations to examine inferred age structure

Next, we plotted the proportions of wild mosquitoes from the RIMDAMAL II trial from which we took wing pictures, both individually and in bins of 0.3 PI units, to observe the overall inferred age structure (Figure 3.3). The plots shows distributions that mimic wild mosquitoes age-graded by the gold standard Polovodova method (estimating age by counting ovarian dilitations) as well as newer techniques such as MIRS, suggesting a population distribution dominated by nulliparous and young

mosquitoes in the lowest PI ranges, and relatively few older females in the long top- or right-skewed tail of the individual or bin distributions, respectively (Figure 3.3)[245,285].

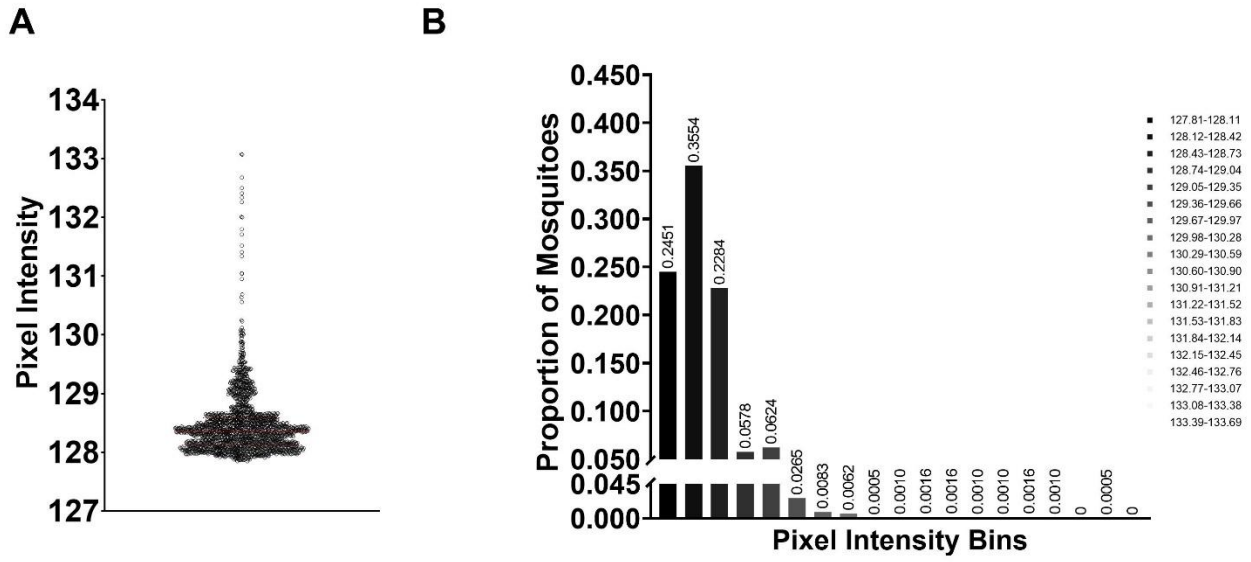

Figure 3.3. Pixel intensities (PI) from wild *Anopheles gambiae* s.l. captured in the RIMDAMAL II trial reflects typical population age distributions from wild mosquitoes. A) The distribution of individual mosquito's mean wing PIs. Each dot represents the mean PI from a set of a mosquito's wings. B) Bins of mosquitoes' mean wing PIs by 0.3 PI units/bin.

Overall, most mosquitoes captured during the trial had PIs of ≤ 128.73 (Range: 127.81-133.43) with a top- or right-skewed distribution tail extending to a PI of 133.43. When the population was split based on mosquitoes captured in each arm of the trial, the top- or right-skewed tail of the distribution was more robust among the population from placebo clusters but not intervention (ivermectin-treated) clusters (Figure 3.4).

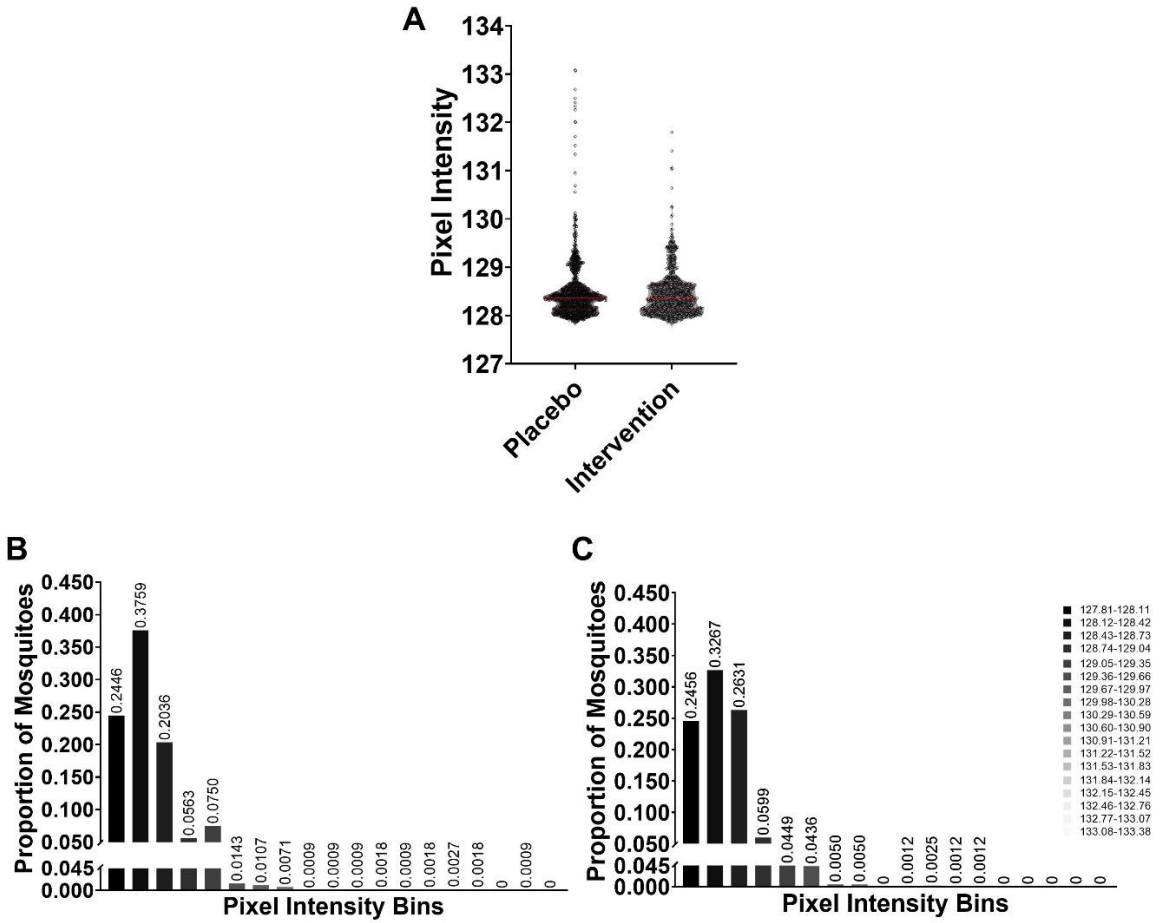

Figure 3.4. Pixel intensities (PI) from wild *Anopheles gambiae* s.l. captured in the RIMDAMAL II trial reflects typical population age distributions from wild mosquitoes. (A) The distribution of individual mosquito's mean wing PIs. Each dot represents the mean PI from a set of a mosquito's wings. (B) Bins of mosquitoes' mean wing PIs captured in the placebo arm by 0.3 PI units/bin. (C) Bins of mosquitoes' mean wing PIs captured in the intervention arm by 0.3 PI units/bin.

Furthermore, when separating the data into the trial years, the top- or right-skewed tail of the distribution was evident among the population captured in 2019 but absent in 2020 (Figure 3.5). The PI bin distributions among the populations captured in 2020 among clusters from both arms were grouped in only 3 of the lowest PI bins (Figure 3.5).

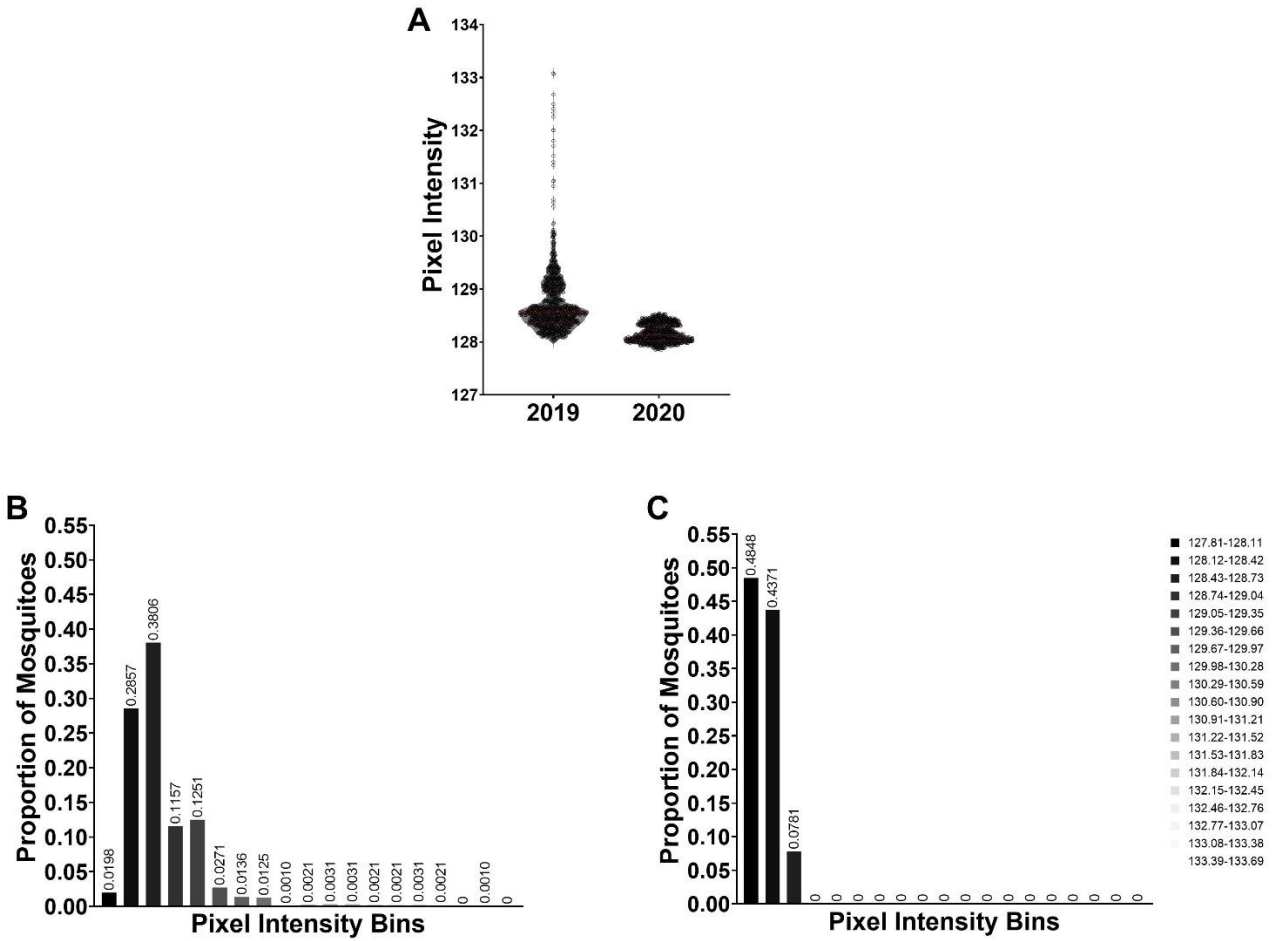

Figure 3.5. Pixel intensities (PI) of wild *Anopheles gambiae* s.l. captured in the RIMDAMAL II trial, grouped by trial year. (A) The distribution of individual mosquitoes' mean wing PIs grouped by the year they were captured during the rainy season intervention periods (late July to early November of 2019 and 2020). Each dot represents the mean PI from a set of a mosquito's wings. (B) Bins of mosquitoes' mean wing PIs, from mosquitoes captured during 2019. (C) Bins of mosquitoes' mean wing PIs, from mosquitoes captured during 2020.

A generalized linear mixed model was generated using individual wing PIs from these mosquitoes, using a gamma distribution with a log link function and a random (grouping) mosquito identification term. This model revealed a small but significant reduction in PI of mosquitoes captured in 2020 compared to 2019 (Ratio (exponentiated model coefficient): 0.9955 [95% CI 0.9950 – 0.9961], $p < 0.001$). No significant difference was detected between control and treatment arms in either 2019 ($p = 0.31$) or 2020 ($p = 0.64$).

These PI distributions associate with the timings of the two mosquito control interventions that occurred during the trial, whereby ivermectin or placebo was distributed in the respective trial arms throughout both years of the trial, and distribution of new dual chemistry Interceptor® G2 (IG2®) nets (containing chlorfenapyr + alpha-cypermethrin) occurred in clusters of both arms in early November 2019, towards the very end of the first rainy season approximately 2-4 weeks after the 4th MDA between sampling weeks 13 and 15 when mosquito capture numbers were very low (Figure 3.6)[170].

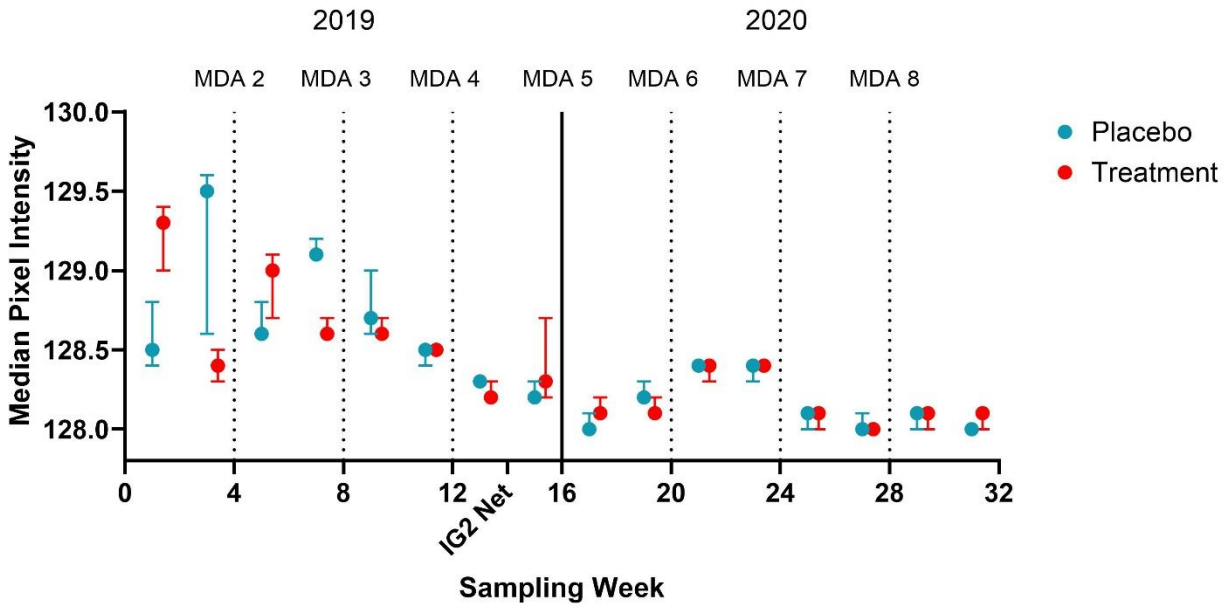

Figure 3.6: Median pixel intensities (PIs) from wild *Anopheles gambiae* s.l. captured in the RIMDAMAL II trial by sampling period and relative to the timing of the mass drug administrations. Median PI of mosquitoes captured from the Placebo (blue: *n* = 1129) and Intervention (red: *n* = 799) arms. Whiskers depict 95% CIs. Mosquito sampling weeks over the 2-year intervention period (late July-early November in 2019 and 2020) are enumerated consecutively on the X-axis, and mass drug administrations (MDA) of either placebo or ivermectin tables are marked with vertical or dotted lines and occurred over a 3-day periods. The period of IG2® net distributions in 2019 to all villages in the health district is marked on the X-axis.

Thus, most of the IG2® nets were not deployed by the populace until 2020 and were used by households from both arms throughout that year. This association can be observed when comparing the median PIs per mosquito population collected one and three weeks after each MDA performed in the trial (Figure 3.7).

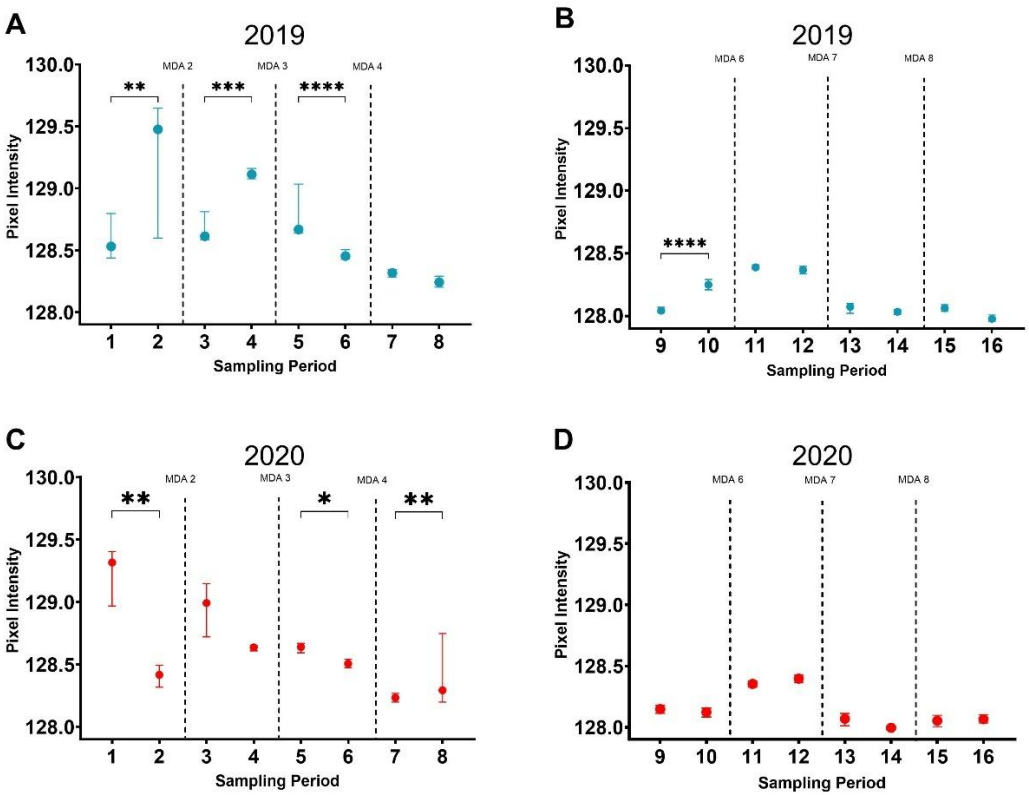

Figure 3.7: Comparisons of median pixel intensities (PIs) from wild *Anopheles gambiae* s.l. captured in the RIMDAMAL II trial by sampling period and relative to the timing of the mass drug administrations. Median PI of mosquitoes captured from each arm were compared by between the two populations sampled 1-week and 3-weeks following each mass drug administration (MDA). Data from mosquitoes captured in the Placebo (blue: n=1129) and Intervention (red: n=799) arms are showed in panel A & B and C & D, respectively. Whiskers depict 95% CIs. Mosquito sampling weeks over the 2-year intervention period (late July-early November in 2019 and 2020) are enumerated consecutively on the X-axis, and mass drug administrations (MDA) of either placebo or ivermectin tables are marked with vertical or dotted lines and occurred over a 3-day periods. Comparisons were ANOVAs and post hoc Kruskal-Wallis tests; (*= $P \leq 0.05$; **= $P \leq 0.01$; ***= $P \leq 0.001$; ****= $P \leq 0.0001$).

In 2019, the median PI among *An.* gambiae s.l. caught in placebo clusters three weeks after each of the first two MDAs were significantly higher relative to the populations captured one week after those MDAs (Sampling period 1 vs 2, $p \leq 0.01$; sampling period 3 vs 4, $p \leq 0.001$), while the median PIs significantly decreased from populations caught in ivermectin-treated clusters over the same sampling time frames (Sampling period 1 vs 2, $p \leq 0.01$), suggesting an ivermectin effect on mosquito population PI structure that manifests by the third week after the 1st and 2nd MDAs (Figure 3.7). This ivermectin effect on wing PI became inapparent after the 3rd MDA in 2019 and through all MDAs in 2020 when the IG2® nets were used throughout the 2020 season. Overall, the new nets seemed to have a dramatic effect on the median PI, lowering it below 128.5 among mosquito populations of both arms beginning with the 4th MDA and lasting through the end of the trial.

3.2.4 Adapting and applying an age model to wild An. gambiae s.l.

To interpolate age for the wild mosquitoes, we sought to use the colonized mosquitoes aged in laboratory mesocosms to develop an age model and use it to predict the ages of the wild mosquito populations from RIMDAMAL II[243]. The range of mean PI scores from these lab mosquitoes of known age was notably constrained (range: 128.30 – 129.45) compared to the range obtained from wild mosquitoes (range: 127.85 – 133.08), but the agreement in the magnitude of PI measured in two the different settings and between the lab and field populations was encouraging (Figure 3.8). The lowest mean PI score from the newly eclosed colony-reared adults (128.35) was 0.5 PI units higher than the lowest mean PI score obtained from wild mosquitoes

(127.85), suggesting wings from the wild mosquitoes tended to have more and/or darker scales than those from the lab colony, or that wing pictures from the microscope camera in the field were more variable than those in the lab (perhaps due to different lighting conditions, etc.).

A simple linear regression model was first applied to the lab mosquitoes, which had relatively poor fit to the data (r^2 = 0.4011) and predicted the wild mosquitoes to be between -24.31 and 163.17 days old. We then performed stepwise comparisons of multiple non-linear models that may plausibly fit the data and reflect the biology of scale loss over time. The best fit model was a symmetrical sigmoidal curve with a variable slope (difference in AICc from the linear model = 90.33; r^2 = 0.6577), from which the best-fit values were PIs between 128.4 (95% CI 128.3 - 128.5) and 129.0 (95%CI 129.0 - 129.1) (Figure 3.8). With this model, PIs from 128.30-128.55 were predicted for mosquitoes between <1-4 days old, PIs from 128.56-128.96 were predicted for mosquitoes 5-9 days old, and PIs from 128.97-129.45 were predicted for mosquitoes ≥10 days old (Figure 3.8).

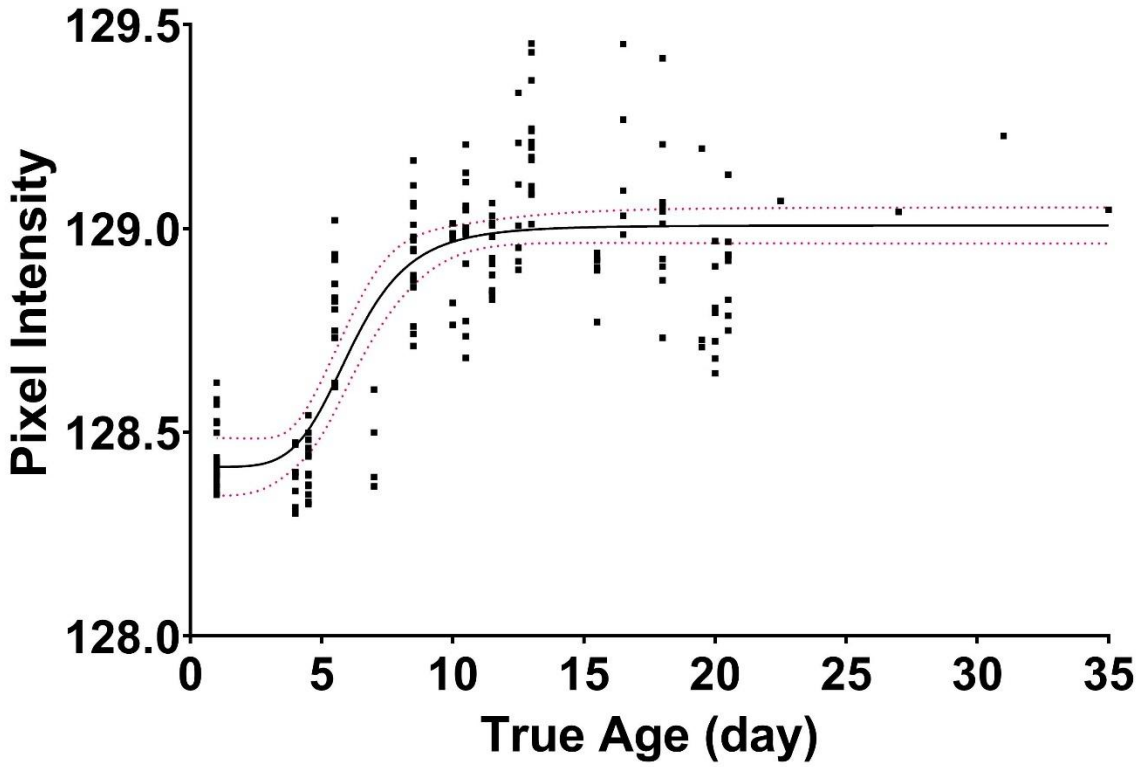

Figure 3.8. Age model derived from colonized, marked *Anopheles gambiae* reared in laboratory mesocosms to known ages. Mean pixel intensities of colonized mosquitoes reared to known ages (n=169) were plotted by their true age and fitted by stepwise comparisons to a linear and multiple non-linear models. The best fit model (depicted) was a variable slope sigmoidal model. The best fit line of the final model is in black and red dotted lines represent 95% confidence bands.

However, given the variance of wild mosquito PI data compared to the model, predicted age could only be accurately interpolated from approximately 30% (578/1928) of the wild mosquitoes (Figure 3.9). Nonetheless, using this model, we binned the mosquitoes into the 3 interpolated pixel intensity groups and observed a slight but non-significant difference in the structure of these binned mosquitoes in 2019, whereby those in from the placebo arm had fewer 'middle aged' mosquitoes with PIs between 128.57-128.96 and more 'old' mosquitoes with PIs between >128.96 in the ivermectin

arm. However, the difference in PI bin structures in 2020 compared to 2019 were noticeable, whereby all mosquitoes tested were predicted to be 'young' (PI < 128.57) in both arms (Figure 3.10).

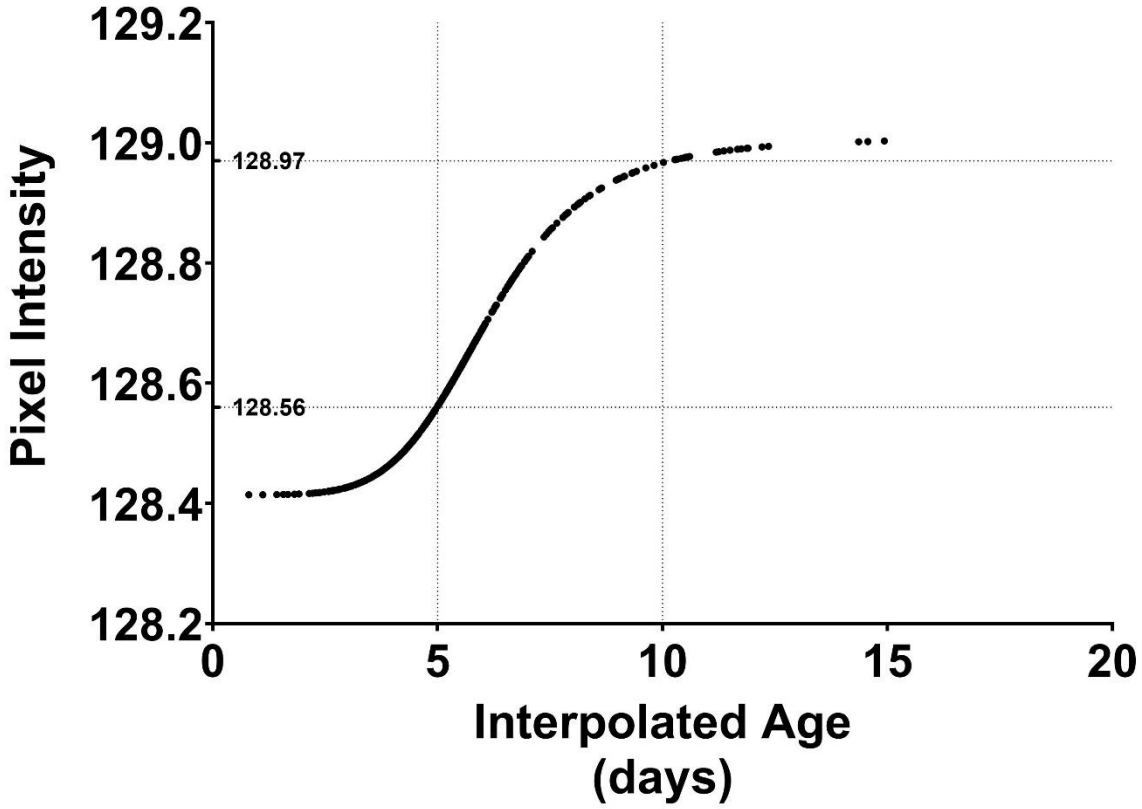

Figure 3.9. Interpolated ages of wild *Anopheles gambiae* s.l. captured in the RIMDAMAL II trial using the pixel intensity-based age model derived from colony mosquitoes. Dots are individual wild mosquitoes placed on the best-fit-line of age model; 30% (n=578) of the wild mosquitoes' pixel intensity (PI) values fit within the model's 95% CI brackets. PIs corresponding to the interpolated ages of 5 and 10 were plotted (dotted lines) using the model.

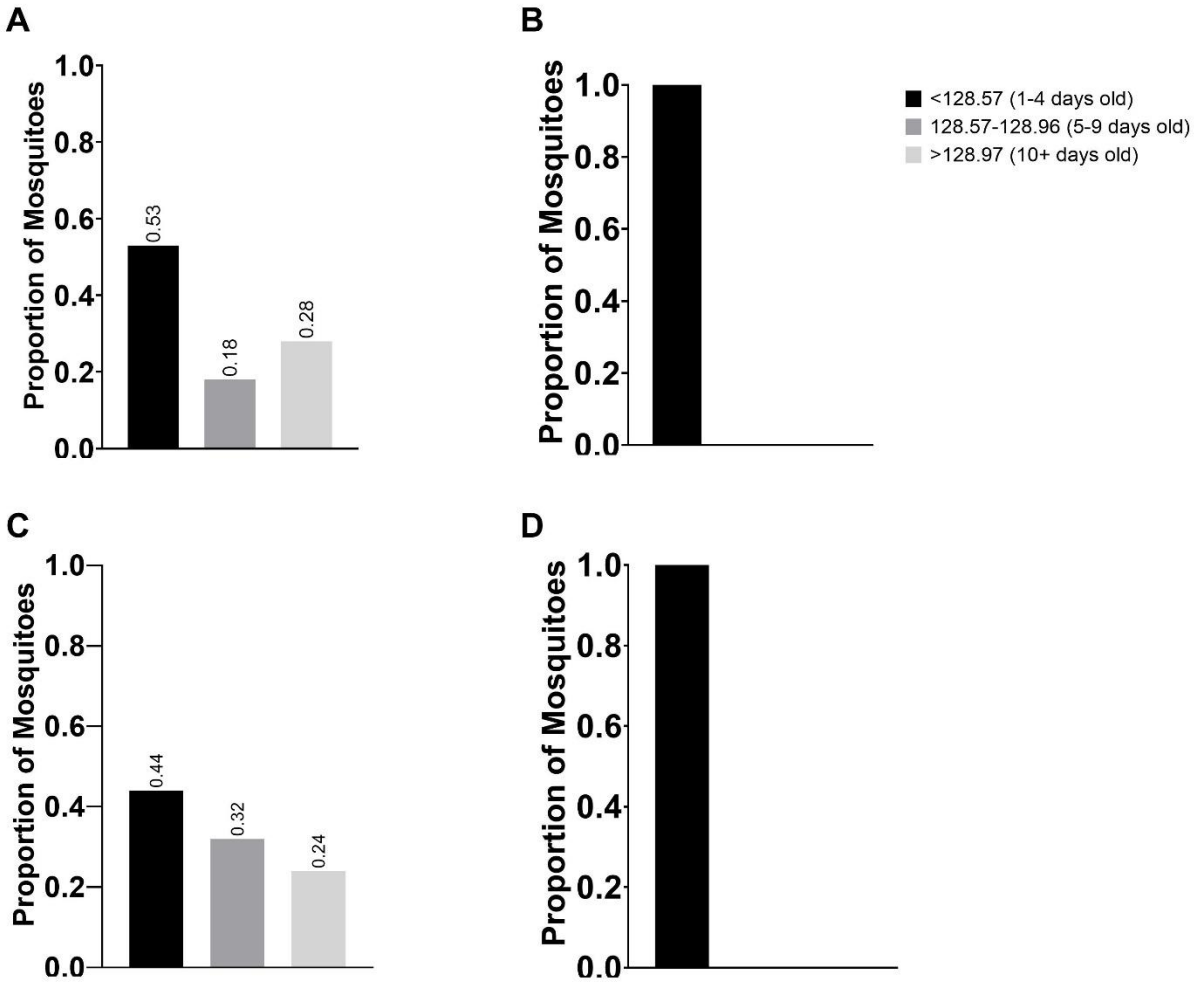

Figure 3.10. Wild *Anopheles gambiae* s.l. captured in the RIMDAMAL II trial grouped in into three, pixel intensity (PI) bins corresponding to interpolated age classes. A) mosquitoes from the first year of the trial (2019) and caught in Placebo clusters. B) mosquitoes from the second year of the trial (2020) and caught in Placebo clusters. C) mosquitoes from the first year of the trial (2019) and caught in Intervention clusters. D) mosquitoes from the second year of the trial (2020) and caught in Intervention clusters.

3.3 Discussion

Here we demonstrate that this revised PI analysis of wing photos enables normalization of the data collected and that the PI distributions, either from individual mosquitoes or with binned data, are similar to mosquito age structures observed from

using the gold standard Polovodova method consisting of ovarian dilation counting, which is sometimes combined with analysis of Christophers stages[245,288,298–301]. Furthermore, we show how this method can be used to observe changes in mosquito population structure in response to two different vector control methods that were performed during the RIMDAMAL II trial, specifically ivermectin mass drug administrations and use of IG2® nets.

The most prominent changes in PI distributions from *An. gambiae* s.l. captured at intervals during the RIMDAMAL II trial were observed in the differences between intervention seasons in 2019 and 2020. These changes were associated with the distribution of new IG2® nets at the end of the 2019 season, just prior to the last mosquito sampling period of that year when the rains had ended and the populations of *An. gambiae* s.l. were nearly gone from the study site. The efficacy of IG2® nets on wild *An. gambiae* has been thoroughly examined, and is known to strongly affect mosquito populations[169,249–251]. The entomological indices we previously reported from the trial suggested a similarly strong effect on malaria vectors from both arms of the trial and that occurred primarily in the in trial's second season (2020)[170,220]. This effect included, a) significant mortality (~50%) of indoor-captured, blood fed mosquitoes held in survival bioassays from both arms, and b) significant reductions in the number of the *An. gambiae* s.l captured in 2020, which were approximately half of those captured in 2019, and a near absence of *An. funestus* captured at the study site in 2020 (n = 49) relative to 2019 (n = 1148) despite similar rainfall and climate at the site across these two years. Similarly, the PI analysis reported from mosquitoes captured in 2020 relative to 2019 (Figure 3.9) supports the strong mosquito killing effect from these nets and

demonstrates how PI can be used to track the efficacy of a robust malaria vector control method like IG2® nets.

The ability of this age-grading method to detect mosquito population changes from the effect of ivermectin mass drug administrations is more nuanced, but the ivermectin intervention itself was not successful in reducing malaria incidence in the trial, nor in reducing the classical entomological indices of density and entomological inoculation rate[170]. The primary entomological index that was affected in treatment clusters compared to placebo clusters was the wild blood fed *An. gambiae* s.l. survival rate, but only in 2019 and only from blood fed mosquitoes captured in the week following the MDAs. Regarding the PI of these mosquito populations, there were modest detectable differences between treatment and control arms at the beginning of the trial in 2019 observed from the mosquito sampling periods that occurred three weeks after MDAs 1-3 were administered. It is interesting that these PI trends mirror the trends of infectious *An. gambiae* s.l. bites per person per night in each arm shown over the trial, suggesting that lower median PIs may correlate with fewer infectious mosquitoes in the population[170]. The observation that the strongest effect of ivermectin MDA on mosquito PI seems to be observed 3 weeks after the MDAs occurred, when the direct mosquitocidal effects are inapparent and the drug is at very low pharmacokinetic levels or undetectable in most of the blood samples tested from the populace, suggests a delayed action of the drug's effect on mosquito population structure and infectiousness[170,215]. Perhaps this delayed effect is due to increased probability of killing the fewer, older mosquitoes that were actively blood feeding immediately after the MDA

was administered, and leaving unharmed most of the younger, newly emerged mosquitoes with lower PIs and that have yet to blood feed.

The age model developed using PIs obtained for mesocosm-aged laboratory colony of *An. gambiae* was somewhat limited due to potential differences in the mosquitoes' wings, as well as the laboratory vs. field conditions experienced by the mosquitoes and possibly also the wing imaging performed. Overall, the lab mosquitoes had a very narrow PI range that limited our ability to interpolate age from wild mosquitoes with PIs residing outside the range of our model. Nonetheless, the best fit symmetrical sigmoidal model that fit the PI data from these laboratory mosquitoes and was used predict the age of the wild mosquitoes from the trial suggests little differences in the PIs among very young (1-4 days old) and very old (≥10 day old) mosquitoes, respectively, but a rapid shift from between these young to old classes in between the ages of 4 to 10 days, presumably due to extensive flying and loss of wing scales during this timeframe. Importantly, wild-type *Anopheles gambiae* do not become infectious until they complete the minimum EIP, which typically correlates with them reaching the 2- or 3-parous state, or approximately 8-11 days old, thus our model's ability to predict proportions of 'old' mosquitoes with cut-off PIs ≥129.7 may be a simple method to classify potentially infectious *An. gambiae* in a population[284,285,299]. Nonetheless, it remains to be seen if this model will similarly fit PI data from wild type mosquitoes reared in large outdoors mesocosms in Africa.

While our newer analytical method allowed for better normalization of wing photos, further work could be done to refine the use of wing pictures to age mosquitoes. Technologies which auto-crop images to only include the wing, or which focus PI or

machine vision analyses on specific wing areas that are more sensitive to scale loss from flying (such as the wing fringe), could lead to a more refined analysis of mosquito age structures. Additionally, further standardization of photo backgrounds and microscope light intensities would likely add more control to the method and allow for easier comparisons across space and time. We believe that these refinements would abrogate the need for regionally calibrated age models at each place and time such analyses were to occur. Finally, due to sample preservation and costs, we were not able to speciate most of the mosquitoes from the entire *Anopheles gambiae* sensu lato complex from RIMDAMAL II. As such, there may be differences in *An. gambiae* sensu strictu, *An. coluzzi* and *An. arabiensis* PIs[170,220]. Therefore, further investigations into the *An. gambiae* species complex are needed to determine if specific species have differing PI ranges.

Overall, we have demonstrated how using PI on wing images can be used to easily age grade *Anopheles gambiae* mosquito populations. This method should easily be expanded to allow investigators and vector control experts across the world, who are implementing and evaluating control of malaria, helminth and arbovirus vectors, to expediently determine mosquito population ages from their surveillance efforts. Such efforts may be highly valuable for evaluation of their control applications and estimations of the risk of mosquito-borne disease spread within their communities.

3.4 Methods and materials

3.4.1 Mosquito rearing

Anopheles gambiae G3 were reared at 27-30°C with 60-80% relative humidity. A standard photoperiod of 16 hours light:8 hours dark was utilized. Larvae were raised in open-top plastic bins and fed a diet of TetraMin fish food (Spectum Brands Pet, LLC). Pupae were transferred into closed-top plastic bins. 24 hours after emergence, adults were aspirated and placed into a closed-top plastic adult bin. Adults were grouped based on their respective date of emergence to ensure adults were the same age. If adult collection was limited, groups were mixed but never exceeded more than two days in age difference.

3.4.2 Mesocosm experiment

These experiments were well described in Gray *et al*, 2022. In brief, 200 *An. gambiae* G3 mosquitoes were marked using florescent pigment powder (Shannon Luminous Materials, Inc.) placed into a large (122 cm long x 61 cm wide x 96.5 cm high) plastic bin in which a fake plant was placed in the middle to force the mosquitoes navigate around as they sought water and bloodmeals that were placed on opposite sides of the bin. Plastic dishes with holes cut into them covered the oviposition papers and sugar cubes. These obstacles were used to replicate a ‘wild’ environment for the lab-reared mosquitoes to force flying behaviors. Twice a week, 15 mosquitoes were removed from the mesocosm, and their wings were detached for analysis.

3.4.3 RIMDAMAL II mosquito collection and photo acquisition

During the RIMDAMAL II clinical trial, entomological sampling was conducted to compare entomological indices, such as bioassay survival, entomological inoculation

rate, and age structure, between the control and treatment arms of the trial. Mosquitoes were collected from 6 (3 treatment; 3 placebo) clusters (villages or village sectors), 1 and 3 weeks after each mass drug administration using a Prokopack aspirator inside predetermined households[302]. Mosquitoes were then transported to the field station, speciated, and *Anopheles* mosquitoes were retained. A portion of *An. gambiae* s.l. mosquitoes were subjected to wing removal. Removed wings were placed on a glass slide and photographed using a Leica EZ4 stereoscope (Leica Microsystems, USA). Photos were then electronically transmitted to Colorado State University for pixel intensity (PI) analyses.

Table 3.1: Proportions and totals number of wild *Anopheles gambiae* s.l. captured from each RIMDAMAL II cluster and arm, and during each year, corresponding to their pixel intensities and associated with their interpolated age class in days.

Cluster	**2019**			**Cluster**	**2020**		
Placebo	**≤128.56 (1-4 days old)**	**128.57-128.96 (5-9 days old)**	**≥128.97 (≥10 days old)**	**Placebo**	**≤128.56 (1-4 days old)**	**128.57-128.96 (5-9 days old)**	**≥128.97 (≥10 days old)**
DB (n=194)	0.572 (n=111)	0.258 (n=50)	0.170 (n=33)	DB (n=223)	1.000 (n=223)	0.000 (n=0)	0.000 (n=0)
DL (n=211)	0.569 (n=120)	0.213 (n=45)	0.218 (n=46)	DL (n=174)	1.000 (n=174)	0.000 (n=0)	0.000 (n=0)
TG (n=194)	0.464 (n=90)	0.082 (n=16)	0.454 (n=88)	TG (n=133)	1.000 (n=133)	0.000 (n=0)	0.000 (n=0)
Intervention	**≤128.56 (1-4 days old)**	**128.57-128.96 (5-9 days old)**	**≥128.97 (≥10 days old)**	**Intervention**	**≤128.56 (1-4 days old)**	**128.57-128.96 (5-9 days old)**	**≥128.97 (≥10 days old)**
KP(n=176)	0.472 (n=83)	0.153 (n=27)	0.375 (n=66)	KP (n=119)	1.000 (n=119)	0.000(n=0)	0.000 (n=0)
KS (n=114)	0.412 (n=47)	0.421 (n=48)	0.167 (n=19)	KS (n=117)	1.000 (n=117)	0.000(n=0)	0.000 (n=0)
(n=140)	0.436 (n=61)	0.457 (n=64)	0.107 (n=15)	SG (n=125)	1.000 (n=125)	0.000(n=0)	0.000 (n=0)

3.4.4 Digital wing photo analysis

Each mosquito had photos taken of both wings using the same Leica EZ4 stereoscope and PI was calculated for each wing using the wing photos processed by the BigPicture program developed by Viden Technologies, LLC. Subsequently, the mean of the left- and right-wing PIs were calculated to establish a PI per individual mosquito (a single PI from the mean of both wings). If a mosquito had only one wing image, or if one wing was folder or torn during the slide mounting process, the individual mosquito was given a PI that came from only one of its wings.

3.4.5 Statistical and mathematical methods

Raw PI values from the trial were modeled using a log-linked gamma generalized linear model. Left- and right-wing PI values were input into the model individually, with a mosquito-level random effect term as a grouping variable. Fixed effects of treatment arm, year, and their interaction term were included. To delineate population PI range differences, mosquitoes were placed into bins with a difference of 0.3 PI. Furthermore, mosquitoes were separated based on the arm location they were captured in to determine differences in PI bins. To establish an age-to-pixel intensity model, mean PIs from mesocosm-reared colonized mosquitoes were first analyzed with a linear model using GraphPad Prism (v10.1.1), and then in a stepwise approach all non-linear models in the program were compared to the linear model using Akaike's Information Criterion. The best fit model emerging from this process was the Sigmoidal Variable Slope model. The predicted ages of the wild mosquitoes captured in the RIMDAMAL II trial were then interpolated using this best-fit model.

CHAPTER 4: DEVELOPMENT OF PIXEL INTENSITY MODELS TO AGE WILD *CULEX TARSALIS* FROM THE MOUNTAIN WEST

4.1 Introduction

Since the introduction of West Nile Virus (WNV) into the United States in 1999, it has spread across North America, becoming endemic on the front range of the Rockies in 2002 and then in most of California in 2003[16,22,303,304]. While WNV is transmitted in an endemic cycle between birds and mosquitoes, infected mosquitoes can transmit the virus to humans and other vertebrates in an epidemic cycle[23]. Viremias in humans do not reach titers that are able to efficiently infect naïve mosquitoes, however, infected people can display a range of symptoms from benign to severe[23]. 80% of those who are infected will be asymptomatic, while 20% will exhibit febrile illness[305]. Only 1/150 people who are infected will develop West Nile Neuroinvasive Disease (WNND), which requires hospitalization[305]. Evidence suggests risk factors such as age and comorbidities including congestive heart failure, chronic obstructive pulmonary disease, diabetes, hypertension can contribute to progression towards WNND[305].

Competent vectors of WNV in the United States include *Culex tarsalis*, *Cx. pipiens*, *Cx. quinquefasciatus,* and *Coquillettidia perturbans*, which have a wide distribution across the United States[20,21,306]. However, *Cx. tarsalis* is considered the main epidemic vector in the western US, and a primary target of mosquito control districts as it accounts for 76% of the WNV positive pools in the west, while *Cx. pipiens*, the primary endemic vector in the west, has the second highest pool positivity rate at

14%[21]. In 2024, the CDC reported that the highest number of (>25) human cases in the western US came from North Dakota (38 cases, 4.77 cases per 100,000), Nebraska (92, 4.59 cases per 100,000), Colorado (76, 1.28 cases per 100,000), Nevada (27, 0.83 cases per 100,000), and California (123, 0.31 cases per 100,000)[307]. It has been suggested that due to the climate of the Great Plains, small pools of water accumulate, condensing both vector and bird populations, creating microcosms of high virus amplification and transmission among these populations[21]. Furthermore, Bolling et al. described how high elevation and low degree days limit the presence of *Cx tarsalis* and *Cx. pipiens,* and thus WNV transmission, to the relatively warmer valleys of the mountain west where people and agriculture are concentrated around the riparian corridors of Colorado, Utah, Idaho and California[21,308]. Additionally, it was found through *Cx. tarsalis* bloodmeal analyses that these mosquitoes shift their feeding behavior towards mammals later in the season, increasing the propensity of human WNV infections occurring in July through September and indicating a flexibility in host preference, making *Cx. tarsalis* specialists at disseminating WNV in both mammals and birds[44,309]. Moreover, *Cx. tarsalis* in these agricultural areas are often insecticide resistant, likely due to its breeding in niches within and surrounding agricultural sites, which are heavily treated with herbicides and insecticides[108,109,112,310]. The species is also known to fly long distances when compared to other mosquitoes, actively flying up to 12.6 km in search of a bloodmeal, however it was found that the vast majority (84%) stay within a 0.5 km range[49,50]. All these traits contribute to *Cx. tarsalis*'s efficient transmission of WNV in the western US and importance for control efforts.

When comparing the control of *Cx. tarsalis* to *Anopheles gambiae* control, it is important to be cognizant of several key traits that differentiate these species as vectors of pathogens. The extrinsic incubation period (EIP) is the time it takes a pathogen to develop in, and be transmitted by, a competent vector. The EIP allows researchers and mosquito control experts to understand when a mosquito population poses the greatest risk to humans and animals. If the majority of a mosquito population's age is less than the EIP, the relative risk of pathogen transmission is lower than if the majority of the population's age is greater than the EIP[311].The EIP for *Plasmodium* species to develop in *An. gambiae* is between 9-16 days, depending on temperature and species, as the parasite needs to undergo sporogony, a specific development within the mosquito that includes fertilization, midgut invasion and multiplying into numerous sporozoites that ultimately disseminate into the salivary glands, making the mosquito infectious[282,312–314]. For this reason, in chapter 3, we focused on wild mosquitoes which had a PI value in our *An. gambiae* age model that corresponded to ≥ 10 days old. However, the EIP of WNV in *Cx. tarsalis* is approximately 8-18 days old depending on temperature, but with a small proportion mosquitoes that may become infectious as early 4 days after taking an infected bloodmeal[13–15].The latter phenomenon occurs when virus disseminates out of the midgut and into the salivary glands in the thorax quickly due to 'leaky midguts', and viruses do not need to undergo a time-dependent process of sexual development within the midgut for the mosquito to become infectious[13–15]. WNV can also be vertically transmitted in some mosquitoes, infecting a subset of eggs from an infected female, and resulting in a limited number of infected progeny able to transmit WNV without taking an initial infected blood meal[315,316]. Additionally, *Cx. tarsalis* must diapause, or overwinter,

as adults, potentially allowing for this vertical transmission cycle to occur when an infected female emerges from diapause in the Spring and lays a new batch of egg rafts[317]. In addition to the wider range of the EIP of WNV in *Cx. tarsalis*, this species is known to be relatively long-lived (Mean adult age: 27.07±1.80 days), allowing females more opportunities to transmit virus[318,319]. Finally, *Cx. tarsalis* can be autogenous, meaning they can lay a batch of eggs without the need for a bloodmeal[49,51]. This capability largely relies on the food sources the mosquito has available to them while in the larvae stage. Considering all of these traits, age-grading of *Cx. tarsalis* populations is necessary to understand their population biology across seasons to help discern the relative risk of populations for WNV transmission to humans. However, the current 'gold-standard' age grading techniques, which focus primarily on parity measures, may not be as sensitive when estimating *Cx. tarsalis* calendar age[49,51]. To rectify this, we hypothesized that the new tools we have developed to age-grade wild *An. gambiae* mosquitoes may also find use for age grading *Cx. tarsalis* populations in the western US while also allowing us to compare the population biology of these very different vectors of mosquito borne pathogens[320].

We have been developing and testing ivermectin-treated bird feed as a novel method to control WNV transmission[221,223]. As part of this effort, we performed limited pre-trial sampling in Northern Colorado in the summer of 2023 and then in the summer of 2024 we initiated a randomized control trial with our finalized formulation, whereby we placed IVM-coated birdseed on homeowners' properties in northern Colorado. Small passerine birds had access to feed on the treated birdseed, which caused them to have mosquitocidal concentrations of IVM in their blood depending on their feeding

frequency. The primary outcome of this two-season, 20 cluster trial (2024 – 2025) is the summarized vector index (VI) in each trial arm, which is the product of mosquito abundance per trap per night and the maximum likelihood estimate of WNV infection rate as measured from pooled mosquitoes tested using quantitative RT-PCR. One key secondary outcome is the estimated *Cx. tarsalis* population structure in each trial arm as measured using wing pixel intensity (PI), with the hypothesis that mosquitoes from sites in the treatment arm would have significantly higher PI values, corresponding to lower predicted ages, which are younger than the EIP compared to mosquitoes from control arm sites. This hypothesized effect is similar to the age structure-related secondary hypothesis for *An. gambiae* sensu lato captured from the RIMDAMAL II clinical trial discussed in chapter 3[320].

A second mosquito control trial supported by our lab was also undertaken in the summer of 2025, managed by mosquito abatement districts in Salt Lake City, UT (Salt Lake City Mosquito Abatement District; SLCMAD) and Davis, UT (Mosquito Abatement District, Davis; MADD) and integrated with our Rockies and High Plains Vector-borne Diseases Training and Evaluation Center (RaHP VEC) to evaluate the efficacy of ultra-low volume (ULV) aerial-treatments of naled for *Cx. tarsalis* control around the wetlands of the Great Salt Lake (GSL). Naled is an organophosphate insecticide mainly used for the control of mosquitoes with some applications in agriculture. It kills mosquitoes by interfering with their central nervous system, inhibiting the enzyme cholinesterase and causing muscles to aberrantly contract, killing the mosquito.

Given our observations of a modest decrease in wild *An. gambiae* PI following the administration of ivermectin MDA and then a much larger decrease following the

distribution IG2® bed nets during the intervention period of the RIMDAMAL II trial in Burkina Faso, we wanted to determine if the same effect could be observed in *Cx. tarsalis* populations from northern Colorado during our trial testing IVM treated bird seed and from populations around the GSL during our testing of naled efficacy in partnership with SLCMAD and MADD[320]. Additionally, we explored the development of an age model for *Cx. tarsalis* using PI to interpolate wild *Cx. tarsalis* population age dynamics in these locations.

4.2 Results

4.2.1 Initial testing of Culex tarsalis wing pixel intensity range using wild caught mosquitoes

Cx. tarsalis mosquitoes were collected during the summer of 2023 during epidemiological weeks 34 and 35 in northern Colorado from volunteers' properties using resting traps and processed to determine their wing pixel intensity. Individual pixel intensity values were plotted in addition to PI bins using a delta of 0.0652947 PI units to establish 19 different bins. Compared to the wild *Anopheles gambiae* sensu lato from the RIMDAMAL II clinical trial discussed in chapter 3, wild *Cx. tarsalis* exhibited a constricted PI range of 128.36-128.95, but with a similar mean PI of 128.63 (95% CI: 128.62 - 128.66) (Figure 4.1). The PI data from the 2023 collection were normally distributed (Shapiro Wilk test; $p = 0.8016$) around the mean, with few mosquitoes in both the low and high ends of the range, in contrast to the top- or right-skewed tail of PI data from wild *An. gambiae* (Figure 3.3)

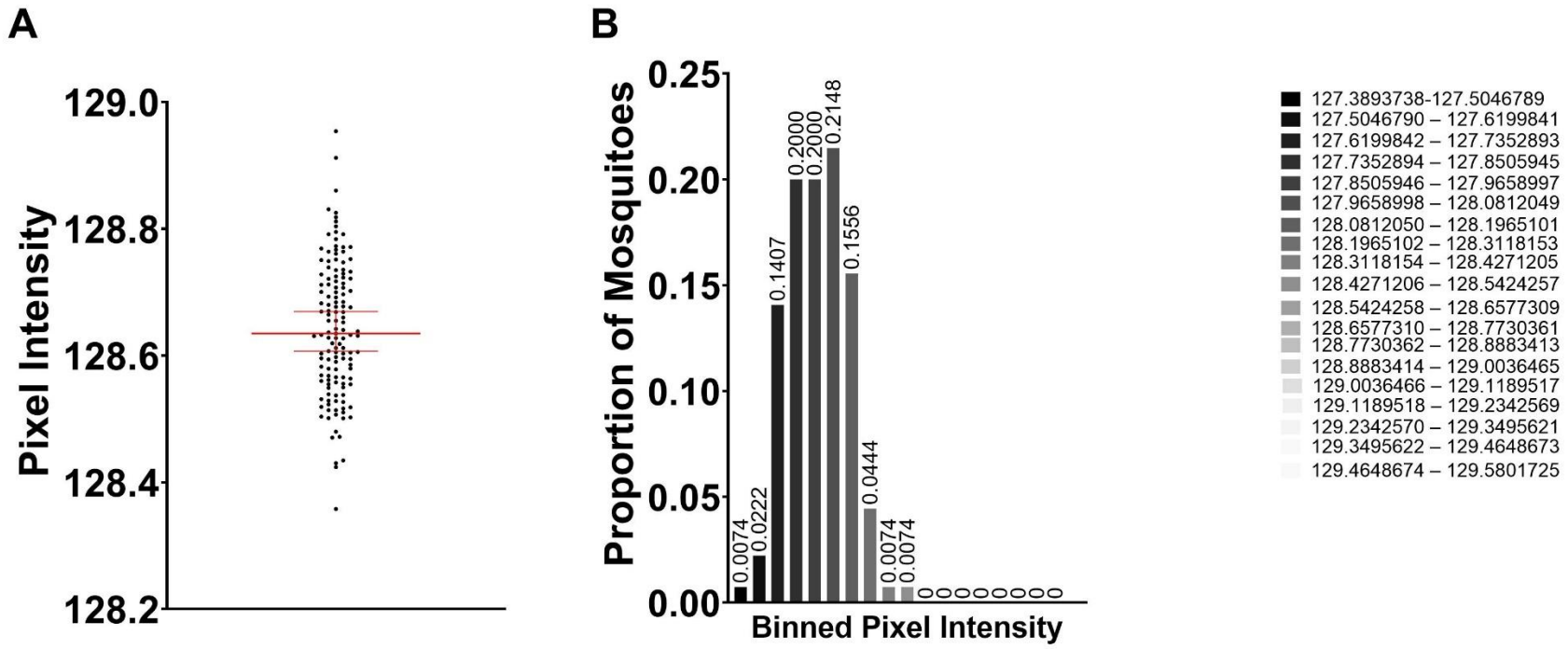

Figure 4.1: Pixel intensity of mosquitoes captured in 2023. (A) Individual plot point data with a mean PI of 128.64, 95% CI: 128.62-128.66, range 128.36 – 128.95. (B) Binned proportions of *Cx. tarsalis*.

4.2.2 Obtaining pixel intensity from Culex tarsalis wings during the 2024 field trial of ivermectin treated birdseed

During the 2024 field trial testing IVM treated birdseed, wild *Cx. tarsalis* mosquitoes were captured using CDC minitraps baited with dry ice from epidemiological weeks 27-35 across 20 sites within cities and towns in northern Colorado. Specifically, 10 broad geographical areas within cities or towns were selected and 2 paired households (sites) within each area were selected for sampling and randomly chosen to be treatment or control sites, and wing images of a proportion of the *Cx. tarsalis* sampled each week were analyzed using PI. First, an analysis of the PI difference between each set of mosquito's wings was performed, whereby a positive difference is associated with higher PI/more scale loss on the left-wing and a negative difference is associated with higher PI/more scale loss on the right-wing. The PI differences in the mosquito population's left and right wings were significant (52.49% (2005/3820) had a positive difference; Binomial test; $p = 0.0022$) (Figure 4.2).

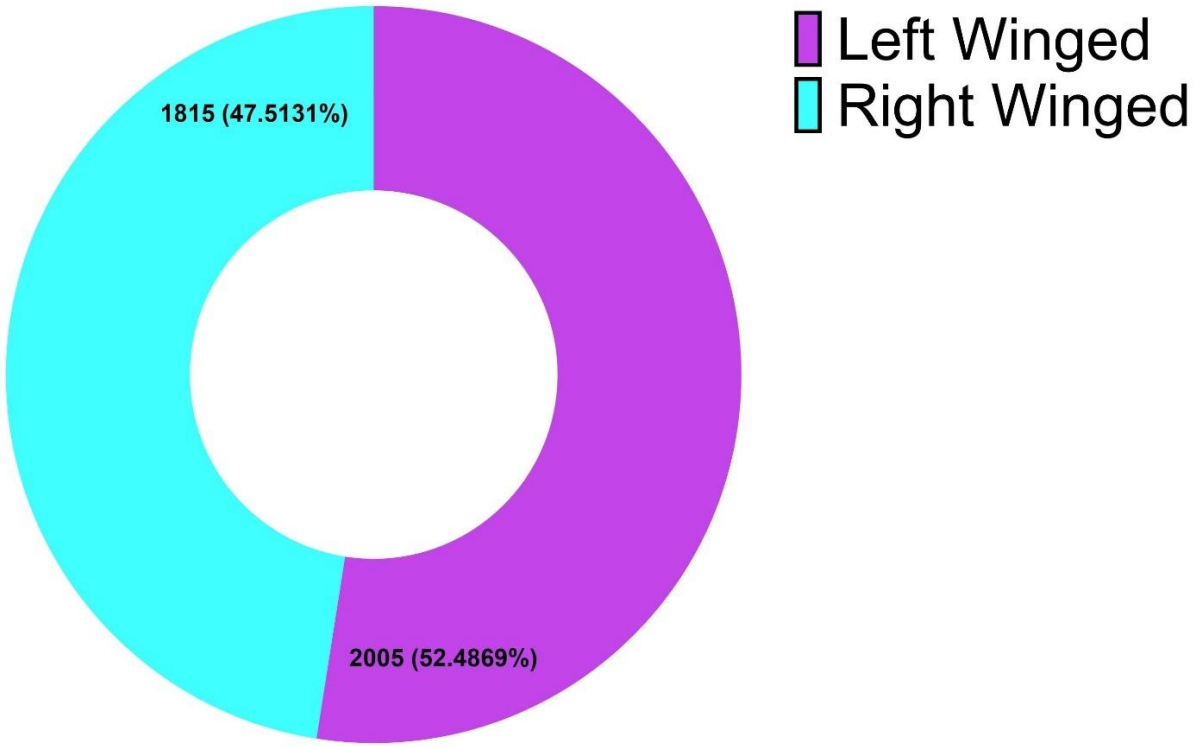

Figure 4.2: Northern Colorado Culex tarsalis wing differences. The difference between the left and right pixel intensities were calculated. A positive difference resulted in a higher left-wing PI and a negative difference resulted in a higher right-wing PI. A binomial test found there was significance (P = 0.0022) between the two populations with the assumption that wing favorability would be evenly split within the population.

All individual *Cx. tarsalis* (*n* = 3990) PIs were then plotted and analyzed as a group from all sites and regardless of capture date or trial arm (Figure 4.3), and this grouping was also plotted as bins to better understand the population's PI distributions (Figure 4.3). The population PI ranges were greater than the wild mosquitoes caught in 2023, with a range of 128.34-129.58 and a median PI of 128.97 (95% CI: 128.96-128.97) (Figure 4.3), but the data were not normally distributed (Shapiro-Wilk test; $p < 0.0001$)

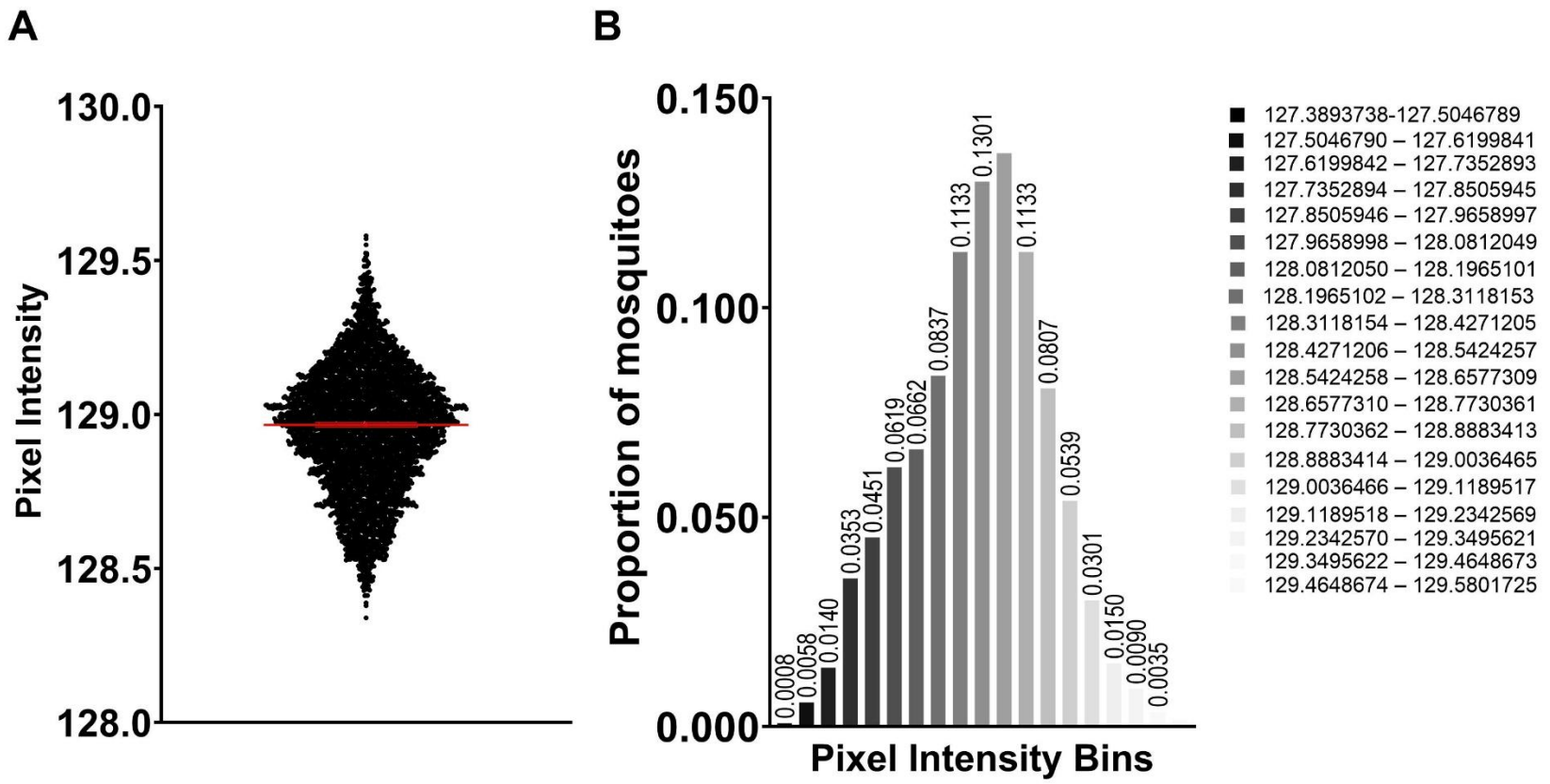

Figure 4.3: Pixel intensity of mosquitoes captured in 2024. (A) Individual plot point data with a median PI of 128.97, 95% CI: 128.96-128.97, range 128.34 – 129.58. (B) Binned proportions of *Cx. tarsalis*.

We then compared the mosquito PI data by trial arm to elucidate if IVM was having an observable effect on PI data (Figure 4.4).

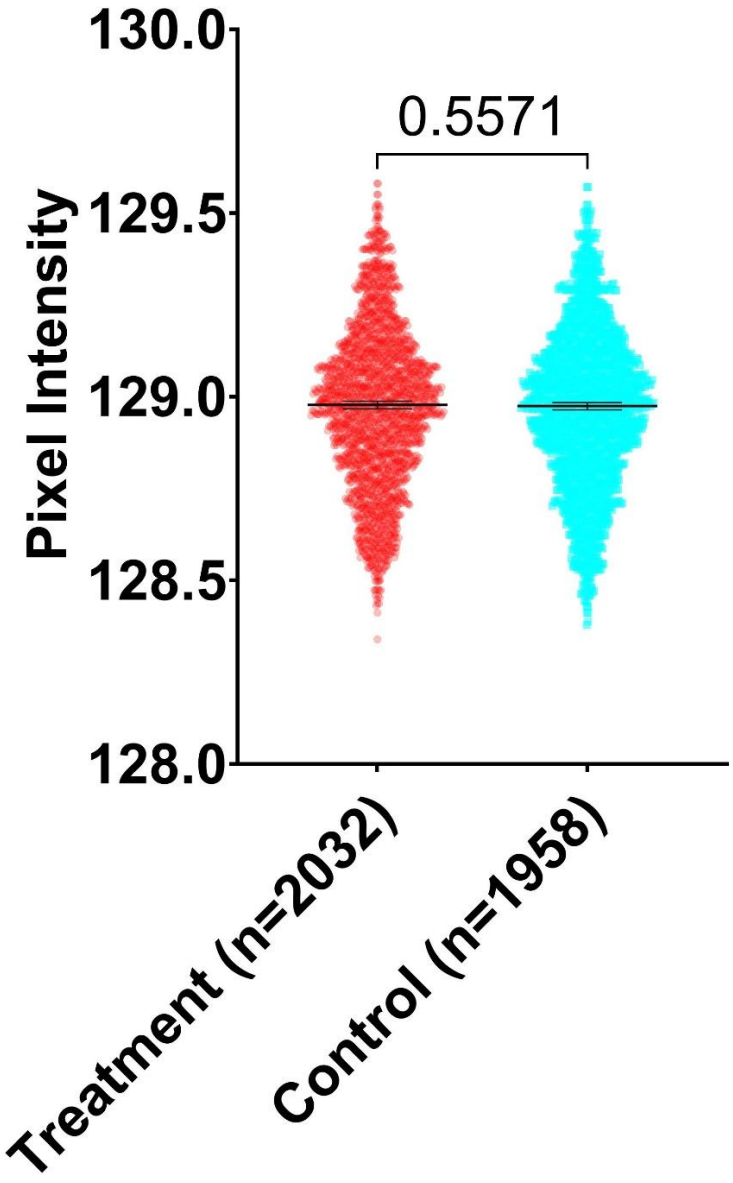

Figure 4.4: Comparisons of the treatment and the control sites median pixel intensities. The treatment sites had a median PI of 128.98 (95% CI: 128.97 – 128.99, range 128.34 – 129.58) while the control sites have a median of 128.97 (95% CI: 128.96 – 128.98, range: 128.38 – 129.57). A Mann-Whitney test indicated no significant difference (p = 0.5571) between the two arms.

Since neither the treatment ($p < 0.0001$) nor the control ($p < 0.0001$) arms indicated normality using a Shapiro-Wilks test, a Mann-Whitney test was used to determine if the arms' PI medians were similar. It was found that the two populations had statistically indistinguishable median PIs (Hodges-Lehmann median difference = -0.004; 95% CI difference -0.02 – 0.01*; p* = 0.5571) (Figures 4.4 & 4.5).

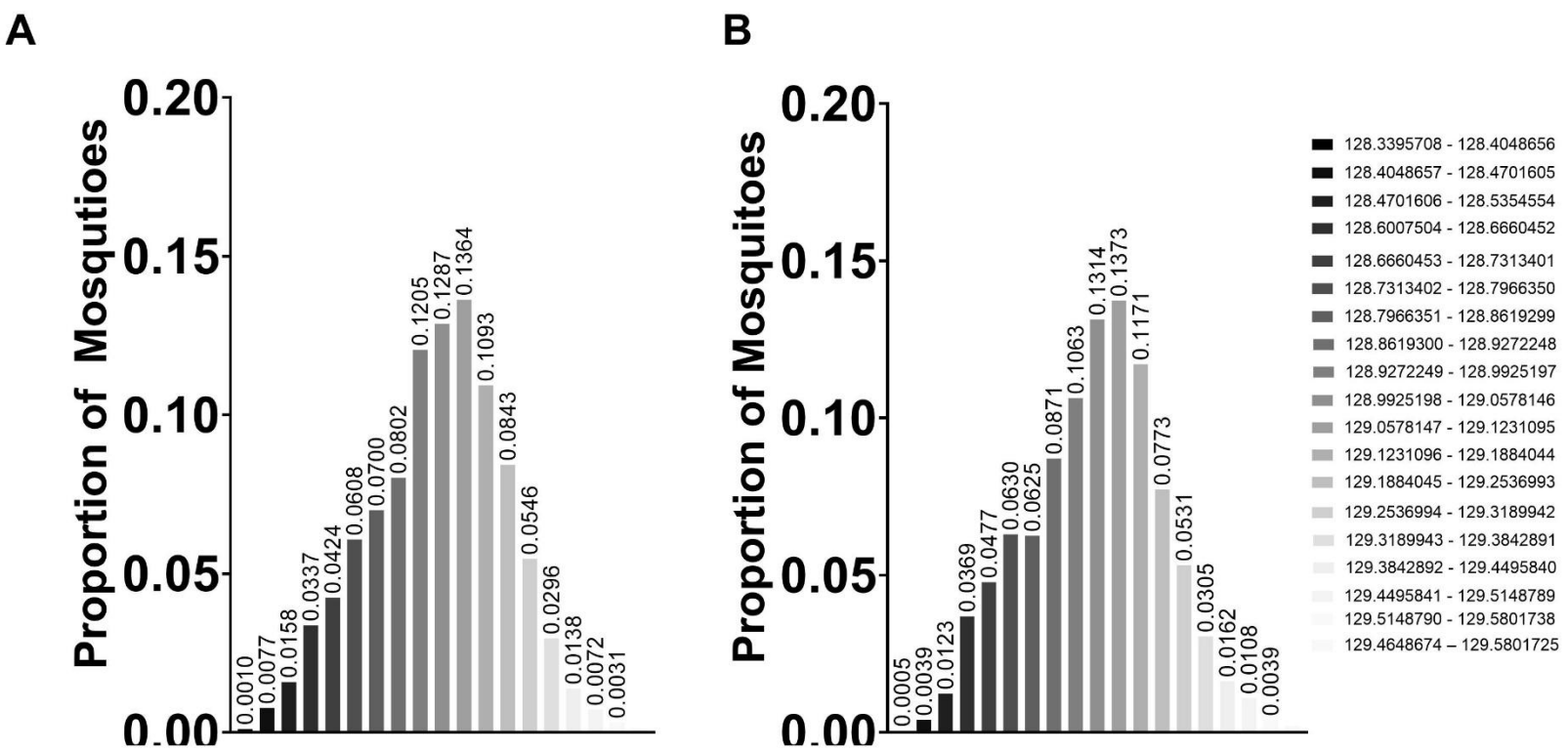

Figure 4.5: Binned pixel intensity proportions of mosquitoes captured in 2024 by arm. (A) Mosquitoes captured in the control arm. (B) Mosquitoes captured in the treatment arm.

We then analyzed the individual sites to determine if the arms within the site were different from one another (Table 4.1). In only one site was the data normally distributed within both arms (NG; Shapiro-Wilk test; Control $p = 0.2777$; Treatment $p = 0.2040$), and in the rest of the sites either one or both arms had non-normal data distributions.

Table 4.1: Comparisons between arms at each test site

Site		P-value
NG		<0.0001^
ET		<0.0001`
FN		0.0012`
TM		0.3968`
FS		0.6548`
SV		0.0158`
SW		0.1868`
SG		0.0012`
AP		0.5159`
NW		0.2515`

^ = unpaired test; ` = Mann-Whitney test

Next we analyzed the data by arm with respect to collection site and capture week (Figures 4.6 & 4.7, respectively).

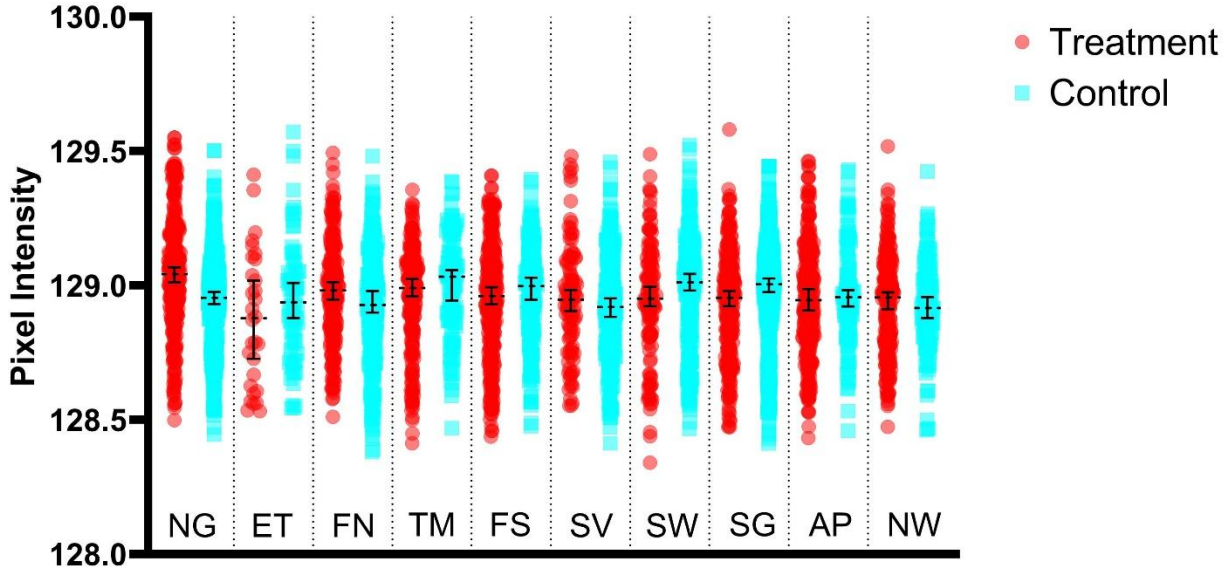

Figure 4.6: *Culex tarsalis* pixel intensity by collection site and arm. Comparisons of PI by arm and site only exhibit significant differences in locations NG ($p < 0.0001$), ET ($p < 0.0001$), FN ($p = 0.0012$), SV ($p = 0.0158$), and SG ($p = 0.0012$). NG was tested using an unpaired t-test, all others were tested with a Mann-Whitney test.

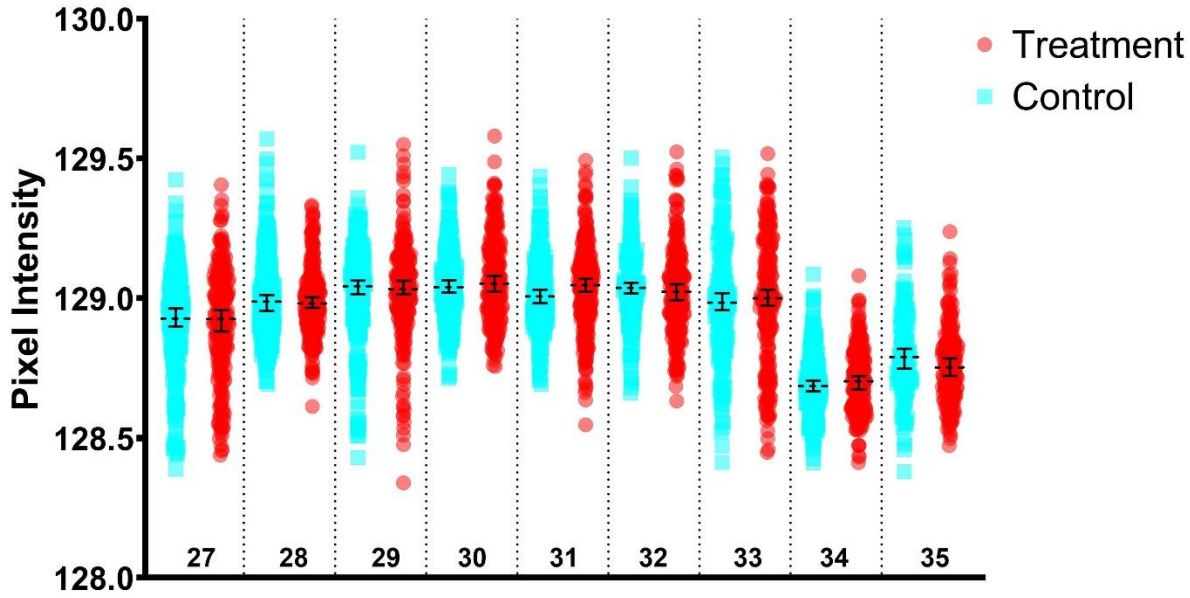

Figure 4.7: *Culex tarsalis* pixel intensity by epidemiological and arm. Comparisons of PI by arm during epidemiological weeks indicated significant differences during week 35 ($p = 0.0172$) using a Mann-Whitney test.

From the individual plot point data grouped by arm and site, the PI of *Cx. tarsalis* populations captured in the NG treatment site was significantly higher (Kruskal-Wallis test; $p < 0.0001$), when compared to all other treatment sites, however, all other treatment sites were similar to one another (Figure 4.6 & Table 4.2). Additionally, when comparing the control sites, it was found that most sites were similar except for FN versus TM ($p = 0.0386$), TM versus SV ($p = 0.0224$), SV versus SW ($p = 0.0404$), and SV versus SG ($p = 0.00241$).

Table 4.2: Treatment site multiple comparisons

Site	Comparison	P-value
NG (*n* = 285)	ET (*n* = 30)	0.0004
NG (*n* = 285)	FN (*n* = 215)	0.006
NG (*n* = 285)	TM (*n* = 218)	0.001
NG (*n* = 285)	FS (*n* = 287)	<0.0001
NG (*n* = 285)	SV (*n* = 103)	0.0003
NG (*n* = 285)	SW (*n* = 125)	0.0004
NG (*n* = 285)	SG (*n* = 255)	<0.0001
NG (*n* = 285)	AP (*n* = 280)	<0.0001
NG (*n* = 285)	NW (*n* = 234)	<0.0001
Post hoc Dunn's multiple comparisons		

Finally, we examined if the PI changes within the arms differed across epidemiological weeks when the study occurred (Figure 4.7 & Table 4.3). It was found that differences between arms only occurred during epidemiological week 35 (Mann-Whitney test; $p = 0.0172$).

Table 4.3: Epidemiological week comparisons between arms		
EpiWeek		**P-value**
27		0.0574`
28		0.7038`
29		0.7567`
30		0.2391`
31		0.1007^
32		0.3460`
33		0.8103`
34		0.3438^
35		0.0172`
^ = unpaired test; ` = Mann-Whitney test		

4.2.4 Using pixel intensity to evaluate the efficacy of ULV aerial-treatment with naled around the Great Salt Lake, Utah

The 2024 trial of naled efficacy around the GSL consisted of seven individual spray events conducted between weeks 24-33, of which four were conducted over the southern GSL wetlands by SLCMAD on June 10, July 8, July 29, and August 12, and three were conducted over the eastern GSL wetlands by MADD on June 25, July 16 and August 6. Mosquito sampling in each region was performed in two adjacent spray blocks that were rotated between treatment and control status each date, and each sampled 1-day pre-treatment, and 1-day post-treatment. SLCMAD is in the process of drafting an analysis of all primary and secondary outcomes of the trial; here we are only presenting the age grading data from one secondary outcome. When collapsing data from all 7 spray events into control and treatment blocks sampled pre- and post-treatment, it was found that mosquitoes collected in the treatment blocks post-naled spraying had a significant (Mann-Whitney test; $p = 0.0083$) decrease in PI when compared to mosquitoes collected in the same blocks prior to the naled applications

(Figure 4.8, panel B), while the mosquitoes captured in control blocks on the same pre- and post-spray days had no change in their PIs (Mann-Whitney test; $p = 0.1211$) (Figure 4.8, panel A). Alternatively, comparisons of the mosquito PIs from the pre-treatment day collections across the Control vs. Treatment blocks (Figure 4.9, panel A, Mann-Whitney test; $p = 0.2590$), and from the post-treatment day collections across the Control vs. Treatment blocks (Figure 4.9, panel B, Mann-Whitney test; $p = 0.9050$) showed no significant differences.

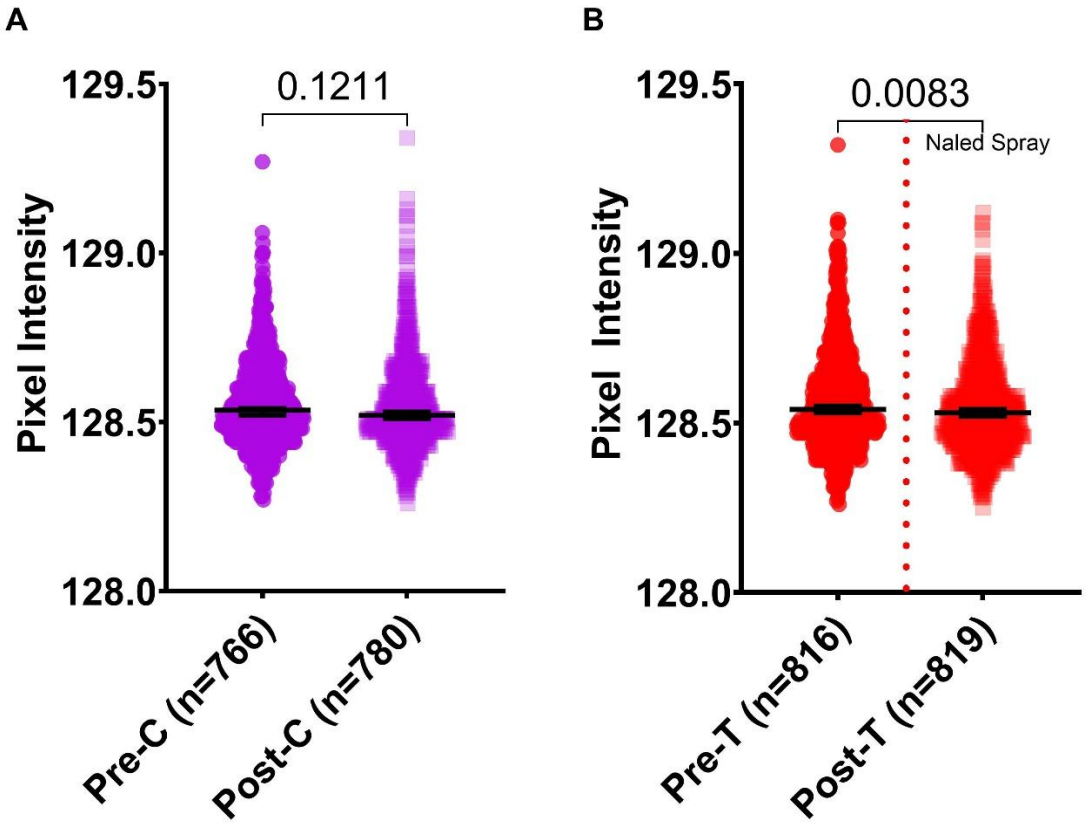

Figure 4.8: Comparisons of site before and after the application of naled. (A) PI of mosquitoes which were captured in the designated control sites before and after naled was applied to the treatment sites. (B) PI of mosquitoes which were captured in the designated treatment sites before and after naled was applied to the treatment sites. Mann-Whitney test indicated a significant difference ($p = 0.0083$) in PI in the treatment sites, but not in the control sites ($p = 0.1211$)

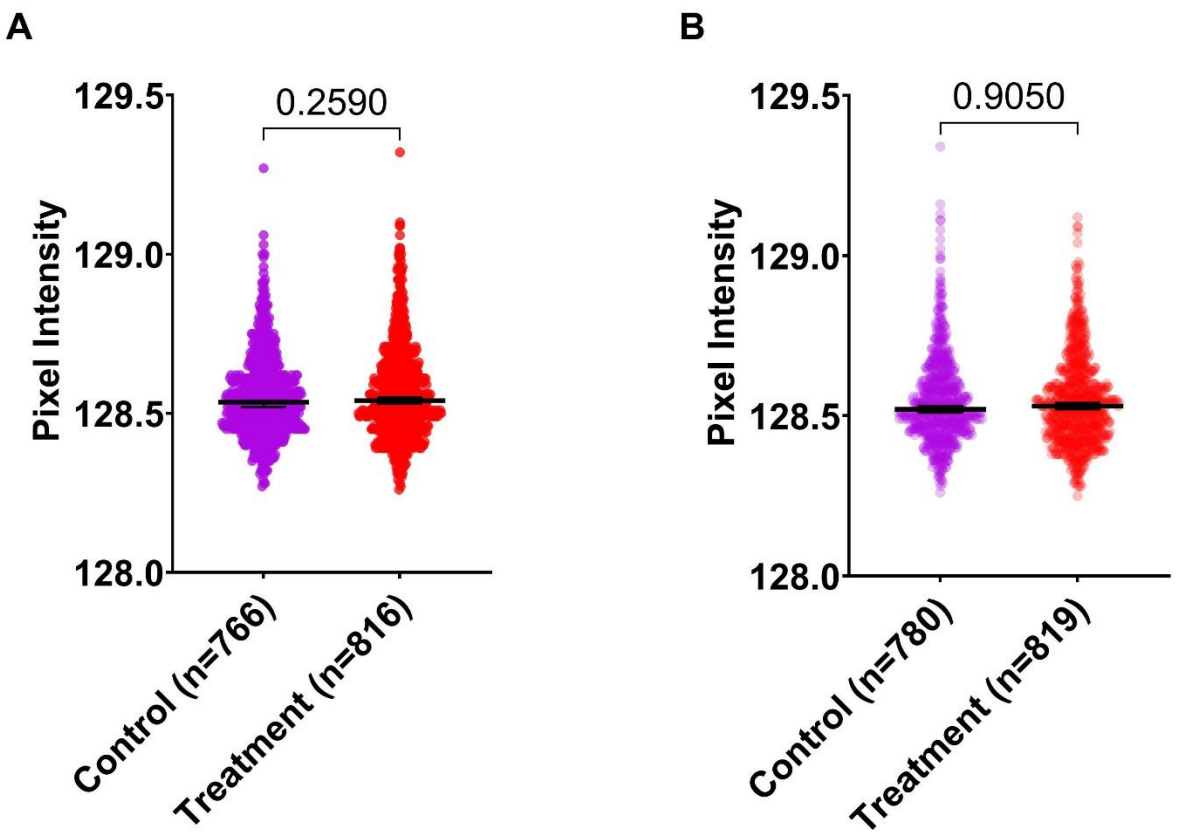

Figure 4.9: Comparisons of arms before and after the application of naled. (A) PI of mosquitoes which were captured before naled was applied to the treatment sites. (B) PI of mosquitoes which were captured after naled was applied to the treatment sites. Mann-Whitney test indicated no significant difference between arms before (p = 0.2590) or after (p = 0.9050) naled was applied to the treatment sites.

To determine if different trial effects occurred among the 7 different spray events that occurred on different days, or occurred between the two GSL locations in which the spray events were conducted by either SLCMAD (southern GSL) or MADD (eastern GSL), we analyzed the mosquito PI data from each spray event separately to understand the differences between the pre-and post-application of naled within each trial (Figures 4.10, 4.11 & Table 4.4).

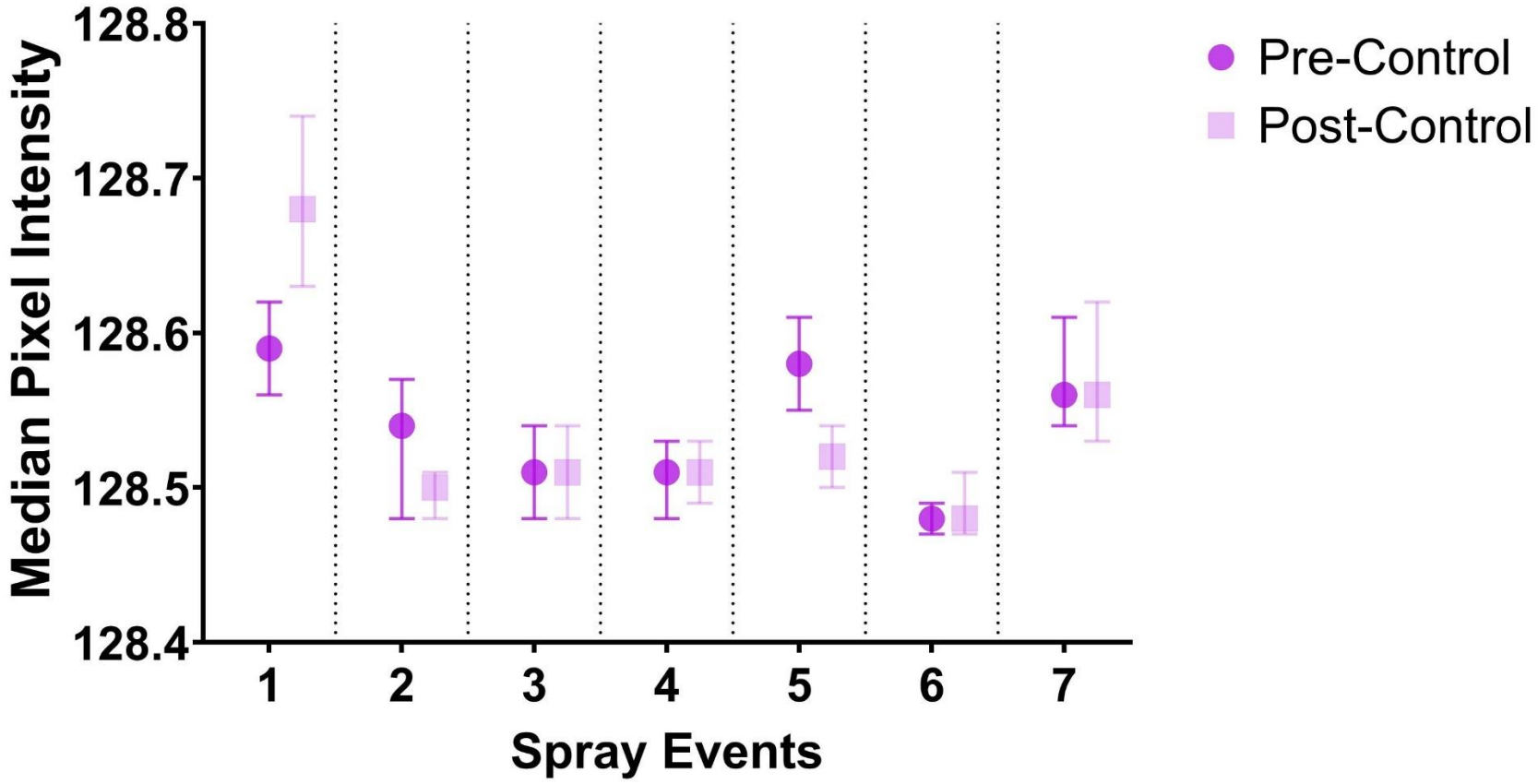

Figure 4.10: Control median pixel intensity before and after naled was applied to the treatment site by spray event. A significant difference was only found during spray events 1 (p = 0.0032), 2 (p = 0.0006), and 5 (p = 0.0002) using a Mann-Whitney test.

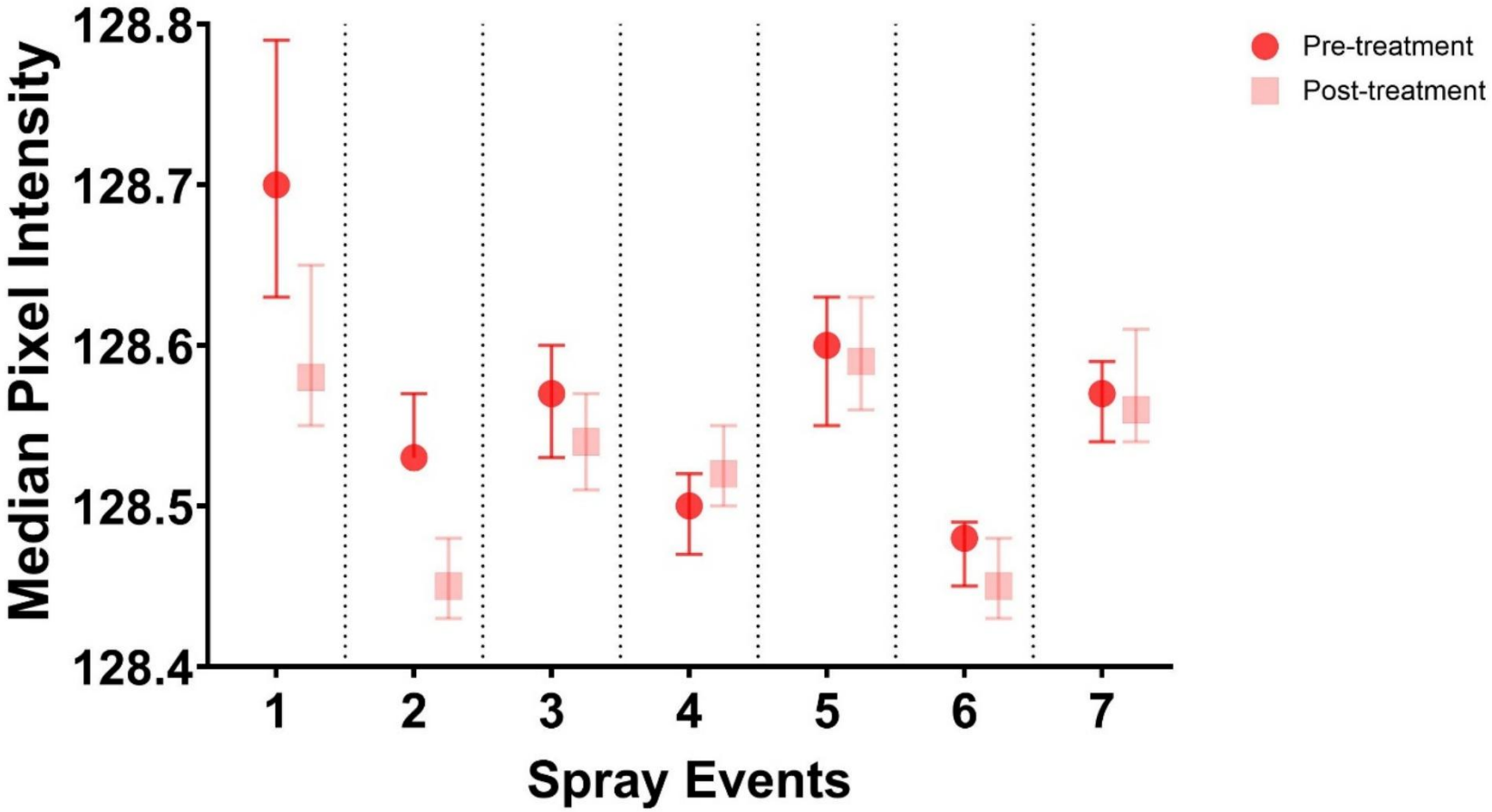

Figure 4.11: Treatment median pixel intensity before and after naled was applied by spray event. A significant difference was only found during spray events 1 (Mann-Whitney; $p = 0.0042$), 2 (Unpaired t-test; $p < 0.0001$), and 4 (Mann-Whitney; $p = 0.0458$).

When examining spray events 1, 3, 5, and 7 (conducted by SLCMAD), the only significant differences found between the control sites were during spray event 1 (Mann-Whitney test; $p = 0.0032$) and 5 (Mann-Whitney test; $p = 0.0002$) (Table 4.4). While the only significant difference in the treatment sites occurred in spray event 1 (Mann-Whitney test; $p = 0.0042$) (Table 4.4). When analyzing data from the MADD site, a significant difference in PI was only found during spray event 2 in both the control arm (Mann-Whitney test; $p = 0.0006$) and the treatment arm (Unpaired t-test; $p < 0.0001$) (Table 4.4).

Table 4.4: GSL trial comparisons between arms

Control			
Spray Event	**Dates**	**Location**	**P-value**
1	6/10-6/13	6/10SLCMAD	0.0032**
2	6/25-6/28	MADD	0.0006**
3	7/8-7/11	SLCMAD	0.9297**
4	7/16-7/19	MADD	0.2590*
5	7/29-8/1	SLCMAD	0.0002**
6	8/6-8/9	MADD	0.5514**
7	8/12-8/15	SLCMAD	0.3559**
Treatment			
Spray Event	**Dates**	**Location**	**P-value**
1	6/10-6/13	SLCMAD	0.0042**
2	6/25-6/28	MADD	<0.0001*
3	7/8-7/11	SLCMAD	0.6320*
4	7/16-7/19	MADD	0.0458**
5	7/29-8/1	SLCMAD	0.6721**
6	8/6-8/9	MADD	0.2182**
7	8/12-8/15	SLCMAD	0.6070**
* = unpaired test; ** = Mann-Whitney test			

4.2.5 Comparing parity rates and pixel intensity to mosquitoes in Salt Lake City, Utah

In the naled efficacy trial conducted in Utah, a portion of the mosquitoes that were assessed for mosquito wing PI were also tested for parity by dissecting their ovaries and examining the ovarial tracheoles skein coiling, which allowed us to compare these two different age grading methods in the context of naled efficacy on the mosquito population. The same groups of mosquitoes were analyzed for increases or decreases in median wing PI and parity over each spray event, from collections occurring pre-spraying and post-spraying, both in the control (Table 4.5) and treatment (Table 4.6) arms. In the control arm (Table 4.5), the direction of changes in mosquito PI and parity were congruent over three spray events (events 1, 2, 5), and in the other spray events, only parity rates changed (events 3, 4, 6 = increased; event 7 = decreased) while mosquito PI remained unchanged. However, in the treatment arm (Table 4.6), mosquito PI and parity decreased over every spray event except for event 4, and the direction of change was congruent between the mosquito PI and parity methods across all seven spray events.

Table 4.5: Comparisons of median pixel intensity and parity data from mosquitoes captured in the control arm during naled evaluation trials conducted near the Great Lake Salt, UT

			Median Pixel Intensity (95% CI)		Parity Rate	
Spray event	**Date**	**Location**	**Pre**	**Post**	**Pre**	**Post**
1	6/10-6/13	SLCMAD	128.59 (128.56-128.62) (*n* = 120)	128.68 (128.63-128.74) (*n* = 119)	0.65 (*n* = 33)	0.73 (*n* = 33)
2	6/25-6/28	MADD	128.54 (128.48-128.57) (*n* = 120)	128.50 (128.48-128.51) (*n* = 100)	0.65 (*n* = 22)	0.61 (*n* = 28)
3	7/8-7/11	SLCMAD	128.51 (128.48-128.54) (*n* = 119)	128.51 (128.48-128.51) (*n* = 100)	0.60 (*n* = 23)	0.62 (*n* = 24)
4	7/16-7/19	MADD	128.51 (128.48-128.53) (*n* = 100)	128.51 (128.49-128.53) (*n* = 120)	0.60 (*n* = 24)	0.61 (*n* = 22)
5	7/29-8/1	SLCMAD	128.58 (128.55-128.61) (*n* = 120)	128.52 (128.50-128.54) (*n* = 120)	0.73 (*n* = 30)	0.66 (*n* = 25)
6	8/6-8/9	MADD	128.48 (128.47-128.49) (*n* = 120)	128.48 (128.47-128.51) (*n* = 120)	0.31 (*n* = 11)	0.32 (*n* = 11)
7	8/12-8/15	SLCMAD	128.56 (128.54-128.61) (*n* = 87)	128.56 (128.53-128.62) (*n* = 81)	0.36 (*n* = 10)	0.35 (*n* = 8)

Nulliparous = 0; parous = 1; green indicates an increase from the pre-population; orange indicates a decrease from the pre-population

Table 4.5: Comparisons of median pixel intensity and parity data from mosquitoes captured in the treatment arm during naled evaluation trials conducted near the Great Lake Salt, UT

			Median Pixel Intensity (95% CI)		Parity Rate	
Spray event	**Date**	**Location**	**Pre**	**Post**	**Pre**	**Post**
1	6/10-6/13	SLCMAD	128.70 (128.63-128.79) (*n* = 121)	128.58 (128.55-128.65) (*n* = 100)	0.77 (*n* = 33)	0.58 (*n* = 31)
2	6/25-6/28	MADD	128.53 (128.53-128.57) (*n* = 120)	128.45 (128.43-128.48) (*n* = 120)	0.74 (*n* = 25)	0.54 (*n* = 21)
3	7/8-7/11	SLCMAD	128.57 (128.53-128.60) (*n* = 80)	128.54 (128.51-128.57) (*n* = 100)	0.73 (*n* = 19)	0.67 (*n* = 22)
4	7/16-7/19	MADD	128.50 (128.47-128.52) (*n* = 140)	128.52 (128.50-128.55) (*n* = 120)	0.60 (*n* = 32)	0.66 (*n* = 31)
5	7/29-8/1	SLCMAD	128.60 (128.55-128.63) (*n* = 116)	128.59 (128.56-128.63) (*n* = 119)	0.65 (*n* = 24)	0.63 (*n* = 26)
6	8/6-8/9	MADD	128.48 (128.45-128.49) (*n* = 120)	128.45 (128.43-128.48) (*n* = 120)	0.46 (*n* = 17)	0.33 (*n* = 12)
7	8/12-8/15	SLCMAD	128.57 (128.54-128.59) (*n* = 120)	128.56 (128.54-128.61) (*n* = 120)	0.38 (*n* = 13)	0.36 (*n* = 12)

Nulliparous = 0; parous = 1; green indicates an increase from the pre-population; orange indicates a decrease from the pre-population

4.2.5 Comparing wing pixel intensities between Salt Lake City, Utah and Northern Colorado Mosquitoes

We then decided to combine PI from wild mosquitoes which were captured in control sites around the GSL (*n* = 1546) and Northern Colorado (NoCo) (*n* = 1958) to compare these wild *Cx. tarsalis* population PI distributions and examine them relative to the wild *An. gambiae* s.l. population PI distributions from Burkina Faso presented in chapter 3. The *Cx. tarsalis* caught around the GSL had a significantly lower median PI (128.53, 95% CI: 125.52-125.53) and range of PI values (128.26 – 129.34) compared those caught in NoCo (median 128.97, 95% CI: 128.96-128.98; range: 128.38 – 129.57) (Mann-Whitney; $p < 0.0001$). Furthermore, the distribution of mosquito PIs from the GSL showed a skewed distribution reminiscent of the wild *An. gambiae* from Burkina Faso, with most mosquitoes having a low PI (presumably younger) and a long thin tail of high PI mosquitoes (presumably older) (Figure 4.12). In contrast mosquitoes caught and analyzed from NoCo had PIs with a well-balanced, near normal distribution, with nearly equal numbers lower (presumably younger) and higher (presumably older) than the median. Furthermore, the bulk of these mosquitoes had the same PI values as some of the highest PI mosquitoes from the GSL, suggesting very different age structures of the captured *Cx. tarsalis* populations between each site (Figure 4.12).

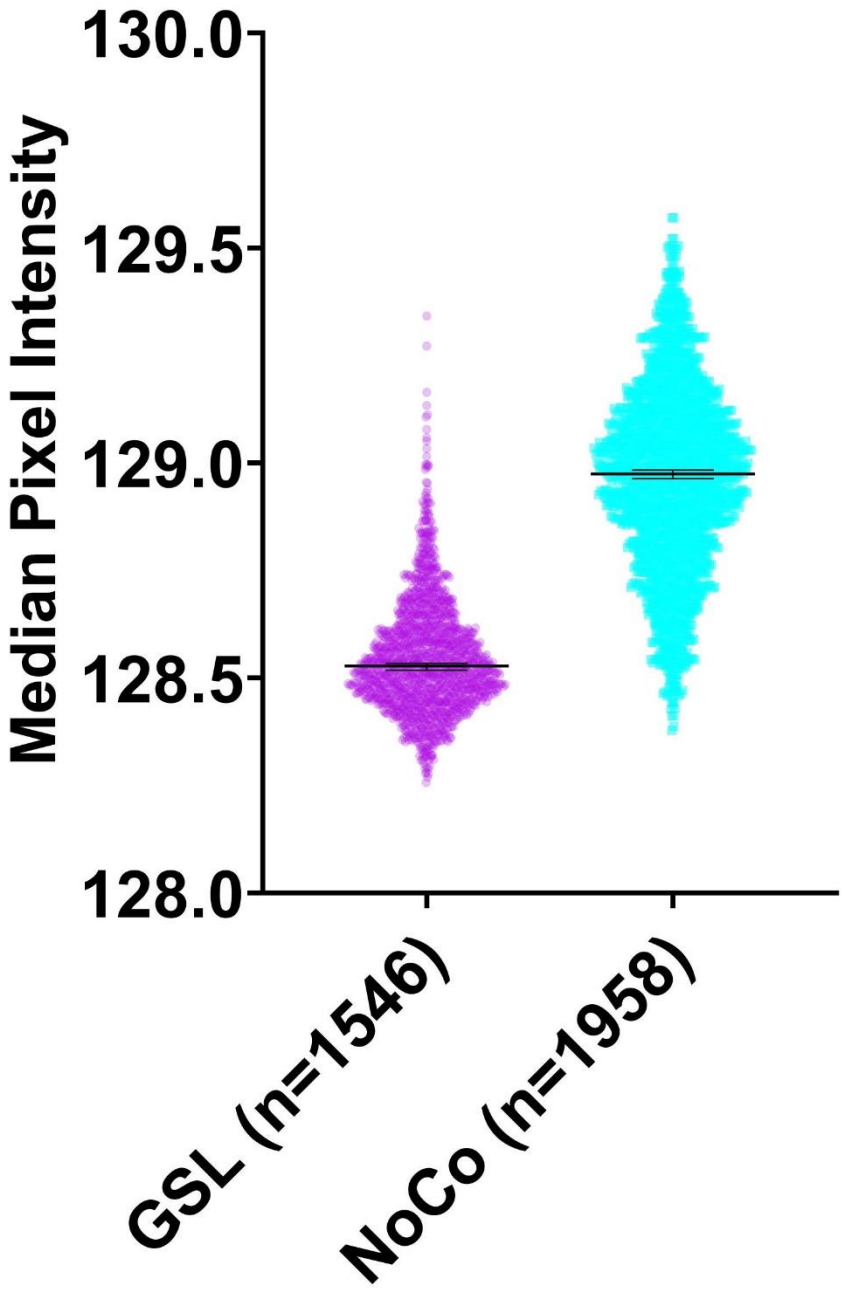

Figure 4.12: Comparison of *Culex tarsalis* pixel intensity of the control populations of both the Great Salt Lake naled application and Northern Colorado ivermectin coated birdseed field test. *Cx tarsalis* captured in control sites during the GSL naled applications had a significantly (Mann-Whitney; $p < 0.0001$) lower median PI (128.53, 95% CI: 125.52-125.53) than those captured in NoCo (128.97, 95% CI: 128.96-128.98).

4.2.6 Starting a known age model for Culex tarsalis

Finally, we aimed to create an age model for *Cx. tarsalis* using the Kern National Wildlife Refuge (KNWR) strain. Mosquitoes were reared post-eclosion to known ages in a large lab mesocosm where they were forced to fly frequently to complete normal life behaviors and then recaptured and their wings scored for PI. Additionally, we collected newly eclosed mosquitoes to establish a base line PI for this strain of *Cx. tarsalis.* Mosquitoes which were collected on day 0 (n = 21) had a median PI of 128.94 (95% CI: 128.84 – 129.01); day 3 mosquitoes (n = 13) had a median PI of 129.00 (95% CI: 128.88 – 129.09); and day 6 mosquitoes (n = 12) had a median PI of 129.02 (95% CI: 128.94 – 129.18) (Figure 4.13). The median PI's from these different age classes were not significantly different from one another (Kruskal-Wallis test, p = 0.1092), nonetheless, they increased at each life stage corresponding to the hypothesis that mosquitoes lose their wing scales as they age and this leads to increased PI at subsequent days post-eclosion. We had originally intended for the known age model to be established up to 21 days post-eclosion, but unfortunately, contamination of the colony with a different species forced us to end the experiment early.

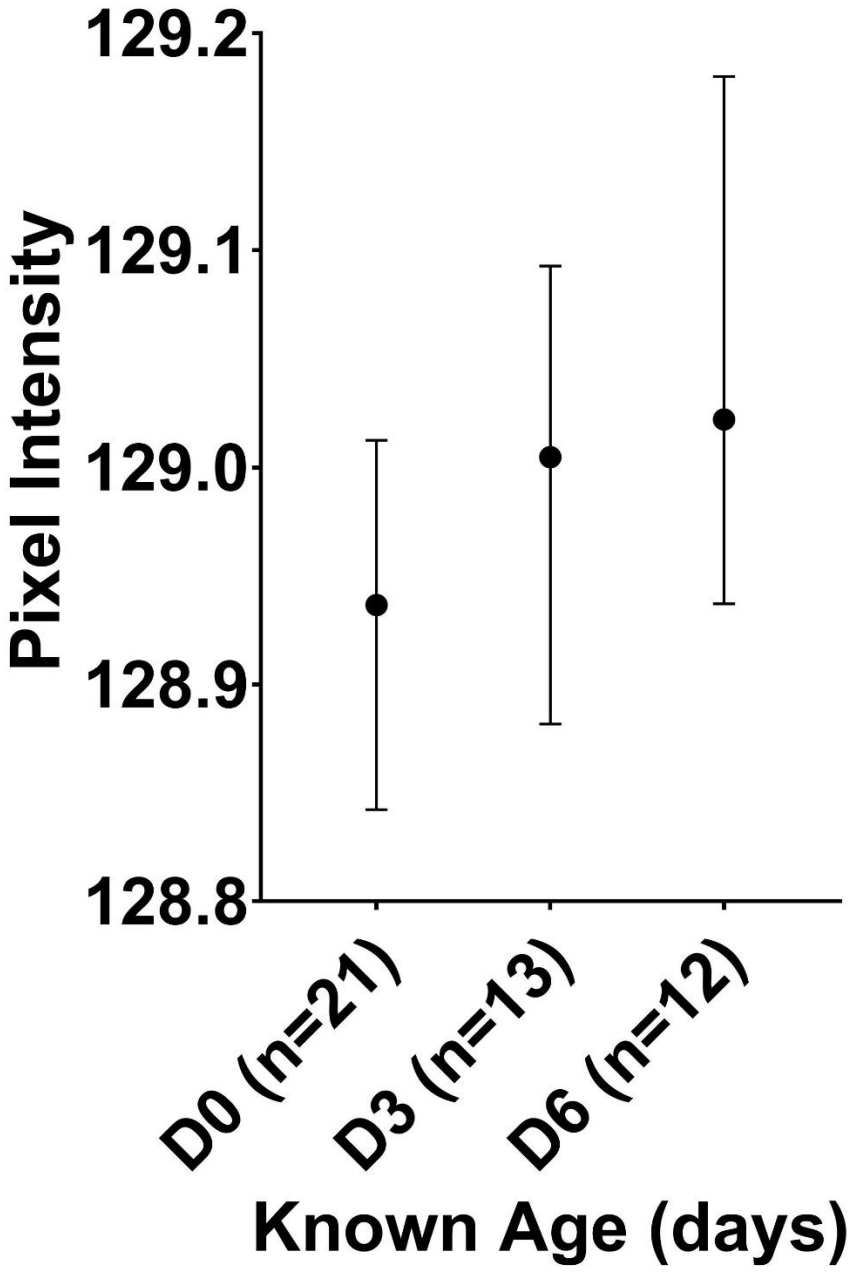

Figure 4.13: *Culex tarsalis* KNWR strain pixel intensity range by known age. Mosquitoes which were captured at known ages show no significant (Kruskal-Wallis test; $p = 0.1092$) difference to one another. However, median pixel intensity was lowest (128.94; 95% CI: 128.84 – 129.01) in day 0 (D0) mosquitoes, while D3s median was 129.00 (95% CI: 128.88 – 129.09), and D6 median was 129.02 (95% CI: 128.94 – 129.18).

4.3 Discussion

In this chapter, we observed photos of wings obtained from wild *Cx. tarsalis* have a more constrained PI range when compared to *An. gambiae* sensu lato captured from Burkina Faso despite having similar median PIs. The reasonings behind this difference may be explained by the differences between the wings of these species or the change in microscope lighting needed to capture a clear picture of the *Cx. tarsalis* wings. *An. gambiae* wings have light and dark scales that create mottled wings, while *Culex tarsalis* scales are uniformly dark resulting wings that are more homogeneous in color.

In the 2023 PI data, the mosquitoes captured represented at the lower end of the PI ranges when compared to mosquitoes captured during 2024 NoCo field trial. However, the sample size was considerably lower in 2023 than in 2024. Interestingly, however, they were captured at the very end of the summer in weeks 34 and 35 and we saw similar lower PI values from mosquitoes captured during the same weeks from the 2024 sampling (Figure 4.9), potentially suggesting lower PI values (presumably younger mosquitoes) at the end of the summer season are a regular phenomenon with *Cx. tarsalis* in NoCo and may be due to most of the older females not host-seeking (e.g. being caught in CO_2 baited traps) but rather having initiated diapause activities prior to the onset of Fall[317]. An alternative explanation is that the mosquitoes in 2023 were captured using resting traps rather than the CDC light traps used in 2024, so perhaps the trapping method also contributed to the differences.

Interestingly, when looking at the mosquitoes' PIs caught in NoCo in 2024 (Figure 4.14), the binned proportions exhibited a normal distribution (p = 0.05) using a Shapiro-Wilks test, indicating a population which is not similar to the skewed mosquito

population age structures (many female mosquitoes with low PIs/young age and a long thin tail of high PI/old aged mosquitoes) observed using traditional methods like the Polovodova age grading method and seen with the *An. gambiae* from Burkina Faso (Figure 3.2) and to a lesser extent with the *Cx. tarsalis* from the GSL region in 2024 (Figure 4.14). It may be that this observation is due to sites from which this population was captured, which were from homeowners' properties in urban and suburban locales, representing local blood feeding sites potentially far away from most breeding sites (standing water in rural fields and riparian wetland) in the region[49,50]. It is known that *Cx. tarsalis* are competent fliers when compared to other genera of mosquitoes, so the breeding sites for these NoCo mosquitoes could be far away from our capture site[51]. Furthermore, the *An. gambiae* in Burkina Faso typically breeding in small rainwater pools only meters from households where they are captured, and the *Cx. tarsalis* from the GSL were captured in the spray blocks that were set up within the large breeding site wetlands on the edges of the GSL that experience high, constant eclosure of new adults. Personal conversations with the director of SLCMAD confirmed that some traps can exceed 10,000 mosquitoes per trap-night. To examine this phenomenon in the future, it may be interesting to trap *Cx. tarsalis* along transects from the GSL wetlands (presumably encompassing most of the regions *Cx. tarsalis* breeding sites) to the western foothills of the Wasatch range in SLC and perform more PI analyses. The foothills area contains few breeding sites but is the area of the valley where most of the WNV positive mosquitoes are captured. From such an experiment, it may be expected that PI would increase over the transect steadily and uncover older *Cx. tarsalis* populations residing in the eastern part of the city, amid the foothills. Similarly, we may

expect a similar phenomenon at our urban/suburban trap sites in NoCo, and thus, it is reasonable to think that the 2024 NoCo population structure stabilized around a relatively older median age with few number of younger mosquitoes with lower PI coming into the population, equaling the few number of older mosquitoes with higher PI leaving the population.

When considering all our data examining *Cx. tarsalis* from across our two sites, it is important to note that potential for genetic differences in *Cx. tarsalis* populations between the GSL and NoCo influencing wing phenotypes that might influence our PI analyses. Indeed, there are three genetic clusters of *Cx. tarsalis* in the United States (Sonoran, Pacific, and Midwest clades) described by Venkatesan and Rasgon in 2010 [321]. They found that *Cx. tarsalis* from Utah county, Utah and Gunnison, Colorado cluster with the Pacific clade while mosquitoes examined in Laramie, Wyoming, belonged to the Midwest clade that was panmictic with mosquitoes from TX, NE, MT and the Dakotas, and separated from the Pacific clade by the Rocky Mountain range[321].

Considering the effects of the two control trials on *Cx.* t*arsalis* PI and assumed age structure, the IVM coated birdseed trial seemed to have no effect on wild *Cx. tarsalis* PI. We do have preliminary evidence that birds captured in our trial indeed had mosquitocidal levels of ivermectin in their blood and initial mosquito density and VI data from the clusters suggest a possible positive trial effect (data not shown). Nonetheless, the lack of effect on mosquito PI could be due to how the 20 clusters in the trial arms were originally constructed. While we originally envisioned each cluster being the size of a neighborhood with many household properties, or encompassing a large park with many adjacent households, due to finical, personnel, and supply constraints, we instead

constructed the clusters as individual household properties, where there were 2 per site randomized as one being the control and one the intervention. The two main drawbacks to this cluster size decision are high expected bird and mosquito movement in and out of the clusters without being exposed to the treatment. In addition to the wide distribution area *Cx. tarsalis* move outside from their breeding sites, birds which were targeted with the IVM coated seed do not stay in one place, obtaining food from a variety of locations. It has been noted that to achieve prime IVM coated birdseed coverage of the neighborhood's properties, approximately 75% of treated houses equated to a stronger percent modeled reduction of infectious mosquito-days in the treated cluster[222]. Due to these factors, it may be more appropriate for a minimum of five to ten adjacent households (e.g. in neighborhood cul-de-sacs) to serve as clusters in future trials with medicated bird feed rather than individual houses. This would allow for more of the natural range of local birds and mosquitoes to be covered by the cluster area, allowing the ability to appropriately elucidate the impact of the IVM coated bird feed on the mosquito population.

From the naled ULV-spray application around the GSL, we found a decrease in the median PI of wild *Cx. tarsalis* in the treatment arm relative to the control arm of the trial. Preliminary data from other trial outcomes are still being analyzed but suggest mixed results. The naled applications were lethal to caged, susceptible sentinel mosquitoes placed in the field, and mosquito densities were temporarily reduced from some spray events, especially the earlier ones. Alternatively, some spray events suffered from unexpected naled drift outside of the spray blocks due to high winds, and there was documented OP resistance in the wild mosquitoes too. *Cx. tarsalis* median

PIs were consistently reduced from pre- to post-spray event sampling across the trial in the treatment arm other than from spray event #4, and more variable (either no change, increased or decreased) in the control arms. Furthermore, the parity rate data from all treatment arm spray events were fully congruent with the changes in mosquito PI. These data themselves suggest that naled treatment was efficacious against a secondary trial outcome, in that it temporarily shifted the mosquito population structure to lower age classes in treatment blocks compared to control blocks as assessed by two independent age structure methods.

While we were not able to generate a successful *Cx. tarsalis* age model to predict median population age from the mosquito PI data, we can still assume an effect using the raw PI data. While this association needs to be investigated further, this relationship could indicate a shift in how mosquito control experts estimate the population age as parity alone cannot give an estimate of true age. Additionally, by utilizing PI, once a known age model is established, control districts might more easily determine if mosquito population they monitor should be treated to limit exposure to WNV.

Overall, we have demonstrated how PI can be used to stratify wild *Cx. tarsalis* populations, suggesting that PI can be a meaningful tool in discerning population age. We also observed a modest yet non-significant decrease in PI when mosquito populations in SLCMAD and MADD were exposed to naled, which seemed to remain stagnant around 198.5 PI units. This may suggest the treatment was targeting newly eclosed mosquitoes rather than established, older populations and that PI might be sensitive enough to identify if mosquito control tools are working on a population if

vector abundance is skewed in areas due to constant high emergence of adults. However, we did not notice any difference in median PI of *Cx. tarsalis* in NoCo due to administration of IVM coated birdseed to treated clusters. This may be due to the modest and slow effects of IVM relative to a rapid neurotoxin like naled, but also likely influence by limit coverage of *Cx. tarsalis* and birds ranging areas due to limitations in the trial's cluster size.

There is a need for new comprehensive and quantitative age-grading models for mosquito populations. These models will help establish best practices for integrated vector management strategies whereby vector populations are controlled in a cost-effective, sustainable, and effective manner, reducing the propensity for resistance development and reducing the relative risk to pathogens to be transmitted to humans. To ensure their use, these novel tools need to be easy to use and cost effective or mosquito control districts will be less likely to utilize them. We have initially demonstrated how the development of wing PI methods to age mosquito populations will allow for a cheaper, yet effective, alternative when compared to other novel methods which most often require expensive machines and advanced knowledge in molecular biology, biochemistry, and statistics to be implemented

4.4 Methods and materials

4.4.1 2023 field trial

Cx. tarsalis mosquitoes were collected during the summer of 2023 during the epidemiological weeks 34 and 35 in northern Colorado from volunteers' properties using fiber resting traps and processed to determine their wing pixel intensity[322]. Resting traps were placed near bird roosting locations on the volunteers' properties and collected

twice a week to identify blood meal contents of fed mosquitoes. Non-blood fed *Cx. tarsalis* from the resting traps were used for PI analysis. Mosquito wings were removed using #5 Dumont Fine Tipped Forceps (Fine Science Tools) and adhered to glass slides using a 10% sucrose solution. Slides were allowed to dry, placed in a slide box, and held in a -20°C freezer until photos were conducted.

4.4.2 2024 field trial

During the 2024 field trial testing IVM treated birdseed, 20 sites within cities and towns in northern Colorado were selected to examine the efficacy of the bird seed (Figure 4.14). Ten broad geographical areas within cities or towns were selected and two paired households (sites) within each area were selected for sampling and randomly chosen to be treatment or control sites. Mosquitoes were captured using standard CDC and 3D printed CO_2 traps, *sans* light[323]. The change from resting traps to CO_2 traps was necessary to create a model which did not interfere with current mosquito control district standard practices and add unneeded steps to their protocols. Traps were set up and collected on two concurrent nights, each week. The morning after the traps were set up, collection cups were removed and brought back to Colorado State University's (CSU) Center for Vector-borne Infectious Diseases (CVID) for processing. Up to ten *Cx. tarsalis* per collection cup were sequestered and had their wings removed and glued to glass slides in the manner stated above. Wingless mosquitoes were added back to collection cups to calculate the vector index for the epidemiological week they were captured in. Wings were retained in the same manner as above.

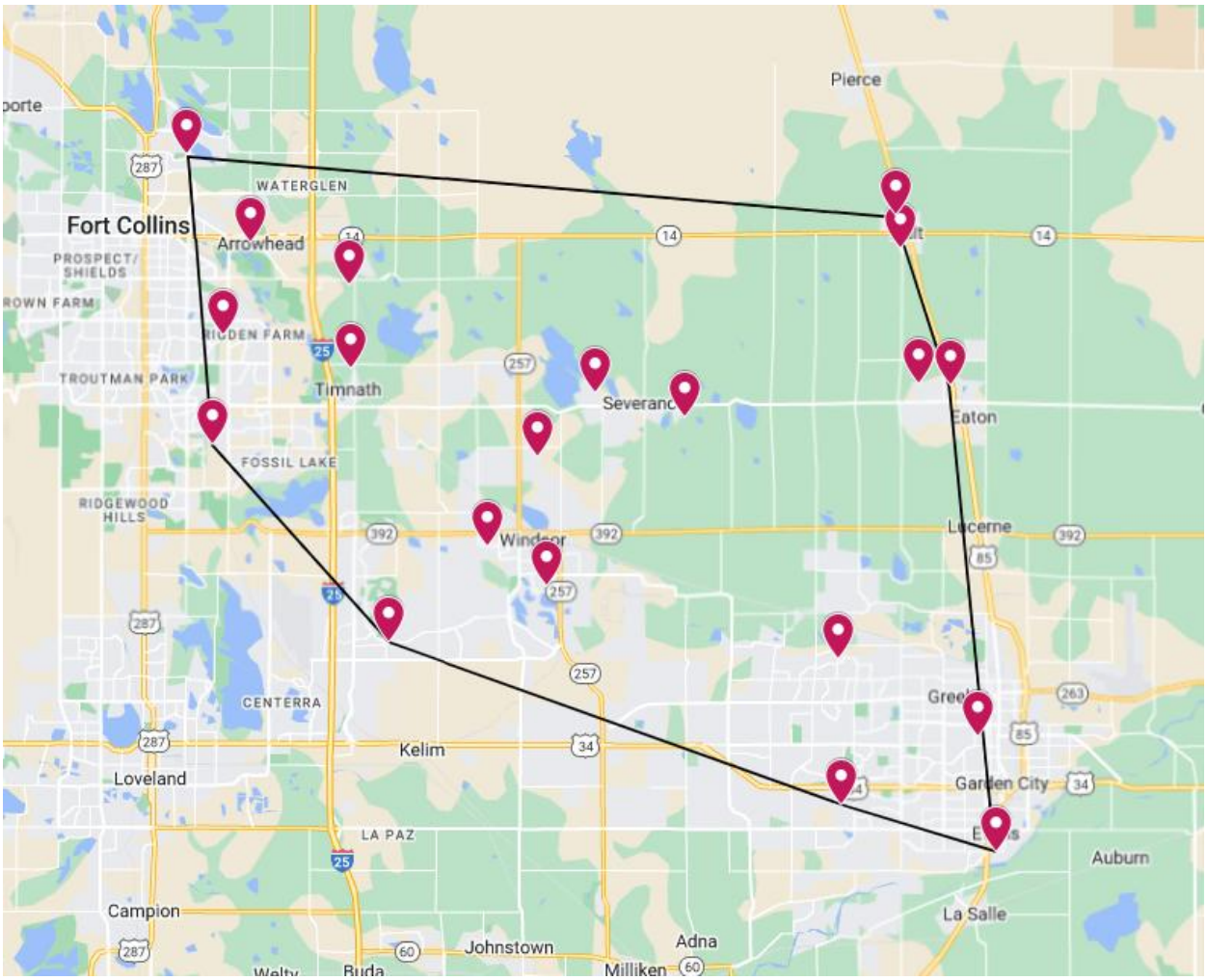

Figure 4.14: Chosen sites for the 2024 ivermectin coated birdseed field trial.

4.4.3 Salt Lake City and Davis Mosquitoes Abatement District naled application

During the SLCMAD and MADD evaluation of naled using an aerial ultra-low volume application process, mosquitoes were captured in the control and treatment zones both before and after the treatment was applied. Up to ten *Cx. tarsalis* from each trap had their wings removed, glued to slides, and stored in the same manner as above. Slide boxes were then sent to CSU's CVID for further analysis. A subset of the

mosquitoes which had their wings removed were stored in the freezer until parity analysis could be conducted.

Mosquitoes which were allocated for parity determination were allowed to thaw and had their ovaries removed and placed on slides to observe if the tracheoles were tightly coiled or loose. Mosquitoes which were found to be tightly coiled were considered nulliparous while those with loose tracheoles were considered parous. Proportion analysis was then conducted to determine the population parity rate per arm, pre and post treatment.

4.4.4 Mosquito rearing and mesocosm experiment

Culex tarsalis KNWR strain were reared at 27-30°C with 60-80% relative humidity. A standard photoperiod of 16 hours light:8 hours dark was utilized. Larvae were raised in open-top plastic bins and fed a diet of TetraMin fish food (Spectum Brands Pet, LLC). Pupae were picked, placed into water cup, then placed into a bin topped with netting to keep mosquitoes from escaping. 24 hours after pupae were picked, the pupae cup was removed and the eclosed adults were taken into mesocosms located in the insectary at CVID using the standard insectary conditions mentioned above. Adults were allowed to free roam the mesocosm and had constant access to raisins and water. To reach these, mosquitoes had to navigate through plastic plants in the room covering the subsistence. Raisins and water were located on the opposite ends of the mesocosm, requiring the mosquitoes to fly from one end to the other to seek their meal and water. Female mosquitoes were collected 3 or 6 days after being placed

into their mesocosm using a variable speed prokopack on the lowest setting. To obtain the day 0 mosquitoes, female mosquitoes which had emerged from pupae within 24 hours were collected using a prokopack. Wing processing occurred in the same manner as used above for consistency.

4.4.5 Digital wing photo analysis

Each wing obtained from all the instances mentioned above were photographed using a Leica EZ4 stereoscope and the Leica LAS EZ program. Each photo was taken at 1080P, a magnification of 20X, 70% brightness, 0.55 gamma, and 77.00 saturation. Additionally, only the bottom light was utilized. These settings were chosen due to *Cx. tarsalis* wings are highly reflective, resulting in a rainbow shine occurring which these settings reduced. PI was calculated for each wing by processing them in the BigPicture program developed by Viden Technologies, LLC. Subsequently, the mean of the left- and right-wing PIs were calculated to establish a PI per individual mosquito (a single PI from the mean of both wings). If a mosquito had only one wing image, or if one wing was folded or torn during the slide mounting process, the individual mosquito was given a PI that came from only one of its wings.

4.4.6 Statistical analysis

Mean PI and parity rates were calculated using excel. All other analyses were made using GraphPad Prism (v10.1.1) using an alpha of 0.05. Normality of data was tested using a Shapiro-Wilk test. If normality was not found Mann-Whitney tests were

utilized. However, if the data was determined to be normal, unpaired t-tests were used. The tests were used to determine the differences between control and treatment arms during the 2024 NoCo field trial and the pre- and post, control, and treatment zones during the SLCMAD and MADD application of naled. Expected versus observed chi-squares were used to determine a difference in wing favorability. Post hoc Dunn's multiple comparisons test was used to determine if the known age mosquitoes median PI were significantly different from one another.

CHAPTER 5: SUMMARY AND FUTURE CONSIDERATIONS

While mosquito-borne disease mortality rates are declining, cases are increasing and VBD ranges are expanding into new areas[2,31]. Invasive mosquito species are occupying niches in areas where other species do not take advantage of, altering the mosquito control landscape[4,6,7]. Rising insecticide resistance to current formulations requires industry to alter their approaches, however, some IR in mosquitoes is cross-protecting, leading to rapid resistance of new formulations of commonly used insecticide backbones[110,113,115,119,120,123,253,254,324,325]. New mosquitocidal drugs are necessary to make an impact on the changing landscape of mosquito population dynamics[114–116,120,144]. Endectocides, such as the avermectin class, have shown promise for their mosquitocidal abilities and are particularly efficacious on anopheline mosquitoes, the vectors of human malaria[211,259,262–264,280]. Currently ivermectin (IVM), an avermectin derivative, is being used as the first endectocide to elucidate if these drugs can make impactful changes to the *Anopheles* mosquito populations across Africa and Southeast Asia, but the literature is lacking in IVMs ability to kill mosquitoes on its own after humans have ingested the endectocide[170,199,203,204,206,207].

Additionally, current mosquito age-grading techniques such as mid- and near-inferred spectrometry have reinvigorated the need for a new tool for control experts and researchers to identify populations which need to be targeted for control[237,241,242,290,291,294,296]. Currently however, these techniques are more equipped to identify very young and old mosquitoes, leading to the mosquitoes in the middle to be incorrectly aged. Additionally, these methods have a high upfront cost if control districts

do not have the current methods to conduct them. Thus, a need for a novel, cost-effective, high-throughput, and accurate age-grading system is needed for control districts to utilize.

5.1 Using ivermectin as a mosquito control tool

Using plasma obtained from participants of the RIMDAMAL II clinical trial, it was found that participants retain a IVM concentration to illicit a mosquitocidal response 7-days post-intervention using a 300μg/kg per day for three days dose. It was found however, that the severity and mosquito survival was dependent on participant age and sex, with the younger participants clearing IVM more quickly than older participants and female participants retaining IVM concentrations longer than males, likely due to sex differences in body fat percentages. While IVM in participants' plasma did illicit a mosquitocidal effect, it was surprisingly short lived, lasting up to 14-days post-intervention, a reduction in the proposed 28-day models[214,215]. While IVM has a short half-life, it may be better to examine other endectocides, such as isoxazolines, which have a longer pharmacokinetic profile compared to IVM[272,276–279]. This would reduce the number of MDAs required to illicit a response and reduce the cost associated with MDAs. However, moving to isoxazoline drugs will not circumvent the exclusion criteria of treating some participants with IVM, which causes select individuals from being treated, thus causing a lap in a treated community.

Additionally, while the mosquitoes in the lab indicated a feeding aversion response to plasma containing IVM, we did not find evidence of this when analyzing the bloodmeal contents of wild caught mosquitoes. Comparing the two groups currently

would be inappropriate due to the nuances of wild mosquitoes versus the structure of insectary operations. A more thorough understanding wild *An. gambiae* s.l. population dynamics is necessary to assess if feeding aversion is occurring. These experiments should be done with wild *An. gambiae* s.l. in outdoor mosquitospheres using two groups of participants, one with an active IVM concentration and one without, confirmed via High-Performance Liquid Chromatography and Mass Spectrometry. Participants would then perform human landing captures on mosquitoes that not only probe but are actively feeding for more than a few seconds. This would allow researchers to identify feeding aversion in a pseudo-wild environment.

Ultimately, the answer might be in providing a multifaceted approach, using indoor residual spraying, insecticide treated bed nets, an endectocide, and attractive toxic sugar baits in conjunction with one another. This could result in a community to be protected from mosquitoes in all facets; however, this level of control would likely be cost prohibitive.

5.2 Developing a novel mosquito age-grading technique

While we can attempt to control all mosquitoes, nuisance or pathogen transmitters, control experts should shift to the mindset of insecticide resistance prevention, only targeting older, possibly infectious mosquitoes with insecticides. While there are a few new methods to examine mosquito population age, these methods are expensive, requiring advanced analytical machinery to run and professionals to analyze the complex data, which most control districts cannot afford. While using techniques that revolve around parity are qualitative, these techniques require an exorbitant amount

of time, meticulously isolating, removing, then grading the ovaries into parous or nulliparous bins. A novel age-grading technique which is high throughput, easy to use, financially accessible, and does not require advanced statistical models to be ran by the user is needed.

Currently, PI of wing photos to measure mosquito population age is in its infancy. It still requires statistical applications to run models, and the development of more robust, known-age models for known vectors are needed. Eventually, we see this as a web-based program where mosquito control districts can submit mosquito wing photos from a sample of their population and the program will analyze, speciate, and deliver a population age estimation to the user. This program needs to be user friendly and enticing to control districts, while academics could use this method, the target demographic should be control districts and local mosquito experts. However, before this goal can be accomplished, more research is needed to establish PI age grading as a contender among novel methods. Additionally, our prior research has indicated that PI can be a valuable tool which is not influenced by wing size[243].

This dissertation has shown that PI based age-grading can be used to estimate wild *An. gambiae* s.l. and observe a difference in the mosquito populations PI once the IG2® nets were used in the community (see chapter 3). We also demonstrated that PI can be used to analyze wild *Cx, tarsalis* in both northern Colorado and Salt Lake City, Utah, suggesting that PI can be utilized for *Cx. tarsalis* as well. Currently though, wild *Cx. tarsalis* age cannot be interpolated due to a lack of a known-age model. The model which is currently developed only extends out to 6 days post-eclosure, thus it is necessary to extend the known-age PI model before ages can be interpolated.

Furthermore, it was noticed that microscope location may influence PI. Photos taken of *Cx, tarsalis* wings in SLCMAD and again at CSU yielded different results. A comparison indicated that the PI ranges were significantly different from one another (data not shown). Both locations used the same settings on the Leica LAS EZ program and in the same photo format, suggesting that the location of the microscope affects the ambient light in the photos, resulting in different PIs. To circumvent this issue, we believe that by building a box-housing for the microscope, preventing any outside light, would keep PI ranges from fluctuating across locations. We also observed a difference in PI when newly eclosed *Cx. tarsalis* were captured via CDC light trap, Prokopak, and mouth aspiration. However, this difference was not unexpected, as the traps are created with their fan in different locations in relation to the traps collection cup. It was expected the mosquitoes which were captured via CDC light trap may undergo more damage, due to mosquitoes going through a fan before arriving at the collection cup. Furthermore, photos taken of the wings result in a wide area which results in wide negative space around the wing. We believe that with the advancement of artificial intelligence tools, we can utilize these tools to crop out all but the wings, making the PI reflective of the wing itself, and not the entire photo.

Future field studies should be conducted to elucidate if PI can be utilized to develop an age-grading method which can satisfy the requirements for mosquito control districts, determining when and where mosquito control techniques would be best used. Additionally, research is needed to determine if the influence the trap type has on PI can be circumvented, possibly with the use of a Biogents BG-Pro All-In-One traps instead of CDC light traps[326]. These traps are modular, meaning the fan can be positioned in a

way that mosquitoes are pulled into a mosquito collection net without going through the fan first, akin to a CDC resting pot trap.

REFERENCES

1. *Spider-Man*. (Sony Pictures, 2002).
2. World Health Organization & UNICEF/UNDP/World Bank/WHO Special Programme for Research and Training in Tropical Diseases. *Global Vector Control Response 2017-2030*. (World Health Organization, Geneva, 2017).
3. Pulkki-Brännström, A.-M., Wolff, C., Brännström, N. & Skordis-Worrall, J. Cost and cost effectiveness of long-lasting insecticide-treated bed nets - a model-based analysis. *Cost Eff. Resour. Alloc. CE* **10**, 5 (2012).
4. Pless, E. *et al.* Multiple introductions of the dengue vector, Aedes aegypti, into California. *PLoS Negl. Trop. Dis.* **11**, e0005718 (2017).
5. Baheshm, Y. A. *et al.* Sequencing confirms Anopheles stephensi distribution across southern Yemen. *Parasit. Vectors* **17**, 507 (2024).
6. Ali, S., Samake, J. N., Spear, J. & Carter, T. E. Morphological identification and genetic characterization of Anopheles stephensi in Somaliland. *Parasit. Vectors* **15**, 247 (2022).
7. Carter, T. E. *et al.* First detection of Anopheles stephensi Liston, 1901 (Diptera: culicidae) in Ethiopia using molecular and morphological approaches. *Acta Trop.* **188**, 180–186 (2018).
8. Seyfarth, M., Khaireh, B. A., Abdi, A. A., Bouh, S. M. & Faulde, M. K. Five years following first detection of Anopheles stephensi (Diptera: Culicidae) in Djibouti, Horn of Africa: populations established—malaria emerging. *Parasitol. Res.* **118**, 725–732 (2019).

9. Hawaria, D. *et al.* Elevated Plasmodium Sporozoite Infection Rates in Primary and Secondary Malaria Vectors in Anopheles stephensi-Infested Areas of Ethiopia. Preprint at https://doi.org/10.20944/preprints202411.2314.v1 (2024).
10. Monaghan, A. J. *et al.* Consensus and uncertainty in the geographic range of Aedes aegypti and Aedes albopictus in the contiguous United States: Multi-model assessment and synthesis. *PLOS Comput. Biol.* **15**, e1007369 (2019).
11. CDC. Historic Data (2010-2024). *Dengue* https://www.cdc.gov/dengue/data-research/facts-stats/historic-data.html (2025).
12. CDC - DPDx - Malaria. https://www.cdc.gov/dpdx/malaria/index.html (2024).
13. Danforth, M. E., Reisen, W. K. & Barker, C. M. Extrinsic Incubation Rate is Not Accelerated in Recent California Strains of West Nile Virus in *Culex tarsalis* (Diptera: Culicidae). *J. Med. Entomol.* **52**, 1083–1089 (2015).
14. Reisen, W. K., Fang, Y. & Martinez, V. M. Effects of Temperature on the Transmission of West Nile Virus by Culex tarsalis (Diptera: Culicidae).
15. McGregor, B. L., Kenney, J. L. & Connelly, C. R. The Effect of Fluctuating Incubation Temperatures on West Nile Virus Infection in Culex Mosquitoes. *Viruses* **13**, 1822 (2021).
16. Nash, D., O'Leary, D. & Sherman, M. The Outbreak of West Nile Virus Infection in the New York City Area in 1999. (2001).
17. Brathwaite Dick, O. *et al.* The History of Dengue Outbreaks in the Americas. *Am. Soc. Trop. Med. Hyg.* **87**, 584–593 (2012).
18. McSherry, J. A. Some Medical Aspects of the Darien Scheme: Was it Dengue? *Scott. Med. J.* **27**, 183–184 (1982).
19. Rush, B. An account of the bilious remitting fever. *Am. J. Med.* **11**, 546–550 (1951).

20. Sardelis, M. R., Turell, M. J., Dohm, D. J. & O'Guinn, M. L. Vector Competence of Selected North American Culex and Coquillettidia Mosquitoes for West Nile Virus. *Emerg. Infect. Dis.* **7**, 1018–1022 (2001).

21. Rochlin, I., Faraji, A., Healy, K. & Andreadis, T. G. West Nile Virus Mosquito Vectors in North America. *J. Med. Entomol.* **56**, 1475–1490 (2019).

22. Roehrig, J. West Nile Virus in the United States — A Historical Perspective. *Viruses* **5**, 3088–3108 (2013).

23. Colpitts, T. M., Conway, M. J., Montgomery, R. R. & Fikrig, E. West Nile Virus: Biology, Transmission, and Human Infection. *Clin. Microbiol. Rev.* **25**, 635–648 (2012).

24. Krambrich, J., Akaberi, D., Lindahl, J. F., Lundkvist, Å. & Hesson, J. C. Vector competence of Swedish Culex pipiens mosquitoes for Japanese encephalitis virus. *Parasit. Vectors* **17**, 220 (2024).

25. Beranek, M. D. *et al.* Culex interfor and Culex saltanensis (Diptera: Culicidae) are susceptible and competent to transmit St. Louis encephalitis virus (Flavivirus: Flaviviridae) in central Argentina. *Trans. R. Soc. Trop. Med. Hyg.* **114**, 725–729 (2020).

26. Barker, C. M. *et al.* Temporal Connections between Culex tarsalis Abundance and Transmission of Western Equine Encephalomyelitis Virus in California. *Am. Soc. Trop. Med. Hyg.* **82**, 1185–1193 (2010).

27. Bingham, A. M., Burkett-Cadena, N. D., Hassan, H. K. & Unnasch, T. R. Vector Competence and Capacity of *Culex erraticus* (Diptera: Culicidae) for Eastern Equine Encephalitis Virus in the Southeastern United States. *J. Med. Entomol.* **53**, 473–476 (2016).

28. Hartman, D. A. *et al.* Susceptibility and barriers to infection of Colorado mosquitoes with Rift Valley fever virus. *PLoS Negl. Trop. Dis.* **15**, e0009837 (2021).

29. Mutsaers, M. *et al.* Vector competence of Anopheles stephensi for O'nyong-nyong virus: a risk for global virus spread. *Parasit. Vectors* **16**, 133 (2023).

30. Nanfack Minkeu, F. & Vernick, K. A Systematic Review of the Natural Virome of Anopheles Mosquitoes. *Viruses* **10**, 222 (2018).

31. World malaria report 2024: addressing inequity in the global malaria response.

32. Neafsey, D. E. *et al.* Genetic Diversity and Protective Efficacy of the RTS,S/AS01 Malaria Vaccine. *N. Engl. J. Med.* **373**, 2025–2037 (2015).

33. Adjei, M. R. *et al.* The impact of the RTS,S malaria vaccine on uncomplicated malaria: evidence from the phase IV study districts, Upper East Region, Ghana, 2020–2022. *Malar. J.* **23**, 305 (2024).

34. Efficacy and safety of RTS,S/AS01 malaria vaccine with or without a booster dose in infants and children in Africa: final results of a phase 3, individually randomised, controlled trial. *The Lancet* **386**, 31–45 (2015).

35. Datoo, M. S. *et al.* Efficacy and immunogenicity of R21/Matrix-M vaccine against clinical malaria after 2 years' follow-up in children in Burkina Faso: a phase 1/2b randomised controlled trial. *Lancet Infect. Dis.* **22**, 1728–1736 (2022).

36. Hobbelen, P. H. F., Samuel, M. D., LaPointe, D. A. & Atkinson, C. T. Modeling Future Conservation of Hawaiian Honeycreepers by Mosquito Management and Translocation of Disease-Tolerant Amakihi. *PLoS ONE* **7**, e49594 (2012).

37. CDC - DPDx - Lymphatic Filariasis. https://www.cdc.gov/dpdx/lymphaticfilariasis/index.html (2019).

38. Smith, D. L. *et al.* Ross, Macdonald, and a Theory for the Dynamics and Control of Mosquito-Transmitted Pathogens. *PLoS Pathog.* **8**, e1002588 (2012).

39. Hartemink, N., Cianci, D. & Reiter, P. R_0 for Vector-Borne Diseases: Impact of the Assumption for the Duration of the Extrinsic Incubation Period. *Vector-Borne Zoonotic Dis.* **15**, 215–217 (2015).

40. Brady, O. J. *et al.* Vectorial capacity and vector control: reconsidering sensitivity to parameters for malaria elimination. *Trans. R. Soc. Trop. Med. Hyg.* **110**, 107–117 (2016).

41. Kenea, O. *et al.* Comparison of two adult mosquito sampling methods with human landing catches in south-central Ethiopia. *Malar. J.* **16**, 30 (2017).

42. Briët, O. J. T. *et al.* Applications and limitations of Centers for Disease Control and Prevention miniature light traps for measuring biting densities of African malaria vector populations: a pooled-analysis of 13 comparisons with human landing catches. *Malar. J.* **14**, 247 (2015).

43. Lima, J. B. P., Rosa-Freitas, M. G., Rodovalho, C. M., Santos, F. & Lourenço-de-Oliveira, R. Is there an efficient trap or collection method for sampling Anopheles darlingi and other malaria vectors that can describe the essential parameters affecting transmission dynamics as effectively as human landing catches? - A Review. *Mem. Inst. Oswaldo Cruz* **109**, 685–705 (2014).

44. Kent, R., Juliusson, L., Weissmann, M., Evans, S. & Komar, N. Seasonal Blood-Feeding Behavior of *Culex tarsalis* (Diptera: Culicidae) in Weld County, Colorado, 2007. *J. Med. Entomol.* **46**, 380–390 (2009).

45. Crabtree, M. B., Kading, R. C., Mutebi, J.-P., Lutwama, J. J. & Miller, B. R. IDENTIFICATION OF HOST BLOOD FROM ENGORGED MOSQUITOES COLLECTED IN WESTERN UGANDA USING CYTOCHROME OXIDASE I GENE SEQUENCES. *J. Wildl. Dis.* **49**, 611–626 (2013).

46. Keven, J. B., Artzberger, G., Gillies, M. L., Mbewe, R. B. & Walker, E. D. Probe-based multiplex qPCR identifies blood-meal hosts in Anopheles mosquitoes from Papua New Guinea. *Parasit. Vectors* **13**, 111 (2020).

47. Alcaide, M. *et al.* Disentangling Vector-Borne Transmission Networks: A Universal DNA Barcoding Method to Identify Vertebrate Hosts from Arthropod Bloodmeals. *PLoS ONE* **4**, e7092 (2009).

48. Kent, R. J. & Norris, D. E. IDENTIFICATION OF MAMMALIAN BLOOD MEALS IN MOSQUITOES BY A MULTIPLEXED POLYMERASE CHAIN REACTION TARGETING CYTOCHROME B. *Am. J. Trop. Med. Hyg.* **73**, 336–342 (2005).

49. Reisen, W. K., Milby, M. M. & Meyer, R. P. Population Dynamics of Adult Culex Mosquitoes (Diptera: Culicidae) Along the Kern River, Kern County, California, in 1990. *J. Med. Entomol.* **29**, 531–543 (1992).

50. Reisen, W. K. & Lothrop, H. D. Population Ecology and Dispersal of Culex tarsalis (Diptera: Culicidae) in the Coachella Valley of California. *J. Med. Entomol.* **32**, 490–502 (1995).

51. Reisen, W. K., Milby, M. M., Reeves, W. C., Meyer, R. P. & Bock, M. E. Population Ecology of Culex tarsalis (Dipteral Culicidae) in a Foothill Environment of Kern County, California: Temporal Changes in Female Relative Abundance, Reproductive Status, and Survivorship.

52. Stuart, J. D. *et al.* Mosquito tagging using DNA-barcoded nanoporous protein microcrystals. *PNAS Nexus* **1**, pgac190 (2022).

53. Faiman, R. *et al.* A novel fluorescence and DNA combination for versatile, long-term marking of mosquitoes. *Methods Ecol. Evol.* **12**, 1008–1016 (2021).

54. Johnson, B. J., Hugo, L. E., Churcher, T. S., Ong, O. T. W. & Devine, G. J. Mosquito Age Grading and Vector-Control Programmes. *Trends Parasitol.* **36**, 39–51 (2020).

55. Fiorenzano, J. M., Koehler, P. G. & Xue, R.-D. Attractive Toxic Sugar Bait (ATSB) For Control of Mosquitoes and Its Impact on Non-Target Organisms: A Review. *Int. J. Environ. Res. Public. Health* **14**, 398 (2017).

56. Honório, N. A., Câmara, D. C. P., Wiggins, K., Eastmond, B. & Alto, B. W. High-Throughput Method for Detection of Arbovirus Infection of Saliva in Mosquitoes Aedes aegypti and Ae. albopictus. *Viruses* **12**, 1343 (2020).

57. Hall-Mendelin, S. *et al.* Exploiting mosquito sugar feeding to detect mosquito-borne pathogens. *Proc. Natl. Acad. Sci.* **107**, 11255–11259 (2010).

58. Brugman, V. A. *et al.* Detection of malaria sporozoites expelled during mosquito sugar feeding. *Sci. Rep.* **8**, 7545 (2018).

59. Guidez, A. *et al.* Impact on Aedes aegypti Mosquitoes Exposed to Honey-Impregnated Flinders Technology Associates (FTA®) Cards. *Trop. Med. Infect. Dis.* **9**, 165 (2024).

60. Braddick, M., Yuen, A., Feldman, R. & Friedman, N. D. Early detection of Murray Valley encephalitis virus activity in Victoria using mosquito surveillance. *Med. J. Aust.* **219**, 40–41 (2023).

61. Osório, H., Zé-Zé, L., Amaro, F. & Alves, M. Mosquito Surveillance for Prevention and Control of Emerging Mosquito-Borne Diseases in Portugal — 2008–2014. *Int. J. Environ. Res. Public. Health* **11**, 11583–11596 (2014).

62. Tedrow, R. E. *et al.* Anopheles mosquito surveillance in Madagascar reveals multiple blood feeding behavior and Plasmodium infection. *PLoS Negl. Trop. Dis.* **13**, e0007176 (2019).

63. Balthazar, T. D. *et al.* Entomological surveillance of mosquitoes (Diptera: Culicidae), vectors of arboviruses, in an ecotourism park in Cachoeiras de Macacu, state of Rio de Janeiro-RJ, Brazil. *PLOS ONE* **16**, e0261244 (2021).

64. Olson, M. F. *et al.* Mosquito surveillance on U.S military installations as part of a Japanese encephalitis virus detection program: 2016 to 2021. *PLoS Negl. Trop. Dis.* **17**, e0011422 (2023).

65. Li, Y. *et al.* Comparative evaluation of the efficiency of the BG-Sentinel trap, CDC light trap and Mosquito-oviposition trap for the surveillance of vector mosquitoes. *Parasit. Vectors* **9**, 446 (2016).

66. Ritchie, S. A. *et al.* A Simple Non-Powered Passive Trap for the Collection of Mosquitoes for Arbovirus Surveillance. *J. Med. Entomol.* **50**, 185–194 (2013).

67. Johnson, B. J. & Ritchie, S. A. The Siren's Song: Exploitation of Female Flight Tones to Passively Capture Male *Aedes aegypti* (Diptera: Culicidae). *J. Med. Entomol.* **53**, 245–248 (2016).

68. Eiras, A. E., Costa, L. H., Batista-Pereira, L. G., Paixão, K. S. & Batista, E. P. A. Semi-field assessment of the Gravid Aedes Trap (GAT) with the aim of controlling Aedes (Stegomyia) aegypti populations. *PLOS ONE* **16**, e0250893 (2021).

69. Staunton, K. M. *et al.* A Low-Powered and Highly Selective Trap for Male Aedes (Diptera: Culicidae) Surveillance: The Male Aedes Sound Trap. *J. Med. Entomol.* tjaa151 (2020) doi:10.1093/jme/tjaa151.

70. González-Pérez, M. I. *et al.* A novel optical sensor system for the automatic classification of mosquitoes by genus and sex with high levels of accuracy. *Parasit. Vectors* **15**, 190 (2022).

71. González-Pérez, M. I. *et al.* Field evaluation of an automated mosquito surveillance system which classifies Aedes and Culex mosquitoes by genus and sex. *Parasit. Vectors* **17**, 97 (2024).

72. Wood, B. *et al.* Distinguishing high and low anopheline-producing rice fields using remote sensing and GIS technologies. *Prev. Vet. Med.* **11**, 277–288 (1991).

73. Chang, A. Y. *et al.* Combining Google Earth and GIS mapping technologies in a dengue surveillance system for developing countries. *Int. J. Health Geogr.* **8**, 49 (2009).

74. Ahmad, R. *et al.* Mapping of mosquito breeding sites in malaria endemic areas in Pos Lenjang, Kuala Lipis, Pahang, Malaysia. *Malar. J.* **10**, 361 (2011).

75. Valiakos, G. *et al.* Use of Wild Bird Surveillance, Human Case Data and GIS Spatial Analysis for Predicting Spatial Distributions of West Nile Virus in Greece. *PLoS ONE* **9**, e96935 (2014).

76. Tokarz, R. & Novak, R. J. Spatial–temporal distribution of Anopheles larval habitats in Uganda using GIS/remote sensing technologies. *Malar. J.* **17**, 420 (2018).

77. Uelmen, J. A. *et al.* Global mosquito observations dashboard (GMOD): creating a user-friendly web interface fueled by citizen science to monitor invasive and vector mosquitoes. *Int. J. Health Geogr.* **22**, 28 (2023).

78. VectorSurv - Vectorborne Disease Surveillance System. https://vectorsurv.org/.

79. Castillo-Neyra, R. *et al.* The potential of canine sentinels for reemerging Trypanosoma cruzi transmission. *Prev. Vet. Med.* **120**, 349–356 (2015).

80. Chaskopoulou, A. *et al.* Detection and Early Warning of West Nile Virus Circulation in Central Macedonia, Greece, Using Sentinel Chickens and Mosquitoes. *Vector-Borne Zoonotic Dis.* **13**, 723–732 (2013).

81. Komar, N. West Nile Virus Surveillance using Sentinel Birds. *Ann. N. Y. Acad. Sci.* **951**, 58–73 (2001).

82. Reisen, W. K. *et al.* Patterns of avian seroprevalence to western equine encephalomyelitis and Saint Louis encephalitis viruses in California, USA. *J. Med. Entomol.* **37**, 507–27 (2000).

83. Chiou, S.-S., Chen, J.-M., Chen, Y.-Y., Chia, M.-Y. & Fan, Y.-C. The feasibility of field collected pig oronasal secretions as specimens for the virologic surveillance of Japanese encephalitis virus. *PLoS Negl. Trop. Dis.* **15**, e0009977 (2021).

84. Kardena, I. M. *et al.* Seroconversion, genotyping, and potential mosquito vector identification of Japanese encephalitis virus in pig sentinel settings in Bali, Indonesia. *Vet. World* 89–98 (2024) doi:10.14202/vetworld.2024.89-98.

85. Webb, J. L. A. The long arc of mosquito control. in *Mosquitopia* 49–60 (Routledge, London, 2021). doi:10.4324/9781003056034-6.

86. Goldberg, L. J. & Margalit, J. A bacterial spore demonstrating rapid larvicidal activity against Anopheles sergentii, Uranotaenia unguiculata, Culex univittatus, Aedes aegypti and Culex pipiens. *Mosq. News* **37**, 355–358 (1977).

87. Boyce, R. *et al. Bacillus thuringiensis israelensis* (*B ti*) for the control of dengue vectors: systematic literature review. *Trop. Med. Int. Health* **18**, 564–577 (2013).

88. Paris, M. *et al.* Persistence of Bacillus thuringiensis israelensis (Bti) in the environment induces resistance to multiple Bti toxins in mosquitoes. *Pest Manag. Sci.* **67**, 122–128 (2011).

89. Araújo, A. P. *et al.* The susceptibility of Aedes aegypti populations displaying temephos resistance to Bacillus thuringiensis israelensis: a basis for management. *Parasit. Vectors* **6**, 297 (2013).

90. Su, T. & Liu, H. History and future perspectives of spinosad for mosquito control. *Pest Manag. Sci.* **n/a**,.

91. Wang, Y., Suman, D. S., Bertrand, J., Dong, L. & Gaugler, R. Dual-treatment autodissemination station with enhanced transfer of an insect growth regulator to mosquito oviposition sites. *Pest Manag. Sci.* **70**, 1299–1304 (2014).

92. Suman, D. S. *et al.* Point-source and area-wide field studies of pyriproxyfen autodissemination against urban container-inhabiting mosquitoes. *Acta Trop.* **135**, 96–103 (2014).

93. US EPA, O. DDT - A Brief History and Status. https://www.epa.gov/ingredients-used-pesticide-products/ddt-brief-history-and-status (2014).

94. Smith, A. G. Toxicology of DDT and Some Analogues. in *Hayes' Handbook of Pesticide Toxicology* 1975–2032 (Elsevier, 2010). doi:10.1016/B978-0-12-374367-1.00093-8.

95. Wilson, B. W. Cholinesterases. *Handb. Pestic. Toxicol.*

96. Blacker, A. M., Lunchick, C., Lasserre-Bigot, D., Payraudeau, V. & Krolski, M. E. Toxicological Profile of Carbaryl. in *Hayes' Handbook of Pesticide Toxicology* 1607–1617 (Elsevier, 2010). doi:10.1016/B978-0-12-374367-1.00074-4.

97. Timchalk, C. Organophosphorus Insecticide Pharmacokinetics. in *Hayes' Handbook of Pesticide Toxicology* 1409–1433 (Elsevier, 2010). doi:10.1016/B978-0-12-374367-1.00066-5.

98. Soderlund, D. M. Toxicology and Mode of Action of Pyrethroid Insecticides. in *Hayes' Handbook of Pesticide Toxicology* 1665–1686 (Elsevier, 2010). doi:10.1016/B978-0-12-374367-1.00077-X.

99. Ngufor, C., Fongnikin, A., Rowland, M. & N'Guessan, R. Indoor residual spraying with a mixture of clothianidin (a neonicotinoid insecticide) and deltamethrin provides improved control and long residual activity against pyrethroid resistant Anopheles gambiae sl in Southern Benin. *PLOS ONE* **12**, e0189575 (2017).

100. Okumu, F. O. & Moore, S. J. Combining indoor residual spraying and insecticide-treated nets for malaria control in Africa: a review of possible outcomes and an outline of suggestions for the future. *Malar. J.* **10**, 208 (2011).

101. Barreaux, A. M. G. *et al.* Semi-field studies to better understand the impact of eave tubes on mosquito mortality and behaviour. *Malar. J.* **17**, 306 (2018).

102. Snetselaar, J. *et al.* Eave tubes for malaria control in Africa: prototyping and evaluation against Anopheles gambiae s.s. and Anopheles arabiensis under semi-field conditions in western Kenya. *Malar. J.* **16**, 276 (2017).

103. Oumbouke, W. A. *et al.* Screening and field performance of powder-formulated insecticides on eave tube inserts against pyrethroid resistant Anopheles gambiae s.l.: an investigation into 'actives' prior to a randomized controlled trial in Côte d'Ivoire. *Malar. J.* **17**, 374 (2018).

104. Maia, M. F. *et al.* Attractive toxic sugar baits for controlling mosquitoes: a qualitative study in Bagamoyo, Tanzania. *Malar. J.* **17**, 22 (2018).

105. Tenywa, F. C., Kambagha, A., Saddler, A. & Maia, M. F. The development of an ivermectin-based attractive toxic sugar bait (ATSB) to target Anopheles arabiensis. *Malar. J.* **16**, (2017).

106. Fongnikin, A. *et al.* Mosquito Shield^{TM}, a transfluthrin passive emanator, protects against pyrethroid-resistant Anopheles gambiae sensu lato in central Benin. *Malar. J.* **23**, 225 (2024).

107. Sukkanon, C., Nararak, J., Bangs, M. J., Hii, J. & Chareonviriyaphap, T. Behavioral responses to transfluthrin by Aedes aegypti, Anopheles minimus, Anopheles harrisoni, and Anopheles dirus (Diptera: Culicidae). *PLOS ONE* **15**, e0237353 (2020).

108. Mortola, B. M. *et al.* Assessing pyrethroid resistance mechanisms in individual *Culex tarsalis* (Diptera: Culicidae). *J. Med. Entomol.* **62**, 584–592 (2025).

109. Tsecouras, J. C., Thiemann, T. C., Hung, K. Y., Henke, J. A. & Gerry, A. C. Prevalence of Permethrin Resistance in Culex Tarsalis Populations in Southern California. *J. Am. Mosq. Control Assoc.* **39**, 236–242 (2023).

110. Namountougou, M. *et al.* Multiple Insecticide Resistance in Anopheles gambiae s.l. Populations from Burkina Faso, West Africa. *PLoS ONE* **7**, e48412 (2012).

111. Yahouédo, G. A. *et al.* Contributions of cuticle permeability and enzyme detoxification to pyrethroid resistance in the major malaria vector Anopheles gambiae. *Sci. Rep.* **7**, 11091 (2017).

112. Strong, A. C., Kondratieff, B. C., Doyle, M. S. & Black, W. C. Resistance to Permethrin in Culex tarsalis in Northeastern Colorado. *J. Am. Mosq. Control Assoc.* **24**, 281–288 (2008).

113. Soma, D. D. *et al.* Insecticide resistance status of malaria vectors Anopheles gambiae (s.l.) of southwest Burkina Faso and residual efficacy of indoor residual spraying with microencapsulated pirimiphos-methyl insecticide. *Parasit. Vectors* **14**, 58 (2021).

114. Das, S., Saha, A., Das, P., Raha, D. & Saha, D. Target-site mediated insecticide resistance in major mosquito (Diptera: Culicidae) vectors: A systematic review. *Asian Pac. J. Trop. Med.* **17**, 481–490 (2024).

115. Badolo, A. *et al.* Three years of insecticide resistance monitoring in Anopheles gambiae in Burkina Faso: resistance on the rise? *Malar. J.* **11**, 232 (2012).

116. Awolola, T. S. *et al.* Pyrethroids resistance intensity and resistance mechanisms in Anopheles gambiae from malaria vector surveillance sites in Nigeria. *PLOS ONE* **13**, e0205230 (2018).

117. Li, L. *et al.* A Leg Cuticle Protein Enhances the Resistance of Anopheles sinensis Mosquitoes to Deltamethrin. *Int. J. Mol. Sci.* **26**, 2182 (2025).

118. Xu, Y. *et al.* Transcription factor FTZ-F1 regulates mosquito cuticular protein CPLCG5 conferring resistance to pyrethroids in Culex pipiens pallens. *Parasit. Vectors* **13**, 514 (2020).

119. Edi, C. V. *et al.* CYP6 P450 Enzymes and ACE-1 Duplication Produce Extreme and Multiple Insecticide Resistance in the Malaria Mosquito Anopheles gambiae. *PLoS Genet.* **10**, e1004236 (2014).

120. Boussougou-Sambe, S. T. *et al.* Resistance of Anopheles gambiae s.s. against commonly used insecticides and implication of cytochrome P450 monooxygenase in resistance to pyrethroids in Lambaréné (Gabon). *BMC Infect. Dis.* **24**, 1221 (2024).

121. Liu, N., Li, T., Reid, W. R., Yang, T. & Zhang, L. Multiple Cytochrome P450 Genes: Their Constitutive Overexpression and Permethrin Induction in Insecticide Resistant Mosquitoes, Culex quinquefasciatus. *PLoS ONE* **6**, e23403 (2011).

122. Yang, T. *et al.* Multiple cytochrome P450 genes: conferring high levels of permethrin resistance in mosquitoes, Culex quinquefasciatus. *Sci. Rep.* **11**, 9041 (2021).

123. Weedall, G. D. *et al.* A cytochrome P450 allele confers pyrethroid resistance on a major African malaria vector, reducing insecticide-treated bednet efficacy. *Sci. Transl. Med.* **11**, eaat7386 (2019).

124. Reddy, M. R. *et al.* Outdoor host seeking behaviour of Anopheles gambiae mosquitoes following initiation of malaria vector control on Bioko Island, Equatorial Guinea. *Malar. J.* **10**, 184 (2011).

125. Cooke, M. K. *et al.* 'A bite before bed': exposure to malaria vectors outside the times of net use in the highlands of western Kenya. *Malar. J.* **14**, 259 (2015).

126. Pyke, G. H. Plague Minnow or Mosquito Fish? A Review of the Biology and Impacts of Introduced *Gambusia* Species. *Annu. Rev. Ecol. Evol. Syst.* **39**, 171–191 (2008).

127. Trimble, R. M. & Smith, S. M. Geographic variation in development time and predation in the tree-hole mosquito, *Toxorhynchites rutilus septentrionalis* (Diptera: Culicidae). *Can. J. Zool.* **56**, 2156–2165 (1978).

128. Focks, D. A., Sackett, S. R., Dame, D. A. & Bailey, D. L. Effect of Weekly Releases of Toxorhynchites amboinensis (Doleschall) on Aedes aegypti (L.) (Diptera: Culicidae) in New Orleans, Louisiana. *J. Econ. Entomol.* **78**, 622–626 (1985).

129. Focks, D. A., Sackett, S. R. & Bailey, D. L. FIELD EXPERIMENTS ON THE CONTROL OF AEDES AEGYPT1 AND CULEX QUINQUEFASCIATUS BY TOXORHYNCHITES RUTILUS RUTILUS (DIPTERA: CULICIDAE).

130. Homski, D., Goren, M. & Gasith', A. Comparative evaluation of the larvivorous fish Gambusia a&is and Aphanius dispar as mosquito control agents.

131. Cassiano, E. J., Hill, J. E., Tuckett, Q. & Watson, C. A. Eastern Mosquitofish, Gambusia holbrooki, for Control of Mosquito Larvae. *EDIS* **2018**, (2018).

132. Angelon, K. A. & Petranka, J. W. CHEMICALS OF PREDATORY MOSQUITOFISH (Gambusia affinis) INFLUENCE SELECTION OF OVIPOSITION SITE BY Culex MOSQUITOES.

133. Why, A. M. & Walton, W. E. Oviposition Behavior of *Culex tarsalis* (Diptera: Culicidae) Responding to Semiochemicals Associated with the Western Mosquitofish, *Gambusia affinis (Cyprinodontiformes: Poecilliidae)*. *J. Med. Entomol.* **57**, 343–352 (2020).

134. Mathavan, S. Satiation time and predatory behaviour of the dragonfly nymph Mesogomphus lineatus. *Hydrobiologia* **50**, 55–64 (1976).

135. Acquah-Lamptey, D. & Brandl, R. Effect of a dragonfly (<i>Bradinopyga strachani</i> Kirby, 1900) on the density of mosquito larvae in a field experiment using mesocosms. *Web Ecol.* **18**, 81–89 (2018).

136. Lubelczyk, C. B. *et al.* Importation of Dragonfly Nymphs (Odonata: Anisoptera) to Control Mosquito Larvae (Diptera: Culicidae) in Southern Maine. *Northeast. Nat.* **27**, 330 (2020).

137. Cabrera, M. B. *et al.* Risks associated with introduction of poeciliids for control of mosquito larvae: first record of the non-native *GAMBUSIA HOLBROOKI* in Argentina. *J. Fish Biol.* **91**, 704–710 (2017).

138. Jaber, S., Mercier, A., Knio, K., Brun, S. & Kambris, Z. Isolation of fungi from dead arthropods and identification of a new mosquito natural pathogen. *Parasit. Vectors* **9**, 491 (2016).

139. Lovett, B. *et al.* Transgenic *Metarhizium* rapidly kills mosquitoes in a malaria-endemic region of Burkina Faso. *Science* **364**, 894–897 (2019).

140. Bilgo, E. *et al.* Transmission of transgenic mosquito-killing fungi during copulation. *Sci. Rep.* **15**, 2181 (2025).

141. Clark, B., Kellen, R., Fukuda, T. & Lindegren, J. E. Field and Laboratory Studies on the Pathogenicity of the Fungus Beuuveria bassiunuto Three Genera of Mosquitoes.

142. Fang, W. *et al.* Development of Transgenic Fungi That Kill Human Malaria Parasites in Mosquitoes. *Science* **331**, 1074–1077 (2011).

143. Thomas, D. D., Donnelly, C. A., Wood, R. J. & Alphey, L. S. Insect Population Control Using a Dominant, Repressible, Lethal Genetic System. *Science* **287**, 2474–2476 (2000).

144. Alphey, N., Coleman, P. G., Donnelly, C. A. & Alphey, L. Managing Insecticide Resistance by Mass Release of Engineered Insects.

145. Fu, G. *et al.* Female-specific flightless phenotype for mosquito control. *Proc. Natl. Acad. Sci.* **107**, 4550–4554 (2010).

146. Wise De Valdez, M. R. *et al.* Genetic elimination of dengue vector mosquitoes. *Proc. Natl. Acad. Sci.* **108**, 4772–4775 (2011).

147. Harris, A. F. *et al.* Field performance of engineered male mosquitoes. *Nat. Biotechnol.* **29**, 1034–1037 (2011).

148. Harris, A. F. *et al.* Successful suppression of a field mosquito population by sustained release of engineered male mosquitoes. *Nat. Biotechnol.* **30**, 828–830 (2012).

149. Carvalho, D. O. *et al.* Suppression of a Field Population of Aedes aegypti in Brazil by Sustained Release of Transgenic Male Mosquitoes. *PLoS Negl. Trop. Dis.* **9**, e0003864 (2015).

150. Kandul, N. P. *et al.* Transforming insect population control with precision guided sterile males with demonstration in flies. *Nat. Commun.* **10**, 84 (2019).

151. Apte, R. A. *et al.* Eliminating malaria vectors with precision-guided sterile males. *Proc. Natl. Acad. Sci.* **121**, e2312456121 (2024).

152. Li, M. *et al.* Suppressing mosquito populations with precision guided sterile males. *Nat. Commun.* **12**, 5374 (2021).

153. Regulations.gov. https://www.regulations.gov/document/EPA-HQ-OPP-2019-0274-0360.

154. Oxitec's Friendly™ mosquito technology receives U.S. EPA approval for pilot projects in U.S. *Oxitec* https://www.oxitec.com/en/news/oxitecs-friendly-mosquito-technology-receives-us-epa-approval-for-pilot-projects-in-us (2020).

155. Fraser, J. E. *et al.* Novel Wolbachia-transinfected Aedes aegypti mosquitoes possess diverse fitness and vector competence phenotypes. *PLOS Pathog.* **13**, e1006751 (2017).

156. Beebe, N. W. *et al.* Releasing incompatible males drives strong suppression across populations of wild and *Wolbachia* -carrying *Aedes aegypti* in Australia. *Proc. Natl. Acad. Sci.* **118**, e2106828118 (2021).

157. Caragata, E., Dutra, H. & Moreira, L. Inhibition of Zika virus by Wolbachia in Aedes aegypti. *Microb. Cell* **3**, 293–295 (2016).

158. Ye, Y. H. *et al.* Wolbachia Reduces the Transmission Potential of Dengue-Infected Aedes aegypti. *PLoS Negl. Trop. Dis.* **9**, e0003894 (2015).

159. Ant, T. H., Herd, C., Louis, F., Failloux, A. B. & Sinkins, S. P. Wolbachia transinfections in Culex quinquefasciatus generate cytoplasmic incompatibility. *Insect Mol. Biol.* **29**, 1–8 (2020).

160. Atyame, C. M. *et al.* Wolbachia-Based Population Control Strategy Targeting Culex quinquefasciatus Mosquitoes Proves Efficient under Semi-Field Conditions. *PLOS ONE* **10**, e0119288 (2015).

161. Atyame, C. M. *et al.* Cytoplasmic Incompatibility as a Means of Controlling Culex pipiens quinquefasciatus Mosquito in the Islands of the South-Western Indian Ocean. *PLoS Negl. Trop. Dis.* **5**, e1440 (2011).

162. Dodson, B. L. *et al.* Wolbachia Enhances West Nile Virus (WNV) Infection in the Mosquito Culex tarsalis. *PLoS Negl. Trop. Dis.* **8**, e2965 (2014).

163. Subbaraman, N. Science snipes at Oxitec transgenic-mosquito trial. *Nat. Biotechnol.* **29**, 9–10 (2011).

164. Nading, A. M. The lively ethics of global health GMOs: The case of the Oxitec mosquito. *BioSocieties* **10**, 24–47 (2015).

165. Fongnikin, A., Odjo, A., Akpi, J., Kiki, L. & Ngufor, C. Pirikool® 300 CS, a new long-lasting capsule suspension formulation of the organophosphate insecticide pirimiphos-methyl for indoor residual spraying against pyrethroid-resistant malaria vectors. *PLOS ONE* **17**, e0267229 (2022).

166. Govoetchan, R. *et al.* VECTRON^{TM} T500, a new broflanilide insecticide for indoor residual spraying, provides prolonged control of pyrethroid-resistant malaria vectors. *Malar. J.* **21**, 324 (2022).

167. Hien, A. S. *et al.* Long-lasting residual efficacy of a new indoor residual spraying product, VECTRON^{TM} T500 (broflanilide), against pyrethroid-resistant malaria vectors and its acceptance in a community trial in Burkina Faso. *Parasit. Vectors* **17**, 484 (2024).

168. N'Guessan, R. *et al.* Mosquito Nets Treated with a Mixture of Chlorfenapyr and Alphacypermethrin Control Pyrethroid Resistant Anopheles gambiae and Culex quinquefasciatus Mosquitoes in West Africa. *PLoS ONE* **9**, e87710 (2014).

169. N'Guessan, R., Odjo, A., Ngufor, C., Malone, D. & Rowland, M. A Chlorfenapyr Mixture Net Interceptor® G2 Shows High Efficacy and Wash Durability against Resistant Mosquitoes in West Africa. *PLOS ONE* **11**, e0165925 (2016).

170. Somé, A. F. *et al.* Safety and efficacy of repeat ivermectin mass drug administrations for malaria control (RIMDAMAL II): a phase 3, double-blind, placebo-controlled, cluster-randomised, parallel-group trial. *Lancet Infect. Dis.* S1473309924007515 (2025) doi:10.1016/S1473-3099(24)00751-5.

171. CDC. Integrated Mosquito Management. *Mosquitoes* https://www.cdc.gov/mosquitoes/php/toolkit/integrated-mosquito-management-1.html (2025).

172. US EPA, O. Success in Mosquito Control: An Integrated Approach. https://www.epa.gov/mosquitocontrol/success-mosquito-control-integrated-approach (2016).

173. Campbell, W. C., Fisher, M. H., Stapley, E. O., Albers-Schönberg, G. & Jacob, T. A. Ivermectin: A Potent New Antiparasitic Agent. *Science* **221**, 823–828 (1983).

174. Davey, P. G. *et al.* Lotilaner Ophthalmic Solution, 0.25%, for the Treatment of Demodex Blepharitis. *Healthcare* **12**, 1487 (2024).

175. Õmura, S. & Crump, A. The life and times of ivermectin — a success story. *Nat. Rev. Microbiol.* **2**, 984–989 (2004).

176. Miglianico, M. *et al.* Repurposing isoxazoline veterinary drugs for control of vector-borne human diseases. *Proc. Natl. Acad. Sci.* **115**, E6920–E6926 (2018).

177. Foy, B. D., Kobylinski, K. C., Silva, I. M. da, Rasgon, J. L. & Sylla, M. Endectocides for malaria control. *Trends Parasitol.* **27**, 423–428 (2011).

178. Meyers, J. I. *et al.* Characterization of the target of ivermectin, the glutamate-gated chloride channel, from *Anopheles gambiae*. *J. Exp. Biol.* **218**, 1478–1486 (2015).

179. Kane, N. S. *et al.* Drug-resistant *Drosophila* indicate glutamate-gated chloride channels are targets for the antiparasitics nodulisporic acid and ivermectin. *Proc. Natl. Acad. Sci.* **97**, 13949–13954 (2000).

180. Ozoe, Y., Asahi, M., Ozoe, F., Nakahira, K. & Mita, T. The antiparasitic isoxazoline A1443 is a potent blocker of insect ligand-gated chloride channels. *Biochem. Biophys. Res. Commun.* **391**, 744–749 (2010).

181. Gassel, M., Wolf, C., Noack, S., Williams, H. & Ilg, T. The novel isoxazoline ectoparasiticide fluralaner: Selective inhibition of arthropod γ-aminobutyric acid- and l-glutamate-gated chloride channels and insecticidal/acaricidal activity. *Insect Biochem. Mol. Biol.* **45**, 111–124 (2014).

182. Zhao, C. & Casida, J. E. Insect γ-Aminobutyric Acid Receptors and Isoxazoline Insecticides: Toxicological Profiles Relative to the Binding Sites of [^{3} H]Fluralaner, [^{3} H]-4′-Ethynyl-4- *n* -propylbicycloorthobenzoate, and [^{3} H]Avermectin. *J. Agric. Food Chem.* **62**, 1019–1024 (2014).

183. Pampiglione, S., Majori, G., Petrangeli, G. & Romi, R. Avermectins, MK-933 and MK-936, for mosquito control. *Trans. R. Soc. Trop. Med. Hyg.* **79**, 797–799 (1985).

184. Bockarie, M. J. *et al.* Mass treatment with ivermectin for filariasis control in Papua New Guinea: impact on mosquito survival. *Med. Vet. Entomol.* **13**, 120–123 (1999).

185. Jiang, S., Tsikolia, M., Bernier, U. R. & Bloomquist, J. R. Mosquitocidal Activity and Mode of Action of the Isoxazoline Fluralaner. *Int. J. Environ. Ressearch Public Health* **14**, (2017).

186. Kolaczinski, J. & Curtis, C. Laboratory evaluation of fipronil, a phenylpyrazole insecticide, against adultAnopheles (Diptera: Culicidae) and investigation of its possible cross-resistance with dieldrin inAnopheles stephensi. *Pest Manag. Sci.* **57**, 41–45 (2001).

187. Uragayala, S., Verma, V., Natarajan, E., Velamuri, P. S. & Kamaraju, R. Adulticidal & larvicidal efficacy of three neonicotinoids against insecticide susceptible & resistant mosquito strains. *Indian J. Med. Res.* **142**, S64–S70 (2015).

188. Hovda, L. R. & Hooser, S. B. Toxicology of newer pesticides for use in dogs and cats. *Vet. Clin. North Am. Small Anim. Pract.* **32**, 455–467 (2002).

189. Gaens, D., Rummel, C., Schmidt, M., Hamann, M. & Geyer, J. Suspected neurological toxicity after oral application of fluralaner (Bravecto®) in a Kooikerhondje dog. *BMC Vet. Res.* **15**, 283 (2019).

190. Medicine, C. for V. Fact Sheet for Pet Owners and Veterinarians about Potential Adverse Events Associated with Isoxazoline Flea and Tick Products. *FDA* (2023).

191. The Ivermectin Roadmappers. A Roadmap for the Development of Ivermectin as a Complementary Malaria Vector Control Tool. *Am. J. Trop. Med. Hyg.* **102**, 3–24 (2020).

192. Lucas, K. J. *et al.* Evaluation of a novel triple-action adulticide containing a pyrethroid, macrocyclic lactone, and fatty acid against pyrethroid-resistant *Aedes aegypti* and *Culex quinquefasciatus (Diptera: Culicidae)*. *J. Med. Entomol.* **61**, 701–709 (2024).

193. A new weapon in the global fight against malaria | Syngenta. https://www.syngenta.com/media/media-releases/2025/new-weapon-global-fight-against-malaria (2025).

194. ReMoa Tri® – Valent BioSciences – Public Health. https://www.valentbiosciences.com/publichealth/products/remoa-tri/.

195. merus3.0-infosheet.

196. Sovrenta 15® WP. *Vector Control* https://www.syngentavectorcontrol.com/product/crop-protection/vector-control/sovrenta-15r-wp (2025).

197. Nicolas, P. *et al.* Potential metabolic resistance mechanisms to ivermectin in Anopheles gambiae: a synergist bioassay study. *Parasit. Vectors* **14**, 172 (2021).

198. Mansouri, V. & Gholizadeh, S. Molecular detection of novel Glutamate-gated chloride channel mutations in field collected human head lice (Phthiraptera: Pediculidae) from Iran. *BMC Res. Notes* **18**, 115 (2025).

199. Foy, B. D. *et al.* Efficacy and risk of harms of repeat ivermectin mass drug administrations for control of malaria (RIMDAMAL): a cluster-randomised trial. *The Lancet* **393**, 1517–1526 (2019).

200. Chaccour, C., Lines, J. & Whitty, C. J. M. Effect of Ivermectin on *Anopheles gambiae* Mosquitoes Fed on Humans: The Potential of Oral Insecticides in Malaria Control. *J. Infect. Dis.* **202**, 113–116 (2010).

201. Chaccour, C., Hammann, F. & Rabinovich, N. R. Ivermectin to reduce malaria transmission I. Pharmacokinetic and pharmacodynamic considerations regarding efficacy and safety. *Malar. J.* **16**, 161 (2017).

202. Kobylinski, K. C. *et al.* Ivermectin susceptibility and sporontocidal effect in Greater Mekong Subregion Anopheles. *Malar. J.* **16**, 280 (2017).

203. Kobylinski, K. C. *et al.* Safety, Pharmacokinetics, and Mosquito-Lethal Effects of Ivermectin in Combination With Dihydroartemisinin-Piperaquine and Primaquine in Healthy Adult Thai Subjects. *Clin. Pharmacol. Ther.* **107**, 1221–1230 (2020).

204. Smit, M. R. *et al.* Safety and mosquitocidal efficacy of high-dose ivermectin when co-administered with dihydroartemisinin-piperaquine in Kenyan adults with uncomplicated malaria (IVERMAL): a randomised, double-blind, placebo-controlled trial. *Lancet Infect. Dis.* **18**, 615–626 (2018).

205. Dabira, E. D. *et al.* Mass drug administration of ivermectin and dihydroartemisinin–piperaquine against malaria in settings with high coverage of standard control interventions: a cluster-randomised controlled trial in The Gambia. *Lancet Infect. Dis.* **22**, 519–528 (2022).

206. Chaccour, C. *et al.* BOHEMIA: Broad One Health Endectocide-based Malaria Intervention in Africa—a phase III cluster-randomized, open-label, clinical trial to study the safety and efficacy of ivermectin mass drug administration to reduce malaria transmission in two African settings. *Trials* **24**, 128 (2023).

207. Hutchins, H. *et al.* Adjunctive ivermectin mass drug administration for malaria control on the Bijagos Archipelago of Guinea-Bissau (MATAMAL): a quadruple-blinded, cluster-

randomised, placebo-controlled trial. *Lancet Infect. Dis.* S1473309924005802 (2024) doi:10.1016/S1473-3099(24)00580-2.

208. Ouedraogo, A. L. *et al.* Efficacy and Safety of the Mosquitocidal Drug Ivermectin to Prevent Malaria Transmission After Treatment: A Double-Blind, Randomized, Clinical Trial. *Clin. Infect. Dis.* **60**, 357–365 (2015).
209. Kobylinski, K. C., Foy, B. D. & Richardson, J. H. Ivermectin inhibits the sporogony of Plasmodium falciparum in Anopheles gambiae. *Malar. J.* **11**, 381 (2012).
210. Kobylinski, K. C. *et al.* The effect of oral anthelmintics on the survivorship and re-feeding frequency of anthropophilic mosquito disease vectors. *Acta Trop.* **116**, 119–126 (2010).
211. Fritz, M. L. *et al.* Toxicity of bloodmeals from ivermectin-treated cattle to *Anopheles gambiae* s.l. *Ann. Trop. Med. Parasitol.* **103**, 539–547 (2009).
212. Foy, B. D., Rao, S., Parikh, S., Slater, H. C. & Dabiré, R. K. Analysis of the RIMDAMAL trial – Authors' reply. *The Lancet* **394**, 1006–1007 (2019).
213. Bradley, J., Moulton, L. H. & Hayes, R. Analysis of the RIMDAMAL trial. *The Lancet* **394**, 1005–1006 (2019).
214. Smit, M. R. *et al.* Efficacy and Safety of High-Dose Ivermectin for Reducing Malaria Transmission (IVERMAL): Protocol for a Double-Blind, Randomized, Placebo-Controlled, Dose-Finding Trial in Western Kenya. *JMIR Res. Protoc.* **5**, e213 (2016).
215. Slater, H. C. *et al.* Ivermectin as a novel complementary malaria control tool to reduce incidence and prevalence: a modelling study. *Lancet Infect. Dis.* **20**, 498–508 (2020).
216. Dabira, E. D. *et al.* Mass Drug Administration With High-Dose Ivermectin and Dihydroartemisinin-Piperaquine for Malaria Elimination in an Area of Low Transmission

With High Coverage of Malaria Control Interventions: Protocol for the MASSIV Cluster Randomized Clinical Trial. *JMIR Res. Protoc.* **9**, e20904 (2020).

217. Kobylinski, K. C. *et al.* Ivermectin susceptibility and sporontocidal effect in Greater Mekong Subregion Anopheles. *Malar. J.* **16**, 280 (2017).

218. Lyimo, I. N., Kessy, S. T., Mbina, K. F., Daraja, A. A. & Mnyone, L. L. Ivermectin-treated cattle reduces blood digestion, egg production and survival of a free-living population of Anopheles arabiensis under semi-field condition in south-eastern Tanzania. *Malar. J.* **16**, 239 (2017).

219. Foy, B. D. *et al.* Repeat Ivermectin Mass Drug Administrations for Malaria Control II: Protocol for a Double-blind, Cluster-Randomized, Placebo-Controlled Trial for the Integrated Control of Malaria. *JMIR Res. Protoc.* **12**, e41197 (2023).

220. Lado, P. *et al.* Changing species dynamics and species-specific associations observed between *Anopheles* and *Plasmodium* genera in Diebougou health district, southwest Burkina Faso. Preprint at https://doi.org/10.1101/2024.10.09.24315124 (2024).

221. Holcomb, K. M., Nguyen, C., Komar, N., Foy, B. D. & Barker, C. M. 29791 Bird-delivered ivermectin as a novel urban West Nile virus prevention strategy. *J. Clin. Transl. Sci.* **5**, 130–130 (2021).

222. Holcomb, K. M. *et al.* Predicted reduction in transmission from deployment of ivermectin-treated birdfeeders for local control of West Nile virus. *Epidemics* **44**, 100697 (2023).

223. Nguyen, C. *et al.* Evaluation of a novel West Nile virus transmission control strategy that targets Culex tarsalis with endectocide-containing blood meals. *PLoS Negl. Trop. Dis.* **13**, e0007210 (2019).

224. Perry, M. Malaria in the Jeypore Hill tract and adjoining coastland. *Palud. 5* 32–40 (1912).

225. Detinova, T. S. & Gillies, M. T. Observations on the Determination of the Age Composition and Epidemiological Importance of Populations of Anopheles gambiae Giles and Anopheles funestus Giles in Tanganyika.

226. Polovodova, V. P. Changes with age in the female genitalia of Anopheles and the age composition of mosquito populations. *Mosk. Thesis* (1947).

227. Lehane, M. J., Chadwick, J., Howe, M. A. & Mail, T. S. Improvements in the Pteridine Method for Determining Age in Adult Male and Female Stomoxys calcitrans (Diptera: Muscidae). *J. Econ. Entomol.* **79**, 1714–1719 (1986).

228. Wu, D. & Lehane, M. J. Pteridine fluorescence for age determination of *Anopheles* mosquitoes. *Med. Vet. Entomol.* **13**, 48–52 (1999).

229. Lardeux, F., Ung, A. & Chebret, M. Spectrofluorometers Are Not Adequate for Aging Aedes and Culex (Diptera: Culicidae) Using Pteridine Fluorescence. *J. Med. Entomol.* **37**, 769–773 (2000).

230. Desena, M. L., Edman, J. D., Clark, J. M., Symington, S. B. & Scott, T. W. *Aedes aegypti* (Diptera: Culicidae) Age Determination by Cuticular Hydrocarbon Analysis of Female Legs. *J. Med. Entomol.* **36**, 824–830 (1999).

231. Desena, M. L. *et al.* Potential for Aging Female *Aedes aegypti* (Diptera: Culicidae) by Gas Chromatographic Analysis of Cuticular Hydrocarbons, Including a Field Evaluation. *J. Med. Entomol.* **36**, 811–823 (1999).

232. Blomquist, G. J., Nelson, D. R. & De Renobales, M. Chemistry, biochemistry, and physiology of insect cuticular lipids. *Arch. Insect Biochem. Physiol.* **6**, 227–265 (1987).

233. Cook, P. E. *et al.* The use of transcriptional profiles to predict adult mosquito age under field conditions. *Proc. Natl. Acad. Sci.* **103**, 18060–18065 (2006).

234. Hugo, L. E., Kay, B. H., O'neill, S. L. & Ryan, P. A. Investigation of Environmental Influences on a Transcriptional Assay for the Prediction of Age of Aedes aegypti (Diptera: Culicidae) Mosquitoes. *J. Med. Entomol.* **47**, 1044–1052 (2010).

235. Hugo, L. E. *et al.* Proteomic Biomarkers for Ageing the Mosquito Aedes aegypti to Determine Risk of Pathogen Transmission. *PLoS ONE* **8**, e58656 (2013).

236. Hugo, L. E. *et al.* Adult Survivorship of the Dengue Mosquito Aedes aegypti Varies Seasonally in Central Vietnam. *PLoS Negl. Trop. Dis.* **8**, e2669 (2014).

237. Mayagaya, V. S. *et al.* Non-destructive Determination of Age and Species of Anopheles gambiae s.l. Using Near-infrared Spectroscopy. *Am. J. Trop. Med. Hyg.* **81**, 622–630 (2009).

238. Sikulu, M. *et al.* Near-infrared spectroscopy as a complementary age grading and species identification tool for African malaria vectors. (2010).

239. Lambert, B. *et al.* Monitoring the Age of Mosquito Populations Using Near-Infrared Spectroscopy. *Sci. Rep.* **8**, 5274 (2018).

240. Khoshmanesh, A. *et al.* Screening of *Wolbachia* Endosymbiont Infection in *Aedes aegypti* Mosquitoes Using Attenuated Total Reflection Mid-Infrared Spectroscopy. *Anal. Chem.* **89**, 5285–5293 (2017).

241. Liebman, K. *et al.* The Influence of Diet on the Use of Near-Infrared Spectroscopy to Determine the Age of Female Aedes aegypti Mosquitoes. *Am. Soc. Trop. Med. Hyg.* **92**, 1070–1075 (2015).

242. González Jiménez, M. *et al.* Prediction of mosquito species and population age structure using mid-infrared spectroscopy and supervised machine learning [version 3; peer review: 2 approved]. *Wellcome Open Res.* **4**, (2019).

243. Gray, L. *et al.* Back to the Future: Quantifying Wing Wear as a Method to Measure Mosquito Age. *Am. J. Trop. Med. Hyg.* **107**, 689–700 (2022).

244. Alout, H. *et al.* Evaluation of ivermectin mass drug administration for malaria transmission control across different West African environments. *Malar. J.* **13**, 417 (2014).

245. Siria, D. J. *et al.* Rapid age-grading and species identification of natural mosquitoes for malaria surveillance. *Nat. Commun.* **13**, 1501 (2022).

246. Sinka, M. E. *et al.* The dominant Anopheles vectors of human malaria in Africa, Europe and the Middle East: occurrence data, distribution maps and bionomic précis. *Parasit. Vectors* **3**, 117 (2010).

247. Sinka, M. E. *et al.* A new malaria vector in Africa: Predicting the expansion range of *Anopheles stephensi* and identifying the urban populations at risk. *Proc. Natl. Acad. Sci.* **117**, 24900–24908 (2020).

248. N'Guessan, R. *et al.* Control of pyrethroid and DDT-resistant Anopheles gambiae by application of indoor residual spraying or mosquito nets treated with a long-lasting organophosphate insecticide, chlorpyrifos-methyl. *Malar. J.* **9**, 44 (2010).

249. Tungu, P. K., Michael, E., Sudi, W., Kisinza, W. W. & Rowland, M. Efficacy of interceptor® G2, a long-lasting insecticide mixture net treated with chlorfenapyr and alpha-cypermethrin against Anopheles funestus: experimental hut trials in north-eastern Tanzania. *Malar. J.* **20**, 180 (2021).

250. Mbewe, N. J. *et al.* Efficacy of bednets with dual insecticide-treated netting (Interceptor® G2) on side and roof panels against Anopheles arabiensis in north-eastern Tanzania. *Parasit. Vectors* **15**, 326 (2022).

251. Bayili, K. *et al.* Evaluation of efficacy of Interceptor® G2, a long-lasting insecticide net coated with a mixture of chlorfenapyr and alpha-cypermethrin, against pyrethroid resistant Anopheles gambiae s.l. in Burkina Faso. *Malar. J.* **16**, 190 (2017).

252. Bhatt, S. *et al.* The effect of malaria control on Plasmodium falciparum in Africa between 2000 and 2015. *Nature* **526**, 207–211 (2015).

253. Keïta, M. *et al.* Multiple Resistance Mechanisms to Pyrethroids Insecticides in *Anopheles gambiae sensu lato* Population From Mali, West Africa. *J. Infect. Dis.* **223**, S81–S90 (2021).

254. Namountougou, M. *et al.* Multiple Insecticide Resistance in Anopheles gambiae s.l. Populations from Burkina Faso, West Africa. *PLoS ONE* **7**, e48412 (2012).

255. Oruni, A. *et al.* Significant variations in tolerance to clothianidin and pirimiphos-methyl in *Anopheles gambiae* and *Anopheles funestus* populations during a dramatic malaria resurgence despite sustained indoor residual spraying in Uganda. Preprint at https://doi.org/10.1101/2025.02.13.638152 (2025).

256. Zinszer, K. *et al.* The Impact of Multiple Rounds of Indoor Residual Spraying on Malaria Incidence and Hemoglobin Levels in a High-Transmission Setting. *J. Infect. Dis.* **221**, 304–312 (2020).

257. Chaccour, C. J. & Rabinovich, N. R. Oral, Slow-Release Ivermectin: Biting Back at Malaria Vectors. *Trends Parasitol.* **33**, 156–158 (2017).

258. Kobylinski, K. C. *et al.* Ivermectin susceptibility, sporontocidal effect, and inhibition of time to re-feed in the Amazonian malaria vector Anopheles darlingi. *Malar. J.* **16**, 474 (2017).

259. Mekuriaw, W. *et al.* The effect of ivermectin® on fertility, fecundity and mortality of Anopheles arabiensis fed on treated men in Ethiopia. *Malar. J.* **18**, 357 (2019).

260. Otabil, K. B. *et al.* Persistence of onchocerciasis and associated dermatologic and ophthalmic pathologies after 27 years of ivermectin mass drug administration in the middle belt of Ghana. *Trop. Med. Int. Health* **28**, 844–854 (2023).

261. The Ivermectin Roadmappers. A Roadmap for the Development of Ivermectin as a Complementary Malaria Vector Control Tool. *Am. J. Trop. Med. Hyg.* **102**, 3–24 (2020).

262. Tesh, R. B. & Guzman, H. Mortality and Infertility in Adult Mosquitoes After the Ingestion of Blood Containing Ivermectin. *Am. J. Trop. Med. Hyg.* **43**, 229–233 (1990).

263. Mahmood, F., Walters, L. L., Guzman, H. & Tesh, R. B. Effect of Ivermectin on the Ovarian Development of Aedes aegypti (Diptera: Culicidae). *J. Med. Entomol.* **28**, 701–707 (1991).

264. Foley, D. H., Bryan, J. H. & Lawrence, G. W. The potential of ivermectin to control the malaria vector Anopheles farauti. *Trans. R. Soc. Trop. Med. Hyg.* **94**, 625–628 (2000).

265. Chaccour, C., Lines, J. & Whitty, C. J. M. Effect of Ivermectin on *Anopheles gambiae* Mosquitoes Fed on Humans: The Potential of Oral Insecticides in Malaria Control. *J. Infect. Dis.* **202**, 113–116 (2010).

266. Baraka, O. Z. *et al.* Ivermectin distribution in the plasma and tissues of patients infected with Onchocerca volvulus. *Eur. J. Clin. Pharmacol.* **50**, 407–410 (1996).

267. Schulz, J. D., Coulibaly, J. T., Schindler, C., Wimmersberger, D. & Keiser, J. Pharmacokinetics of ascending doses of ivermectin in Trichuris trichiura-infected children aged 2–12 years. *J. Antimicrob. Chemother.* **74**, 1642–1647 (2019).

268. Brussee, J. M., Schulz, J. D., Coulibaly, J. T., Keiser, J. & Pfister, M. Ivermectin Dosing Strategy to Achieve Equivalent Exposure Coverage in Children and Adults. *Clin. Pharmacol. Ther.* **106**, 661–667 (2019).

269. Day, M. The Mechanism of Food Distribution to Midgut or Diverticula in the Mosquito. *Aust. J. Biol. Sci.* 515–524 (1954) doi:https://doi.org/10.1071/BI9540515.

270. Dapples, C. C., Foster, W. A. & Lea, A. O. Ultrastructure of the accessory gland of the male mosquito, Aedes Aegypti (L.) (Diptera: CUlicidae). *Int. J. Insect Morphol. Embryol.* **3**, 279–291 (1974).

271. Dapples, C. C. & Lea, A. O. Inner surface morphology of the alimentary canal in Aedes aegypti (L.) (diptera: culicidae). *Int. J. Insect Morphol. Embryol.* **3**, 433–442 (1974).

272. Evans, C. C. *et al.* Treatment of dogs with Bravecto® (fluralaner) reduces mosquito survival and fecundity. *Parasit. Vectors* **16**, (2023).

273. Knape, K. *et al.* Fluralaner treatment of chickens kills the southern house mosquito, Culex quinquefasciatus. *Med. Vet. Entomol.* **n/a**,.

274. Shah, H. K. *et al.* Evaluation of the mosquitocidal efficacy of fluralaner, a potential candidate for drug based vector control. *Sci. Rep.* **14**, (2024).

275. Soré, H. *et al.* The mosquitocidal activity of isoxazoline derivatives afoxolaner, lotilaner, and fluralaner are not affected by mosquito sugar or antibiotic treatment. *Sci. Rep.* **15**, (2025).

276. Kilp, S., Ramirez, D., Allan, M. J. & Roepke, R. K. Comparative pharmacokinetics of fluralaner in dogs and cats following single topical or intravenous administration. *Parasit. Vectors* **9**, 296 (2016).

277. Kilp, S., Ramirez, D., Allan, M. J., Roepke, R. K. & Nuernberger, M. C. Pharmacokinetics of fluralaner in dogs following a single oral or intravenous administration. *Parasit. Vectors* **7**, 85 (2014).

278. Murphy, M. *et al.* Laboratory evaluations of the immediate and sustained efficacy of lotilaner (Credelio^{TM}) against four common species of ticks affecting dogs in North America. *Parasit. Vectors* **10**, 523 (2017).

279. Toutain, C. E., Seewald, W. & Jung, M. The intravenous and oral pharmacokinetics of lotilaner in dogs. *Parasit. Vectors* **10**, 522 (2017).

280. Pooda, S. H. *et al.* Proof-of-concept study for a long-acting formulation of ivermectin injected in cattle as a complementary malaria vector control tool. *Parasit. Vectors* **16**, 66 (2023).

281. Charlwood, J. D., Pinto, J., Sousa, C. A., Ferreira, C. & Petrarca, V. 'A mate or a meal' – Pre-gravid behaviour of female Anopheles gambiae from the islands of São Tomé and Príncipe, West Africa. *Malar. J.* 11 (2003).

282. Ohm, J. R. *et al.* Rethinking the extrinsic incubation period of malaria parasites. *Parasit. Vectors* **11**, 178 (2018).

283. Guissou, E. *et al.* A non-destructive sugar-feeding assay for parasite detection and estimating the extrinsic incubation period of Plasmodium falciparum in individual mosquito vectors. *Sci. Rep.* **11**, 9344 (2021).

284. Gillies, M. T. & Wilkes, T. J. A study of the age-composition of populations of Anopheles gambiae Giles and A. funestus Giles in North-Eastern Tanzania. *Bull. Entomol. Res.* **56**, 237–262 (1965).

285. Ryan, S. J., Ben-Horin, T. & Johnson, L. R. Malaria control and senescence: the importance of accounting for the pace and shape of aging in wild mosquitoes. *Ecosphere* **6**, art170 (2015).

286. Gillett, J. D. Age Analysis in the Biting-Cycle of the Mosquito Taeniorhynchus (Mansonioides) Africanus Theobald, based on the Presence of Parasitic Mites. *Ann. Trop. Med. Parasitol.* **51**, 151–158 (1957).

287. Detinova, T. S. AGE-GROUPING METHODS IN DIPTERA OF MEDICAL IMPORTANCE. 213 (1962).

288. Beklemishev, W. N., Detinova, T. S. & Polovodova, V. P. Determination of Physiological Age in Anophelines and of Age Distribution in Anopheline Populations in the USSR. *Bull Wld Hlth Org* **21**, 223–232 (1959).

289. Sikulu, M. T. *et al.* Mass spectrometry identification of age-associated proteins from the malaria mosquitoes Anopheles gambiae s.s. and Anopheles stephensi. *Data Brief* **4**, 461–467 (2015).

290. Sikulu-Lord, M. T., Devine, G. J., Hugo, L. E. & Dowell, F. E. First report on the application of near-infrared spectroscopy to predict the age of Aedes albopictus Skuse. *Sci. Rep.* **8**, 9590 (2018).

291. Ong, O. T. W. *et al.* Ability of near-infrared spectroscopy and chemometrics to predict the age of mosquitoes reared under different conditions. *Parasit. Vectors* **13**, 160 (2020).

292. Gao, Z. *et al.* Accurate age-grading of field-aged mosquitoes reared under ambient conditions using surface-enhanced Raman spectroscopy and artificial neural networks. *J. Med. Entomol.* **60**, (2023).

293. Wang, D. *et al.* Quantitative age grading of mosquitoes using surface-enhanced Raman spectroscopy. *Anal. Sci. Adv.* **3**, 47–53 (2022).

294. Krajacich, B. J. *et al.* Analysis of near infrared spectra for age-grading of wild populations of Anopheles gambiae. *Parasit. Vectors* **10**, 552 (2017).

295. Somé, B. M. *et al.* Adapting field-mosquito collection techniques in a perspective of near-infrared spectroscopy implementation. *Parasit. Vectors* **15**, 338 (2022).

296. Mwanga, E. P. *et al.* Using transfer learning and dimensionality reduction techniques to improve generalisability of machine-learning predictions of mosquito ages from mid-infrared spectra. *BMC Bioinformatics* **24**, 11 (2023).

297. Johnson, B. J., Hugo, L. E., Churcher, T. S., Ong, O. T. W. & Devine, G. J. Mosquito Age Grading and Vector-Control Programmes. *Trends Parasitol.* **36**, 39–51 (2020).

298. Hugo, L. E., Quick-Miles, S., Kay, B. H. & Ryan, P. A. Evaluations of Mosquito Age Grading Techniques Based on Morphological Changes. *J. Med. Entomol.* **45**, 17 (2008).

299. Anagonou, R. *et al.* Application of Polovodova's method for the determination of physiological age and relationship between the level of parity and infectivity of Plasmodium falciparum in Anopheles gambiae s.s, south-eastern Benin. *Parasit. Vectors* **8**, 117 (2015).

300. Kirstein, O. D. *et al.* Targeted indoor residual insecticide applications shift Aedes aegypti age structure and arbovirus transmission potential. *Sci. Rep.* **13**, 21271 (2023).

301. Christophers, S. The development of the egg follicle in anophelines. *Paludism* **1911**, 73–88 (1911).

302. Vazquez-Prokopec, G. M., Galvin, W. A., Kelly, R. & Kitron, U. A New, Cost-Effective, Battery-Powered Aspirator for Adult Mosquito Collections. *J. Med. Entomol.* **46**, 1256–1259 (2009).

303. CDC. Outbreak of West Nile-Like Viral Encephalitis — New York, 1999. *Morb. Mortal. Wkly. Rep.* **48**, 845–849 (1999).

304. Nicholas Komar. West Nile Virus: Epidemiology and Ecology in North America. in *Advances in Virus Research* vol. 61 185–234 (Elsevier, 2003).

305. CDC. West Nile: Symptoms, Diagnosis, & Treatment. *West Nile Virus* https://www.cdc.gov/west-nile-virus/symptoms-diagnosis-treatment/index.html (2025).

306. Darsie, R. F. & Ward, R. A. *Identification and Geographical Distribution of the Mosquitoes of North America, North of Mexico*. (Gainsville : University Press of Florida, 2005).

307. CDC. Current Year Data (2024). *West Nile Virus* https://www.cdc.gov/west-nile-virus/data-maps/current-year-data.html (2025).

308. Bolling, B. G., Barker, C. M., Moore, C. G., Pape, W. J. & Eisen, L. Seasonal Patterns for Entomological Measures of Risk for Exposure to *Culex* Vectors and West Nile Virus in Relation to Human Disease Cases in Northeastern Colorado. *J. Med. Entomol.* **46**, 1519–1531 (2009).

309. Wekesa, J. W., Yuval, B., Washino, R. K. & De Vasquez, A. M. Blood feeding patterns of *Anopheles freeborni* and *Culex tarsalis* (Diptera: Culicidae): effects of habitat and host abundance. *Bull. Entomol. Res.* **87**, 633–641 (1997).

310. Wirth, M., Georghiou, G. P., Pasteur, N. & Luna, L. L. Evolution of Resistance and Change in Relative Density in a Culex tarsalis (Diptera: Culicidae) Population Under Heavy Insecticidal Control. *J. Med. Entomol.* **24**, 494–497 (1987).

311. Bellan, S. E. The Importance of Age Dependent Mortality and the Extrinsic Incubation Period in Models of Mosquito-Borne Disease Transmission and Control. *PLoS ONE* **5**, e10165 (2010).

312. Hien, D. F. D. S. *et al.* Plant-Mediated Effects on Mosquito Capacity to Transmit Human Malaria. *PLOS Pathog.* **12**, e1005773 (2016).

313. Guissou, E. *et al.* Intervention reducing malaria parasite load in vector mosquitoes: No impact on Plasmodium falciparum extrinsic incubation period and the survival of Anopheles gambiae. *PLOS Pathog.* **19**, e1011084 (2023).

314. Guissou, E. *et al.* A non-destructive sugar-feeding assay for parasite detection and estimating the extrinsic incubation period of Plasmodium falciparum in individual mosquito vectors. *Sci. Rep.* **11**, 9344 (2021).

315. Anderson, J. F., Main, A. J., Cheng, G., Ferrandino, F. J. & Fikrig, E. Horizontal and Vertical Transmission of West Nile Virus Genotype NY99 by Culex salinarius and Genotypes NY99 and WN02 by Culex tarsalis. *Am. Soc. Trop. Med. Hyg.* **86**, 134–139 (2012).

316. Goddard, L. B., Roth, A. E., Reisen, W. K. & Scott, T. W. Vertical Transmission of West Nile Virus by Three California <I>Culex</I> (Diptera: Culicidae) Species. *J. Med. Entomol.* **40**, 743–746 (2003).

317. Nelms, B. M., Macedo, P. A., Kothera, L., Savage, H. M. & Reisen, W. K. Overwintering Biology of <I>Culex</I> (Diptera: Culicidae) Mosquitoes in the Sacramento Valley of California. *J. Med. Entomol.* **50**, 773–790 (2013).

318. Moser, S. K. *et al.* Scoping review of Culex mosquito life history trait heterogeneity in response to temperature. *Parasit. Vectors* **16**, 200 (2023).

319. Mahmood, F., Reisen, W. K., Chiles, R. E. & Fang, Y. Western Equine Encephalomyelitis Virus Infection Affects the Life Table Characteristics of *Culex tarsalis* (Diptera: Culicidae). *J. Med. Entomol.* **41**, 982–986 (2004).

320. Pugh, G. *et al.* Pixel intensity of wing photos used to predict age of Anopheles gambiae caught during the RIMDAMAL II clinical trial. *bioRxiv* 2025.02.27.640698 (2025) doi:10.1101/2025.02.27.640698.

321. Venkatesan, P. Malaria vaccine development—where are we? *Lancet Infect. Dis.* **21**, 1218 (2021).

322. Panella, N. A., Kent Crockett, R. J., Biggerstaff, B. J. & Komar, N. The Centers for Disease Control and Prevention Resting Trap: A Novel Device for Collecting Resting Mosquitoes. *J. Am. Mosq. Control Assoc.* **27**, 323–325 (2011).

323. Bibbs, C. S. *et al.* Do it yourself: 3D-printed miniature CDC trap for adult mosquito (Diptera: Culicidae) surveillance. *PLoS Negl. Trop. Dis.* **18**, e0011899 (2024).

324. Guillet, P. *et al.* The role of agricultural use of insecticides in resistance to pyrethroids in Anopheles gambiae s.l. in Burkina Faso. *Am. J. Trop. Med. Hyg.* **67**, 617–622 (2002).

325. Soma, D. D. *et al.* Malaria vectors diversity, insecticide resistance and transmission during the rainy season in peri-urban villages of south-western Burkina Faso. *Malar. J.* **20**, 63 (2021).

326. BG-Pro All-In-One small set of 4. *Biogents US Webshop For Researchers* https://us-research-shop.biogents.com/products/bg-pro-all-in-one-set-of-4.